# MESENTERIC VASCULAR-PROJECTING NEURONS IN THE CELIAC AND SPLANCHNIC GANGLIA PROJECT WIDELY AND CONTRIBUTE TO THE REGULATION OF SYSTEMIC ARTERIAL PRESSURE

By

Bradley Dustin Hammond

A DISSERTATION

Submitted to
Michigan State University
in partial fulfillment of the requirements
for the degree of

Neuroscience-Doctor of Philosophy

2015

## ABSTRACT

MESENTERIC VASCULAR-PROJECTING NEURONS IN THE CELIAC AND SPLANCHNIC GANGLIA PROJECT WIDELY AND CONTRIBUTE TO THE REGULATION OF SYSTEMIC ARTERIAL PRESSURE

By

Bradley Dustin Hammond

The splanchnic circulation holds one third of the body's total blood volume, making it a critical target for the regulation of systemic hemodynamics by sympathetic neurons in prevertebral ganglia. Mesenteric arteries and veins are innervated by separate subpopulations of neurons in prevertebral ganglia. The studies described in this dissertation examine the effects of a selective lesion of artery-projecting and vein-projecting neurons on the hemodynamic response to activating sympathetic fibers innervating the splanchnic circulation. The presence of artery-projecting and vein-projecting neurons in both the celiac ganglion and the splanchnic ganglion was demonstrated with retrograde tracers that were applied to the surface of mesenteric arteries and veins. Nicotine application to the celiac ganglion elevated systemic arterial pressure 7.89 ± 1.53 mmHg via activation of postganglionic neurons in the celiac ganglion. Electrical stimulation of the greater splanchnic nerve elevated systemic arterial pressure 7.36 ± 1.07 mmHg via activation of postganglionic nerve fibers of neurons residing in the splanchnic ganglion. Application of a neurotoxin, saporin, conjugated to an antibody against dopamine beta hydroxylase (DβH-sap) onto two small 7 mm segments of mesenteric arteries and veins ablated 94% of neurons in prevertebral ganglia. Three

weeks after application of DβH-sap to the mesenteric vasculature, electrical stimulation of the greater splanchnic nerve elicited a -1.59 ± 1.53 mmHg change in systemic arterial pressure. Lesions generated by DβH-sap indicate prevertebral vascular-projecting neurons have wide fields of innervation and play a role in the regulation of systemic hemodynamics.

## ACKNOWLEDGEMENTS

Much like it takes a village to raise a child, it takes a consortium to educate a doctoral student. I would like to thank my advisor, Dr. David Kreulen for taking me into his lab, because he gave me the opportunity to pioneer many challenging avenues of research. I would also like to thank my committee members: Dr. Gregory Fink, Dr. Anne Dorrance, and Dr. Fredric Manfredsson for individual support, ideas, and questions over the years.

I would also like to thank all of my colleagues in the lab. Amit Shah and Ryan Mui for many conversations about the innervation to the splanchnic circulation. Tim Houchin for showing me how to harvest prevertebral ganglia. My undergrads, Annaliese Durling, and Brian Darios for their continued help with IHC, imaging, and cell counting. Hannah Graver for assisting me with anything rodent related, and Robert Burnett for helping me analysis splanchnic tissues for norepinephrine content.

Lastly I would like to thank my friends and family. My parents and brother for their love and emotional support. My lovely wife for her love, and continued inspiration over the past years.

## TABLE OF CONTENTS

## LIST OF FIGURES

## KEY TO ABBREVIATIONS

| | |
|---|---|
| Ang II | angiotensin II |
| AR | adrenergic receptor |
| ATP | adenosine triphosphate |
| BPM | beats per minute |
| CG | celiac ganglion |
| CTB | cholera toxin subunit B |
| CGRP | calcitonin gene related peptide |
| CGx | celiac ganglionectomy |
| CNS | central nervous system |
| DβH | dopamine beta hydroxylase |
| DβH–MA | DβH–sap applied to mesenteric arteries |
| DβH–MV | DβH–sap applied to mesenteric veins |
| DβH–sap | antibody to dopamine beta hydroxylase conjugated to saporin |
| DOCA | deoxycorticosterone acetate |

| | |
|---|---|
| DRG | dorsal root ganglion |
| GFAP | glial fibrillary acidic protein |
| GFP | green florescent protein |
| GSN | greater splanchnic nerve |
| HBSS | hanks’ balanced salt solution |
| IB | TPBS with 0.3% triton |
| IMG | inferior mesenteric ganglion |
| IP | intraperitoneal |
| IR | immunoreactivity |
| IV | intravenous |
| MA | mesenteric artery |
| MCFP | mean circulatory filling pressure |
| MV | mesenteric vein |
| NE | norepinephrine |
| nAchRs | nicotinic acetylcholine receptors |

| | |
|---|---|
| PBS | phosphate buffered saline |
| PNS | peripheral nervous system |
| PPADs | pyridoxalphosphate-6-azophenyl-2',4'-disulfonic acid |
| PRV | pseudorabies virus |
| PVN | paraventricular nucleus |
| rAAV | recombinant adeno–associated virus |
| RT | room temperature |
| RVLM | rostral ventral lateral medulla |
| SG | splanchnic ganglion |
| TH | tyrosine hydroxylase |
| TPBS | tris phosphate buffered saline |
| VEGF | vascular endothelial growth factor |
| VTA | ventral tegmental area |

# CHAPTER 1: GENERAL INTRODUCTION

The autonomic nervous system links visceral effectors with the central nervous system (CNS) via neural pathways. A branch of the autonomic nervous system is the sympathetic nervous system, which is organized into pathways of centrally located cholinergic preganglionic neurons that innervate ganglia, glands, and other neural networks. Neurons located in ganglia innervate visceral effectors, thereby conferring neural control over viscera, vasculature, and glands. An essential region controlled by sympathetic ganglia is the splanchnic circulation, the body's largest vascular bed. As such, sympathetic control of the splanchnic circulation greatly influences systemic arterial pressure by reducing the amount of blood stored in the splanchnic circulation as well as the resistance that must be overcome to maintain blood flow to abdominal organs, termed splanchnic capacitance and resistance respectively. A plethora of evidence for the impact of sympathetic control over splanchnic resistance and capacitance on systemic arterial pressure arises from studies removing or activating sympathetic innervation to the splanchnic region (Kandlikar & Fink, 2011; Karim & Hainsworth, 1976; King, Osborn, & Fink, 2007). Removing innervation to the splanchnic circulation attenuates rises in systemic arterial pressure during hypertension, however, the relative contribution of splanchnic capacitance or resistance to systemic arterial pressure has not been isolated. It is the aim of this study to isolate and investigate the impacts of splanchnic resistance and capacitance on systemic arterial pressure.

*Splanchnic resistance and capacitance contribute to rises in systemic arterial pressure*

Arterial pressure is positively correlated to cardiac output and total peripheral resistance. Cardiac output is transiently increased during the development of hypertension in humans, as evidenced by increased cardiac–specific spillover (Esler et

al., 1984), but normalizes during later phases and transitions to increased vascular resistance (Julius, 1988). Similarly, in aldosterone and angiotensin (Ang) induced hypertension in sheep, elevated arterial pressure is positively correlated with peripheral resistance, but not correlated at all with cardiac output (May, 1996; 2006). In support, removing sympathetic innervation of cardiac tissues does not affect the development or maintenance of deoxycorticosterone acetate–salt (DOCA) hypertension (Wehrwein et al., 2014). Taken together, increases in cardiac output are not a key factor leading to the development or maintenance of hypertension.

If cardiac output is not a primary player in the development of hypertension, then total peripheral resistance and venous capacitance must play a large role. Arteries have thick inelastic walls that are important for generating resistance, while veins have thinner elastic walls important for the storage of blood. Total peripheral resistance is proportional to the diameter of small arteries and arterioles and, in turn, arterial pressure. In contrast, veins contain up to 66% of systemic blood and constricting veins displaces volumes of blood, which transiently increases cardiac output until the displaced volume of blood is translocated to the arterial circulation. It has been hypothesized that chronic sympathetically mediated translocation of blood from the venous reservoir to the arterial reservoir leads to long–term increases in systemic arterial pressure, because the arterial reservoir is less compliant and small changes in volume drastically increase pressure (Fink, 2008). Therefore, constricting either the arterial or venous circulation contributes to rises in systemic arterial pressure.

*Splanchnic sympathetic neurons are recruited during hypertension*

The splanchnic circulation significantly contributes to the long–term regulation of arterial pressure, since it receives 25–30% of cardiac output and contains 25–30% of total blood volume (Fink, 2008). As such, the splanchnic region is an essential target of sympathetic efferent fibers in Ang II-salt hypertension, where splanchnic sympathetic nerve activity is increased without corresponding increases in markers for lumbar, hindlimb, or renal sympathetic nerve activity (Luft et al., 1989; Osborn, Fink, & Kuroki, 2011). Removing the sympathetic innervation to the viscera and vasculature of the abdominal region (Li, Galligan, Wang, & Fink, 2010) via celiac ganglionectomy (CGx) has been a therapeutic target to lower arterial pressure in hypertensive individuals (Grimson & Orgain, 1949; Kandlikar & Fink, 2011; King et al., 2007; Marlett & Code, 1979). Although, the CG contains a diverse array of neurons and fibers of passage that innervate vascular and visceral targets; so, it is unknown what population of neurons or fibers is responsible for attenuating rises in systemic arterial pressure.

Vasoconstricting the splanchnic circulation contributes to increases in systemic arterial pressure, so the population of CG neurons important for increasing systemic arterial pressure may project to the splanchnic vasculature (Osborn, Fink, Sved, Toney, & Raizada, 2007). In support of this proposal, venous tone estimated by measuring mean circulatory filling pressure (MCFP, Pang, 2001), is increased in Ang II-salt hypertension. MCFP is attenuated by CGx or ganglionic blockade with hexamethonium, indicating constricting splanchnic veins promotes long–term increases in systemic arterial pressure (King et al., 2007). Similarly, splanchnic resistance is increased in Ang II-salt hypertension and is attenuated by ganglionic blockade with hexamethonium (Kuroki, Guzman, Fink, &

Osborn, 2011), Taken together, increasing vasomotor tone to splanchnic arteries, or veins, contributes to long–term increases in systemic arterial pressure, and the critical component attenuating rises in arterial pressure is located in the CG. I hypothesize, both vascular-projecting neurons in the CG, and vascular-projecting fibers passing through the CG, are the critical components leading to increases in splanchnic vascular tone and, in turn, systemic arterial pressure.

Until recently a lack of selective methodology has hindered progress on clarifying the neural component important for the hemodynamic control of the splanchnic circulation. For instance, no study has isolated the contribution of the splanchnic vasculature, let alone arteries or veins, to increases in systemic arterial pressure. Rather, studies have examined the effects of activating several populations of postganglionic fibers in the greater splanchnic nerve (Karim & Hainsworth, 1976), or the effects of removing the majority of sympathetic innervation to the splanchnic region (King et al., 2007) The focus of each chapter in the present study will be to develop techniques facilitating the selective isolation of populations of neurons and fibers, in prevertebral ganglia, important for the hemodynamic control of the splanchnic circulation. The second chapter of this dissertation aims to investigate the innervation patterns and potentially modify genes of vascular–projecting neurons by examining the effectiveness of recombinant adeno-associated viruses (rAAVs) to transduce CG neurons. The third chapter investigates methods to activate prevertebral neurons to isolate the effects of constricting splanchnic arteries and veins on systemic arterial pressure. The methods from chapter three will be used in the fourth chapter to test the effects of removing

sympathetic innervation to mesenteric arteries (MA) or veins (MV) on systemic arterial pressure.

*The sympathetic nervous system exerts control over splanchnic viscera*

Prevertebral ganglia contain sympathetic neurons that exert control over abdominal viscera, therefore understanding the endogenous sympathetic control over splanchnic viscera becomes important to grasping the corollaries of CGx on the function of splanchnic viscera. Stimulating splanchnic nerves mobilizes glucose via elevated glucose metabolism in the liver (Bloom & Edwards, 1978; 1984; Shimazu, 1981), and increased glucagon release in the pancreas (Bloom, Edwards, & Vaughan, 1973). Activating the sympathetic nervous system relaxes the stomach (Nakazato, Sekine, Isogaya, & Ito, 1987), reduces intestinal motility (Kuntz & Saccomanno, 1944), reduces sodium and renin excretion by the kidney (Vander, 1965), and relaxes the body of the bladder, while the neck of the bladder and proximal urethra contract (Kihara & de Groat, 1997). Activating sympathetic innervation to the spleen is correlated to reductions in natural killer cell activity (Katafuchi, Ichijo, Take, & Hori, 1993a; Katafuchi, Take, & Hori, 1993b) and the number of regulatory T cells (Katsuki, Hirooka, Kishi, & Sunagawa, 2015) indicating the sympathetic nervous system exerts control over the immunity conferred by the spleen. A final response to activating the sympathetic nervous system is the release of epinephrine and NE from the adrenal gland, which increases heart rate, glucose metabolism and mean arterial pressure, redistributes blood to the muscles, and enlarges air pathways in the lungs (Ramey & Goldstein, 1957). Epinephrine and norepinephrine (NE) released from the adrenal glands have longer time courses than the initial activation of the sympathetic nervous system, so they serve to reinforce and sustain the actions of

the sympathetic nervous system. Therefore, activating the sympathetic nervous system effects the function of many abdominal organs and removing innervation to the splanchnic region, via CGx, likely has deleterious effects on the function of splanchnic viscera. For example, CGx causes marked diarrhea in dogs (Freedman, Hallenbeck, & Code, 1952; Lillehei & Wangensteen, 1948), however several other studies reported no diarrhea or any disruptions in whole-body metabolism in rodents (Furness et al., 2001; King et al., 2007). Therefore, the effects of removing innervation to the splanchnic viscera remain unclear, and it is an aim of this study to remove innervation to the splanchnic vasculature without removing the innervation to the splanchnic viscera.

*Organization of the sympathetic nervous system influences sympathetic outflow*

Comprehending the organization of the sympathetic nervous system is crucial to understanding how sympathetic outflow reaches and ultimately modulates the function of end organs. Sympathetic outflow to blood vessels begins centrally by integrating several inputs in the paraventricular nucleus of the hypothalamus (PVN). The PVN relays sympathetic outflow to the rostral ventrolateral medulla (RVLM), where outflow is integrated with baroreceptor mediated reflexes (Barman, Orer, & Gebber, 2001). The RVLM sends projections downstream to preganglionic neurons in the spinal cord. Neurons in the RVLM are organized in a viscerotopic fashion in multiple animal models (Dean & Coote, 1986; Dean, Seagard, Hopp, & Kampine, 1992; Lovick, 1987; Lovick & Hilton, 1985; McAllen, May, & Shafton, 1995), suggesting sympathetic outflow can be directed to tissue specific sites throughout the body. For example, vasoconstricting hind-limb and mesenteric vasculature beds is accomplished by injecting an N-methyl-D-aspartate receptor agonist into the ventrolateral medulla adjacent to the inferior olive,

where vasoconstricting the renal vascular bed was evoked by more rostral injections (Lovick & Hilton, 1985).

Preganglionic neurons in the spinal cord innervate postganglionic neurons located in paravertebral and prevertebral ganglia. Postganglionic neurons receive convergent input from many preganglionic neurons (Janig & McLachlan, 1992) while each preganglionic neuron diverges to make synaptic connections with 50-200 postganglionic cells, to comprise an autonomic neural unit (Purves & Wigston, 1983). Autonomic neural units are hypothesized to be organized according to target tissue, providing target specific control (McLachlan, 2003). However, autonomic neural units are not topographically organized and neurons within a neural unit can be separated by distances up to 1-2 mms (Purves & Wigston, 1983). For example, vasoconstrictor neurons projecting to the vasculature of the hindlimb muscles exclusively received all of the inputs from preganglionic neurons containing calcitonin gene related peptide (CGRP; Gibbins, 1992). In contrast, most vasodilator neurons projecting to the vascular bed exclusively received inputs from preganglionic neurons containing substance P (Murphy, Matthew, Rodgers, Lituri, & Gibbins, 1998). The activation of distinct autonomic neural units could provide a level of control over distinct end organs and vascular beds throughout the periphery allowing the sympathetic nervous system to shunt outflow to one region or even to one specific organ. However, the distinct control of different end organs would depend on the innervation fields of postganglionic neurons. For instance, if innervation fields narrowly project to single organs then autonomic neural units could be organized to preferentially activate one target organ. Alternatively, if innervation fields project widely then a graded response of sympathetic innervation to the abdominal region would be generated based

on the number of the neural units recruited. Distinct control over end organs would then be conferred to unique neuroeffector junctions that would determine the response of each organ throughout the abdomen. However, this assertion has yet to be tested experimentally.

*Prevertebral neurons integrate inputs to regulate sympathetic outflow*

In addition to preganglionic fibers (Langley, 1893), prevertebral ganglia receive and integrate input from spinal sensory fibers (Crowcroft & Szurszewski, 1971), intestinofugal afferent neurons (Kreulen & Szurszewski, 1979), and the vagus nerve (Rosas-Ballina et al., 2008). Subthreshold postsynaptic potentials from each input are summated to regulate sympathetic outflow to end organs (Kreulen, 1984). In the third lumbar sympathetic ganglion, single presynaptic inputs to ganglionic neurons were responsible for the propagation of only 32% of all recorded action potentials (Bratton, Davies, Jänig, & McAllen, 2010). The remaining action potentials were driven by secondary synaptic inputs, indicating that the summation of many ganglion inputs determines sympathetic outflow to end organs. For example, stimulating preganglionic nerves elicited much smaller amplitude excitatory junction potential in MA than stimulating postganglionic nerves (Kreulen, 1986). Ganglia are not simple relays, rather they summate several distinct inputs to regulate sympathetic outflow to target tissues, thereby providing another possible avenue for distinct control of target tissues based on the summation of inputs to each prevertebral neuron.

*Prevertebral neurons are organized according to target organ*

Splanchnic sympathetic efferent fibers are supplied by paravertebral and prevertebral ganglia. The paravertebral ganglia form a bilateral chain on either side of the

spinal cord and supply innervation to the vasculature, kidneys, gastrointestinal tract, pancreas, liver, sweat glands, and spleen (Ferguson, Ryan, & Bell, 1986; Hsieh, Liu, & Chen, 2000; Quinson, Robbins, Clark, & Furness, 2001). Prevertebral ganglia are not organized into a chain and can be found in different locations throughout the abdominal region. The celiac plexus consists of two prevertebral ganglia, the celiac ganglia and superior mesenteric ganglia, and is located along the anterior surface of the aorta just caudal of the celiac artery. A third bilateral pair of prevertebral ganglia lies proximal to the celiac plexus along the GSN called the splanchnic ganglia (SG). The final prevertebral ganglia, the inferior mesenteric ganglia (IMG), lies caudal to the celiac plexus along the inferior mesenteric artery (**Fig. 1.1**). Prevertebral ganglia innervate the kidneys, gastrointestinal tract, pancreas, liver, and spleen (Ferguson et al., 1986; Quinson et al., 2001) and contain a large population of neurons innervating the mesenteric vasculature (Hsieh, Liu, & Chen, 2000). The celiac plexus and SG will be the focus of the present study due to the large number of neurons innervating mesenteric vasculature. Conversely, paravertebral ganglia were not studied, because they supply little sympathetic innervation to the vasculature as compared to the innervation supplied by prevertebral ganglia (Hsieh, Liu, & Chen, 2000).

Infusing unique retrograde tracers onto both arteries and veins in rodents has identified subpopulations of prevertebral neurons that provide dual innervation to MA and MV, while others specifically project to either MA or MV. The IMG of guinea pigs contains separate populations of MA- and MV-projecting neurons (Browning, Zheng, Kreulen, & Travagli, 1999), while a similar study in rats revealed 54% of retrogradely traced neurons projected to arteries and veins, 5% projected exclusively to veins, and 41% projected

exclusively to arteries (Hsieh, Liu, & Chen, 2000). Differences between species or method of infusing tracers may have led to the distinct results between the studies undertaken in guinea pigs and the studies undertaken in rats. Furthermore, the tracers used by Hsieh *et al*., Fast blue and diamidino yellow, are taken up by fibers of passage and such uptake was not prevented so tracers were likely taken up by paravascular nerves resulting in overestimated dual innervation of arteries and veins. However, careful studies in our lab that removed paravascular nerves have confirmed a large population of MA- and MV-projecting neurons with a 39.2% overlap between arterial-projecting and venous-projecting neurons (Shah et al., unpublished data). Interestingly, tracers were only applied to a small 7 mm segment of mesenteric MA and MV, which labeled ~22.5% of CG neurons, suggesting vascular-projecting neurons have multiple collaterals that innervate several segments of mesenteric vasculature.

Determining if vascular-projecting neurons have multiple collaterals that project widely is vastly important for understanding how the sympathetic nervous system exerts control over the splanchnic circulation. To investigate the innervation fields of vascular-projecting neurons, our lab applied separate retrograde tracers to segments of vessels supplying the ileum and jejunum to identify neurons projecting to proximally- and distally-located vascular segments. Tracers were co-localized in 46% and 49% percent of arterial-projecting and venous-projecting neurons respectively (Shah et al., unpublished data). Furthermore, vascular-projecting neurons with large fields of innervation have been established in other species and circulatory systems. Anterograde tract tracing of a single human perivascular nerve fiber revealed significant branching with projections covering an area of up to 4.32 mm of MA (De Fontgalland, Wattchow, Costa, & Brookes, 2008).

More extensive fields are seen in neurons innervating 7 mm portions of cutaneous blood vessels in the guinea pig ear. In the same study, 50-100 neurons were found to innervate the same 1 $mm^2$ portion of vessel (Gibbins, Hoffmann, & Morris, 1998). Indicating that prevertebral neurons could extensively diverge while converging onto small segments of vasculature. Taken together, these results suggest the presence of distinct populations of prevertebral vascular-projecting neurons that project to arteries, veins, or both with each population containing narrowly-projecting or widely-projecting neurons. More sophisticated mapping is necessary to more appropriately characterize artery-projecting and vein-projecting populations and better understand the physiological impacts of narrowly-projecting and widely-projecting vasomotor neurons.

*Development of sympathetic innervation to the vasculature suggests selective innervation patterns*

The development of the sympathetic nervous system provides key insights into the innervation fields of prevertebral neurons in adulthood. Sympathetic neurites travel along vasculature to the parenchyma of end organs by sensing artemin, a guidance cue produced by vascular smooth muscle cells that promotes axonal outgrowth towards target tissues (Baloh et al., 1999; Damon, Teriele, & Marko, 2007; Honma et al., 2002). After reaching the end organ, nerve growth factor (NGF) prompts heterogeneous innervation of the end organs, indicating NGF is not the sole determinate of sympathetic innervation to parenchyma of abdominal organs (Glebova & Ginty, 2004). NGF then promotes the survival of sympathetic neurons with strong synaptic connections (Davies, 1996), those with strong connections secrete BDNF to further strengthen connections, while weak connections are pruned (Singh et al., 2008). This process of innervating viscera is

established by birth (Glebova & Ginty, 2004), however sympathetic fibers do not start innervating vasculature until postnatal day 2 in rodents and is completed in a distal to proximal fashion (Hill, Hirst, & Van Helden, 1983) such that the entire vasculature is not innervated until postnatal day 10 (Brunet et al., 2014). Several guidance cues are important for vascular innervation and include netrin, semaphorin3A, and vascular endothelial growth factor (VEGF). Netrin and VEGF promote axonal outgrowth and innervation of the vasculature, while semaphorin3A repels axons by collapsing the growth cones of advancing neurites (Brunet et al., 2014; Long, Jay, Segal, & Madri, 2009). The combination of guidance cues expressed by vascular tissue has been hypothesized to control the innervation densities of different vascular segments. For example, the carotid artery expresses higher levels of semaphorin3A and is significantly less densely innervated by neurons from superior cervical ganglion explants *in vitro* than are femoral arteries (Long et al., 2009). Therefore, the development of sympathetic innervation to end organs is carefully controlled via a plethora of guidance cues to permit heterogeneous innervation of the abdominal region. Heterogeneous innervation patterns could provide a means for the development of distinct control of abdominal organs based on the density of innervation.

*MA and MV are distinctly controlled by the sympathetic nervous system*

Sympathetic nerves innervate MA and MV via closely associated varicosities, and contract vascular smooth muscle via co-release of adenosine triphosphate (ATP), and NE. Stimulating sympathetic nerves rarely causes single varicosities to secrete transmitters in the vas deferens (Macleod, Lavidis, & Bennett, 1994), However, the number of varicosities releasing neurotransmitters increases with stimulating frequency

(Stjärne & Stjärne, 1995). ATP released from varicosities acts via P2X receptors to transiently increase post junctional $Ca^{2+}$ which mediates a fast contraction of smooth muscle, while NE acts via $\alpha_1$-adrenergic receptors (AR) to propagate $Ca^{2+}$ waves via sarcoplasmic reticulum mediated release of intercellular $Ca^{2+}$ which mediates a slow contraction of smooth muscle (Burnstock, 2009; Gourine, Wood, & Burnstock, 2009; Hottenstein & Kreulen, 1987; Pediani, McGrath, & Wilson, 1999). In addition to different postjunctional actions, ATP and NE are also released from separate populations of synaptic vesicles. Differential prejunctional action of angiotensin II, CGRP, atrial natriuretic peptide, and NE via $\beta$-adrenoceptors on the release of ATP and NE suggests they are packaged into different synaptic vesicles (Burnstock, 2009). ATP and NE are also released in a temporally distinct fashion when stimulating guinea-pig vas deferens. ATP release peaked at 20s, while NE release peaked much later at 30s, which further suggested NE and ATP are stored in separate synaptic vesicles (Todorov, Bjur, & Westfall, 1994). Co-release of ATP and NE provides an avenue to distinctly control different vascular targets because each has distinct mechanisms to contract smooth muscle and they are differentially released by different stores of synaptic vesicles.

ATP and NE are co-released on mesenteric vasculature, but each has a distinct effect on the constriction of MA and MV. ATP constricts MA by activating P2X receptors which is abolished by P2X receptor antagonists, like pyridoxalphosphate-6-azophenyl-2',4'-disulfonic acid (Gitterman & Evans, 2001a; Luo et al., 2003; Park, Galligan, Fink, & Swain, 2009). NE also constricts MA via $\alpha_1$-ARs, but concentration–response curves are left-shifted as compared to MV indicating NE comprises a smaller portion of arterial constrictions (Sporkova, Perez-Rivera, & Galligan, 2010). MV are constricted by both ATP

and NE via P2Y receptors, $\alpha_1$-ARs and $\alpha_2$-ARs respectively (Galligan, Hess, Miller, & Fink, 2001; Park et al., 2009; Sporkova et al., 2010). Although, $\alpha_1$-ARs are the primary mediators of venoconstriction since prazosin (α1-AR antagonist) almost completely abolishes constrictions evoked by stimulating perivascular nerves (Luo et al., 2003; Park et al., 2009). Furthermore, activating $\alpha_2$-ARs with UK 14,304 does not directly constrict MV, but does enhance constrictions evoked by $\alpha_1$-AR (Sporkova et al., 2010). NE also acts prejunctionally to inhibit neurotransmitter release via $\alpha_2$-AR receptors, and this effect is greater in arteries compared to veins (Evans & Surprenant, 1992; Park et al., 2009). Unique compositions of neuroeffector junctions on MA and MV may account for the different thresholds required to constrict arteries and veins via activation of the sympathetic nervous system. For example, stimulating lumbar colonic nerve fibers at lower frequencies (0.5-5 Hz) constricts veins to a greater degree compared to arteries (5-10 Hz; Hottenstein & Kreulen, 1987).. Distinct processing of neurotransmitters at the neuroeffector junction supports the hypothesis that separate sympathetic control over MA and MV arises from separate populations of artery-projecting and vein-projecting neurons (Browning et al., 1999). Alternatively, unique compositions of neuroeffector junctions could also allow sympathetic outflow from neurons dually projecting to arteries and veins, observed in the retrograde tracing studies of rats (Hsieh, Liu, & Chen, 2000), to maintain separate control over each target.

*Selectively activating sympathetic efferents fibers projecting to the splanchnic circulation*

The effects of activating sympathetic neurons projecting to the splanchnic circulation on splanchnic resistance and capacitance are well characterized, but their contribution to systemic arterial pressure is not. Actively increasing splanchnic resistance

and decreasing splanchnic capacitance is accomplished by stimulating the GSN, which is a mixed nerve that transverses through the SG and terminates in the CG. GSN activity proximal to the SG is predominantly preganglionic, because only a 16% decrease in nerve activity is observed during ganglionic blockade with hexamethonium (Sapru, Gonzalez, & Krieger, 1982). Activity in the segment distal to the SG is predominantly postganglionic with hexamethonium reducing nerve activity by 73% (Sapru et al., 1982). These results suggested a significant population of postganglionic fibers originating from the SG comprise endogenous nerve activity in the segment of the GSN distal to the SG. Stimulating the GSN actively decreases splanchnic capacitance and increases splanchnic resistance, in a frequency dependent manner, and elevates systemic arterial pressure, but few studies have characterized these pressor responses (Gootman & Cohen, 1970; Karim & Hainsworth, 1976; Marley & Paton, 1961). In the third chapter of the present study the relative contributions of active capacitance and resistance to the systemic pressor responses evoked by stimulating the GSN will be characterized.

An alternative method to studying rises in systemic arterial pressure mediated by the splanchnic circulation is by activating nicotinic acetylcholine receptors (nAChR) localized on CG neurons (Aceto et al., 1979; Ikushima, Muramatsu, Sakakibara, Yokotani, & Fujiwara, 1982). Intraperitoneal (IP) injections of nicotine elicit rises in systemic arterial pressure, but also activates nAChR on adrenal chromaffin cells stimulating release of NE and epinephrine (Kidokoro, Miyazaki, & Ozawa, 1982). A innovative method to elicit systemic rises in systemic arterial pressure without including the release of NE and epinephrine from the adrenal gland is by directly applying nicotine to prevertebral ganglia. The CG is the ideal prevertebral ganglia to target for topical application of nicotine,

because it contains a large population of vascular-projecting neurons, and is readily accessible through an incision in the abdominal wall (Browning et al., 1999; Hsieh, Liu, & Chen, 2000). Directly applying nicotine to the CG provides an avenue to isolate the relative contributions of splanchnic arteries and veins to rises in systemic arterial pressure.

*The contribution of splanchnic arteries and veins to physiological conditions*

In physiological challenges the splanchnic circulation greatly contributes to the redistribution of blood. Submaximal exercise reduces splanchnic blood flow, while increasing cardiac output, and mean arterial pressure (Perko, Nielsen, Skak, Clemmesen, Schroeder, & Secher, 1998). Increasing sympathetic outflow to the splanchnic circulation is the principle factor determining splanchnic blood flow by constricting splanchnic arteries during exercise (Rowell, Blackmon, Kenny, & Escourrou, 1984). Similarly, constricting splanchnic veins leads to increased venous return and likely accounts for increases in cardiac output during exercise via the Frank-Starling mechanism; thereby, redistributing blood from venous reservoirs in the splanchnic circulation to the arterial circulation. Exercise is an example of a physiological condition where both MA and MV contribute to the redistribution of blood from the splanchnic circulation and illustrates the ability of splanchnic efferent neurons to simultaneously constrict splanchnic arteries and veins.

Splanchnic efferents can also preferentially requisition blood from splanchnic veins to prevent tissue ischemia during hemorrhage. The splanchnic circulation contributes 66% of total blood lost during hemorrhage of 15% total blood volume (Greenway & Lister, 1974). Vasoconstriction of splanchnic veins leads to a decrease in splanchnic blood volume, without significant changes in cardiac output, heart rate, arterial pressure,

splanchnic resistance, splanchnic blood flow, or central blood volume (Price et al., 1966; Reilly, Wilkins, Fuh, Haglund, & Bulkley, 2001; Toung, Reilly, Fuh, Ferris, & Bulkley, 2000). The hemodynamic response to hemorrhage is, in part, mediated by the sympathetic nervous system with bilateral splanchnicectomy reducing the volume of splanchnic blood mobilized by 32% (Brooksby & Donald, 1972). Abolishing the sympathetic response to hemorrhage by removing vagal afferents in the cardiopulmonary area suggests constriction of splanchnic veins is mediated by activating baroreceptors (Pelletier, Edis, & Shepherd, 1971; Shen, Knight, Thomas, & Vatner, 1990). These studies suggest splanchnic veins but not arteries are constricted during hemorrhage and is evidence of differential control over splanchnic veins and arteries during activation of the sympathetic nervous system. Separate innervation of arteries and veins is one possible explanation (Browning et al., 1999) for preferentially constricting veins during hemorrhage. Blood in the splanchnic circulation is differentially distributed during physiological challenges like hemorrhage or septic shock. However, blood is not uniformly distributed throughout the splanchnic circulation. Rather, it is thought to be redistributed from tissues with low oxygen demand to tissues with high oxygen demand (Krejci et al., 2000). Evidence of this phenomenon arises from observing intestinal segments after 3 hours of ischemia with the mucosa layer incurring marked necrosis without any observable necrosis in the muscularis layer (Granger, Kvietys, & Korthuis, 2011), suggesting the mucosa is more susceptible to ischemia because it requires more oxygen. Stimulating splanchnic nerves decreases blood flow in the mucosa layer to 49% of baseline, and in the muscularis layer to 9% of baseline (Shepherd & Riedel, 1988), and $\alpha$-adrenergic blockade significantly reduced oxygen extraction by the intestine from 77 ±

7% to 69 ± 6% (Samsel & Schumacker, 1994). Taken together, these results suggest splanchnic sympathetic efferents are important from redistributing blood within the splanchnic circulation based on tissue–specific oxygen demands.

Blood flow is also heterogeneously distributed between abdominal organs as exemplified by the pancreas, where blood flow is decreased to a greater degree than other regions during hemorrhage (Krejci et al., 2000; Robert, Toledano, Toth, Premus, & Dreiling, 1988). Furthermore, microcirculatory blood flow to jejunal mucosa is increased when compared to regional blood flow, but significantly reduced to the pancreas during septic shock (Krejci et al., 2000; Lundgren & Svanvik, 1973; Raper, Sibbald, Hobson, & Rutledge, 1991). Therefore, distribution of blood flow to abdominal viscera is heterogeneous during hemorrhagic and septic shock with the sympathetic nervous system working in concert with local factors to shunt blood from one vascular component to another.

The splanchnic circulation undergoes regional hyperemia during digestion, suggesting regional control over the diameter of MA. The intestinal segment containing chyme experiences increased blood flow, while there is no change in the rest of the intestinal segments (Chou, 1983; Gallavan & Chou, 1985; Gallavan, Chou, Kvietys, & Sit, 1980; Granger et al., 2011). Several mechanisms are hypothesized to account for regional hyperemia, including metabolic–, humoral–, paracrine–, and neural–based mechanisms (Gallavan & Chou, 1985; Matheson, Wilson, & Garrison, 2000). Neural mechanisms play an essential role in controlling the diameter of mesenteric vasculature via sympathetic innervation and peripherally mediated reflexes (Pucovský, Gordienko, & Bolton, 2002). One such peripheral reflex is activating primary sensory neurons via

colonic distension to vasodilate MA via release of nitric oxide and CGRP (Holzer, 1992; Zheng, Shimamura, Anthony, Travagli, & Kreulen, 1998), and veins via endothelium–dependent release of nitric oxide (Ahluwalia & Vallance, 1997). Peripheral reflexes may contribute to regional hyperemia present during digestion by vasodilating large mesenteric feed arteries. Coincidentally, hyperemia causes arterial pressure to fail and is restored via sympathetically mediated increases in cardiac output (van Baak, 2008). Although, no reports determine if elevated cardiac output is influenced by increasing splanchnic sympathetic activity. Increased blood flow in spite of increased sympathetic activity during digestion suggests interplay between the sympathetic nervous system and sensory–based peripheral reflexes to control the diameter of mesenteric vasculature in a regional manner.

The data summarized above indicates activating the sympathetic nervous system differentially recruits vascular targets based on different physiological stimuli, and abdominal sympathetic innervation would need to be organized in a fashion to facilitate multiple hemodynamic states. The discovery of widely–projecting, and narrowly–projecting prevertebral neurons by retrograde tracing studies (Shah et al., unpublished data) suggests the ability of sympathetic efferent fibers to be organized in a regional manner to heterogeneously regulate blood flow. Neurons projecting widely to the entirety of the splanchnic circulation would modulate physiological responses, like exercise, which require recruitment of the entire splanchnic region. Neurons projecting regionally to small portions of the splanchnic vascular bed would be activated in physiological states that require shunting blood from one region to another, like postprandial hyperemia. Therefore, I hypothesize innervation to splanchnic vasculature is tightly organized into

subsets of regionally–projecting and widely–projecting neurons that interact with local factors and peripheral reflexes to carry out a diverse array of hemodynamic responses to satisfy physiological needs.

*rAAVs will be used to transduce prevertebral neurons*

rAAVs consist of a virion shell (capsid), and a single-stranded DNA genome the latter encodes proteins important for integration into the host genome, expression of target genes, and structural proteins that form the capsid. Many different serotypes of rAAV exist and tissue tropism varies widely between serotypes because of interaction with cell receptors, uptake of the virus, intracellular processing, and delivery of the genome to the nucleus (Wu, Asokan, & Samulski, 2006). For example, the best characterized serotype rAAV2, stably transduces the substantia nigra, but often fails to produce robust gene-transfer in dorsal root ganglia as compared to other serotypes (Klein et al., 1998; Mason et al., 2010). Tissue-specific tropisms can also determine the time course of viral transductions, for example, in portal vein injections of rAAV, capsid serotype 2 took 6 to 8 weeks to reach maximal expression in the liver, while capsid serotype6 and 8 took only 4 weeks to reach maximal transgene expression (Thomas, Storm, Huang, & Kay, 2004). Similarly, maximal transgene expression was seen at 4 weeks post injection of rAAV6 into dorsal root ganglion (Glatzel et al., 2000). The wealth of research detailing tissue specific tropisms of neural targets has been undertaken in the CNS, with few viral tropisms of peripheral ganglia being described (Glatzel et al., 2000; Mason et al., 2010). An aim of the current study is to test several serotypes of rAAV to elucidate the viral tropisms of prevertebral ganglia to produce stable, long–lasting, transductions of sympathetic neurons.

rAAVs have been used for many different applications throughout the nervous system; mainly, to map anatomical pathways, and to manipulate gene expression (Chamberlin, Du, de Lacalle, & Saper, 1998; Kaplitt et al., 1994; Peel, Zolotukhin, Schrimsher, Muzyczka, & Reier, 1997; Ruitenberg, Eggers, Boer, & Verhaagen, 2002). Anterograde viral mapping is used throughout the CNS, but no reports of mapping peripheral anatomical pathways exist. When used to map anatomical pathways rAAVs can be injected at nerve terminals, undergoing receptor-mediated endocytosis, subsequently undergoing retrograde transport to the cell body, and translocation to the nucleus, or rAAVs can be injected near the cell body, gaining access to the host cell via receptor-mediated endocytosis. Once the virus transduces the host cell, a marker of choice is expressed (mostly GFP) and transported throughout the processes of the cell (Chamberlin et al., 1998; Foust, Poirier, Pacak, Mandel, & Flotte, 2007; Kaspar, Lladó, Sherkat, Rothstein, & Gage, 2003; Zheng et al., 2009). Therefore, rAAVs can be used to anterogradely map anatomical pathways by way of target organ, by direct application of rAAV to the nerve terminals innervating the organ of interest. I will use rAAV to map the anatomical pathways of vascular-projecting neurons in the abdominal region by selectively applying rAAV to the mesenteric vasculature.

*Dβ-sap will be used to ablate prevertebral neurons projecting to splanchnic vasculature*

Conjugated neurotoxins have been used to create targeted lesions of neurons throughout the nervous system. A particular conjugated neurotoxin of interest is anti-dopamine-beta-hydroxylase (DβH) conjugated to saporin (DβH-sap). Anti-DβH is an antibody against DβH, an enzyme that catalyzes the production of NE from dopamine, that recognizes DβH when it is presented to the synaptic cleft during release of NE from

synaptic vesicles (Jacobowitz, Ziegler, & Thomas, 1975). Uptake of anti-DβH is relatively quick and can be detected in submaxillary gland nerve fibers as early as 15 min after intravenous injection (Jacobowitz, Ziegler, & Thomas, 1975). After uptake into nerve terminals anti-DβH is retrogradely transported to the cell body at a rate of 2 mm/h (Jacobowitz, Ziegler, & Thomas, 1975). Unconjugated saporin is a potent ribosome inactivating neurotoxin that is not readily taken up by eukaryotic cells (Ziegler, Thomas, & Jacobowitz, 1976); therefore, saporin is traditionally conjugated to a compound that will grant it access to neurons, in this case anti-DβH. The time course for saporin mediated cell death occurs over a period of days, saporin applied to L540 Hodgkin's lymphoma cells induced mechanisms of cell death by activating caspase-8 and -9 as early as 4 hours and ablating 50% of cells within 14.4 hours after exposure (Polito et al., 2008).

DβH-sap has been used sparingly to study the peripheral nervous system (PNS). The most extensive research has been done after intravenous injection of DβH-sap. The dose response curve done in this study revealed a critical threshold of 87.5 μg/kg DβH-sap injected intravenously started to show significant neuronal cell death in the superior cervical ganglia (Picklo, Wiley, Lonce, Lappi, & Robertson, 1995). Other studies have focused on IP injection of 15 μg DβH-sap, which produced significant lesion of the duodenum and spleen without affecting sympathetic innervation to the heart (Worlicek et al., 2010). These studies have shown DβH-sap can be used to non-selectively destroy ganglionic neurons projecting to the abdominal region, but has yet to be utilized to selectively destroy neurons projecting to specific targets throughout the abdomen. DβH-sap could be used to selectively destroy vascular-projecting neurons by isolating the saporin conjugate to the mesenteric vasculature, where DβH-sap will be taken up by

vascular-projecting sympathetic neurons and subsequently target them for cell death. Since MA and MV receives distinct sympathetic innervation (Browning et al., 1999) further specificity can be achieved by applying DβH-sap to arteries or veins. In chapter four, producing a specific lesion of mesenteric vascular-projecting neurons will be examined by applying DβH-sap directly to the MA, MV, or both.

**Research Aim**

Prevertebral neurons are the final common pathway of the sympathetic nervous system to splanchnic viscera and vasculature, but the innervation fields of prevertebral neurons are unknown. Discerning innervation fields of prevertebral neurons is of great importance to understanding the impacts of sympathetic innervation to the splanchnic circulation. Therefore it is the aim of the present study to 1) elucidate the innervation fields of prevertebral neurons; 2) investigate methods to activate prevertebral neurons projecting to the splanchnic circulation; 3) investigate the impact of vascular-projecting neurons on the splanchnic circulation by targeting them for cell death.

**Specific Aims and Hypotheses**

**Guiding hypothesis: Ablating artery- or vein-projecting prevertebral neurons will reduce, but not abolish systemic pressor responses to activating splanchnic sympathetic efferents.**

**Specific Aim 1: Injecting rAAV into the CG or applying rAAV to the mesenteric vasculature will transduce CG neurons.** I will determine the best serotype to express GFP using pan neuronal promoters by directly injecting rAAV into the CG. I will also elucidate a method to anterogradely trace innervation fields of vascular-projecting

neurons by applying rAAV to the MA and MV. I hypothesize that direct injection of rAAV will express GFP at four weeks post-injection, and application of rAAV to the mesenteric vasculature will transduce prevertebral neurons innervating the mesenteric vasculature.

**Specific Aim 2: Stimulating prevertebral neurons will elicit responses in systemic arterial pressure and both splanchnic arteries and veins will contribute to the pressor responses.** I will characterize two different methods of stimulating prevertebral neurons, either by direct application of nicotine to the CG, or stimulation of the GSN. I will also investigate the contribution of splanchnic arteries and veins to the pressor response by using pharmacological agents. I hypothesize that both methods will increase systemic arterial pressure by 5-10 mmHg and that arteries and veins both contribute to increases in systemic arterial pressure.

**Specific Aim 3: Chemical ablation of MA- and MV-projecting neurons will reduce systemic arterial pressure responses to stimulating the GSN.** I will chemically ablate artery-projecting and vein-projecting neurons in the prevertebral ganglia with DβH-sap to measure their role in arterial pressure regulation. The effects of ablating artery-projecting and vein-projecting neurons on the control of systemic blood pressure will be evaluated *in vivo* by stimulating the GSN in anesthetized Sprague Dawley rats. I hypothesize ablation of artery-projecting and vein-projecting neurons will attenuate rises in systemic arterial pressure to stimulating the GSN by blocking sympathetic outflow to the mesenteric vasculature.

## Figures

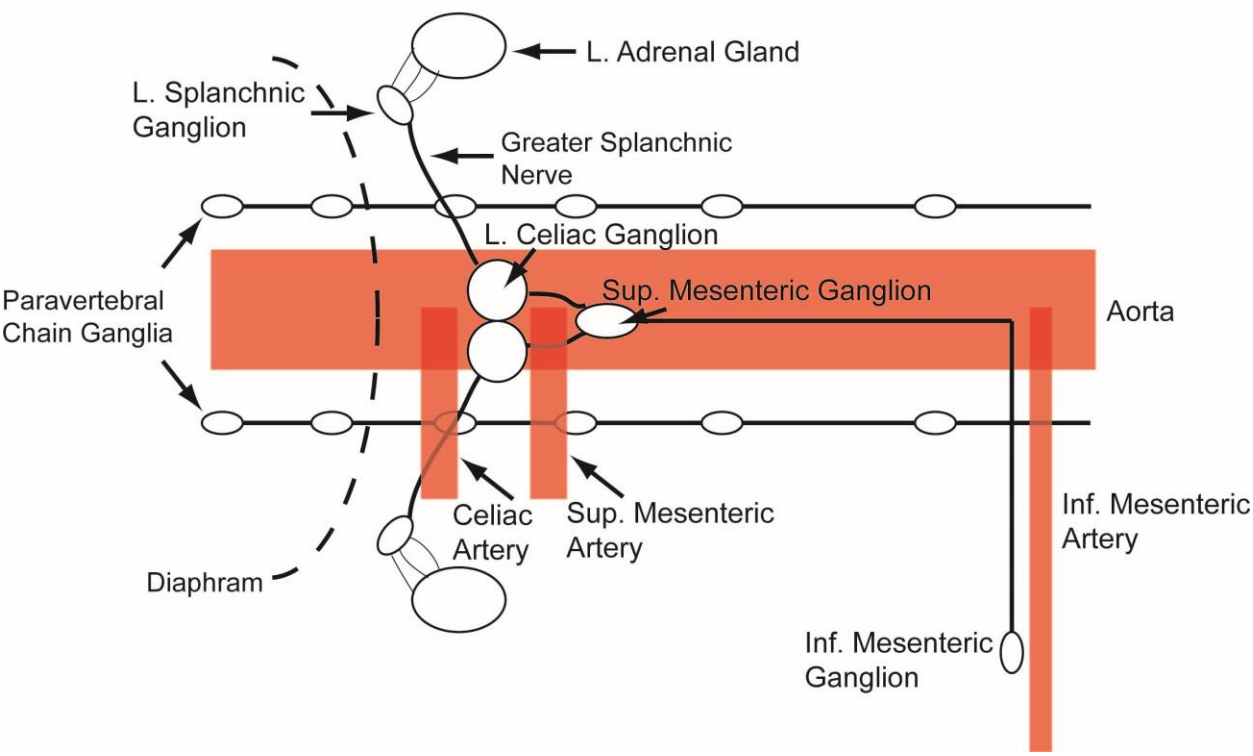


**Figure 1.1: Anatomical locations of para- and pre-vertebral ganglia.** Diagram of para- and pre-vertebral ganglia from a rat. The CG and SG are the focus of the present study and are bilateral structures that can be found in proximity to the celiac artery. Abbreviations in this figure are as followed: L. = left, Sup. = superior, and Inf. = inferior.

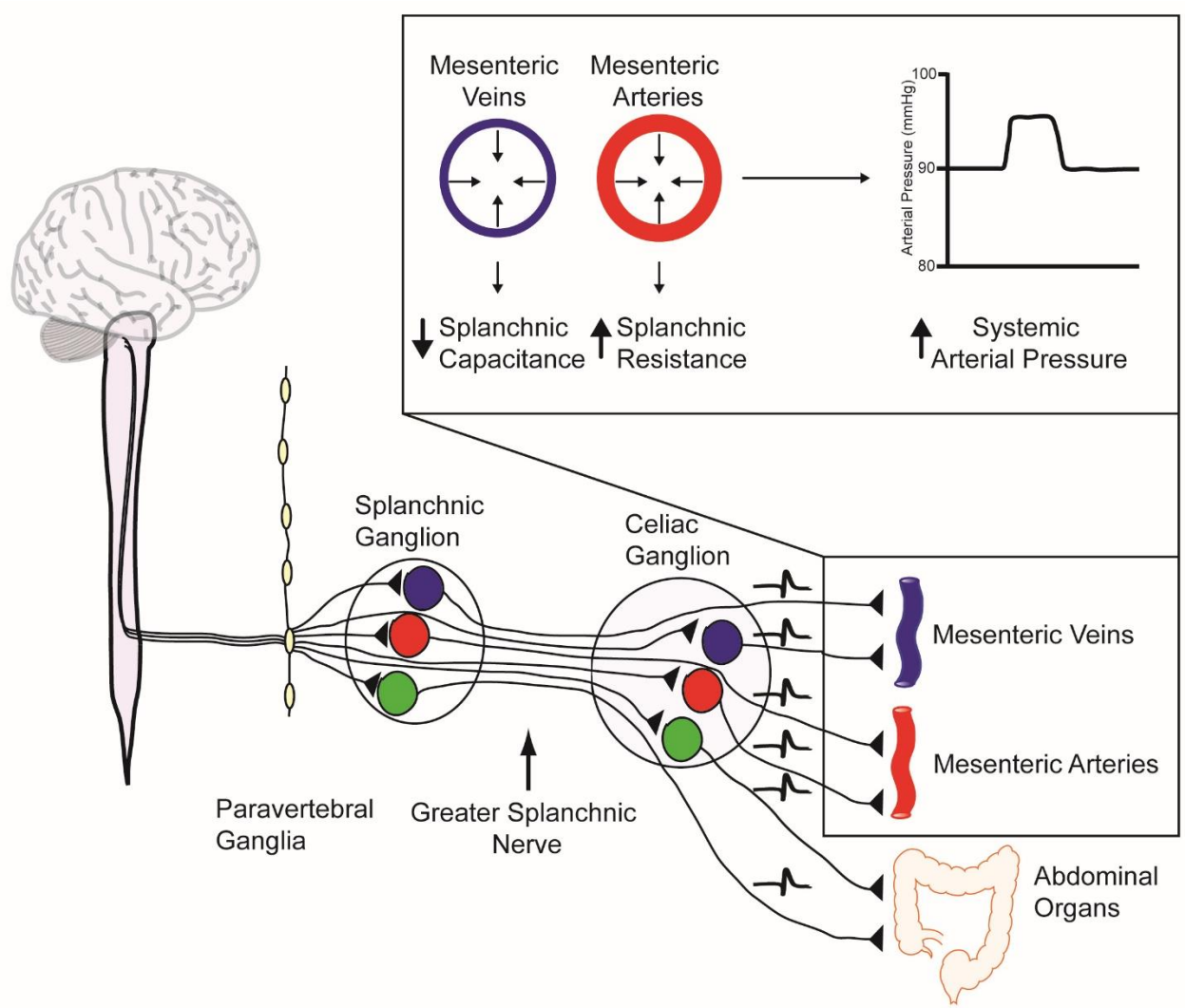


**Figure 1.2: Diagrammatic representation of distinct pathways in prevertebral ganglia.** Prevertebral neurons are organized according to target. Vascular–projecting neurons control splanchnic resistance and capacitance via vasoconstriction of MA and MV. Increased splanchnic resistance and decreased splanchnic capacitance both contribute to increases in systemic arterial pressure.

# CHAPTER TWO: GENE THERAPY OF PREVERTEBRAL GANGLIA

**Abstract**

Gene therapy has played an integral role in advancing our understanding of the central nervous system. However, gene therapy techniques have yet to be widely utilized in the peripheral nervous system. Critical targets for gene therapy within the peripheral nervous system are neurons in sympathetic ganglia, which are the final pathway to end organs. Thus they are the most specific targets for organ-specific neuron modification. This presents challenges because neurons are not viscerotopically organized within the ganglia and therefore cannot be targeted by their location. However, organ-specific neurons have been identified in sympathetic ganglia this offers an opportunity for targeting and transducing neurons by way of their target. In fact, alterations in sympathetic neurons have had pathological effects, and transducing organ-specific sympathetic neurons offers an exciting opportunity to selectively modify sympathetic pathology. In this paper, we describe two methods to virally transduce the celiac ganglion with recombinant adeno–associated virus serotypes 1, 2, 5, 6, and 9; thereby, providing potential avenues to modulate subset specific neurons within the celiac ganglion.

## Introduction

Recombinant adeno-associated viruses (rAAV) produce efficient, long-lasting, and non-toxic transductions; thus, making rAAVs an ideal vector for gene therapy (Blacklow et al., 1971; Kaplitt et al., 1994). Transductions using rAAVs have been used to map anatomical pathways, and drive transgene expression in a variety of regions throughout the central nervous system (Kaplitt et al., 1994; Peel et al., 1997; Ruitenberg et al., 2002; Yamamoto, Goto, Nakai, Ogino, & Ikeda, 1983). However, few have utilized gene therapy to modulate regions in the peripheral nervous system (PNS; Glatzel et al., 2000; Mason et al., 2010). PNS gene therapy would give way to a host of investigations including manipulation of target genes, utilizing optogenetics to modulate subsets of PNS cell types and anterior tracing of PNS neurons. The results of these investigations would provide insight into various avenues of research including: gene function in disease states, function of various cell types throughout the PNS, and innervation patterns of PNS neurons. An unexplored target for gene therapy in the PNS is the celiac ganglion (CG), an important source of innervation to a variety of abdominal organs that are critical for survival. While sympathetic neurons within the CG are not spatially organized, organ-specific neurons have been identified using retrograde tracers (Browning et al., 1999; Hsieh, Liu, & Chen, 2000). Furthermore, there is evidence that neurons are chemically-coded according to their targets (Macrae, Furness, & Costa, 1986; Quinson et al., 2001), which suggests that neurochemical-specific promoters could be used genetically modify neurons based on their target. In the abdomen, CG neurons modulate organ blood flow via the degree of vasoconstriction of arteries and veins; larger recruitment of these vascular neurons contributes to the elevated blood pressure and if it is chronic, neurogenic hypertension (Fink, Johnson, & Galligan, 2000; Foss, Fink, & Osborn, 2013;

Kandlikar & Fink, 2011). While we are learning more about the organization of macroscopic anatomy of the prevertebral ganglia, little is known about the innervation fields of mesenteric vascular-projecting neurons or the specific physiologic consequences of gain or loss of function of selected subsets of neurons within the CG. Gene therapy techniques have the potential to resolve the physiological implications of organ-specific neurons seen in the CG. Until now, little research has investigated virally transducing the CG. Here, we demonstrate viral transduction of the CG either by direct CG injections or application of rAAV to the mesenteric vasculature.

## Materials and Methods

*Animals*

For all protocols involving animals, male Sprague-Dawley rats weighing 225g-400g were used. During viral exposure animals were housed two per cage in a temperature- and humidity-controlled biosafety level 2 facility with a 12-hour light/dark cycle unless noted below. All animals had *ad libitum* access to standard rat chow and water for the duration of this protocol. All protocols involving the use of animals were approved by Michigan State University's Institutional Animal Care and Use Committee.

*Viral transduction of PC12 cells*

PC12 cell lines were thawed from storage in liquid nitrogen, re-suspended in RPMI medium (Gibco) supplemented with penicillin-streptomycin (Gibco), fungizone amphotericin B (Gibco), horse serum (Gibco), fetal bovine serum (Gibco), and plated on 100mmx20mm culture dishes (Corning) coated with collagen from rat tail (Gibco). When cultures reached 90% confluence, the cells were split onto collagen coated glass bottom dishes (MatTek) using 0.05% Trypsin to detach the cells from the culture dish. Cells were plated on glass bottom dishes and exposed to nerve growth factor (Chemicon). After PC12 were differentiated, $1\times10^{10}$ GC/ml rAAV-1, 2, 5, and 6 for one hour. 5 days after transduction, cell cultures were fixed with 4% paraformeldyhe for 30mins, washed with TPBS and coverslipped with ProLong Gold Antifade and stored at 4ºC until image acquisition.

*Direct injections of the CG*

Animals were anesthetized with isoflurane (3%-4% during induction, 2% during surgery) in $0_2$ (0.75 l/min). Then a laparotomy was performed, the abdominal viscera were

retracted to reveal the CG and kept moist by draping the exposed tissue with sterile gauze soaked in hanks' balanced salt solution (HBSS). After the CG was located, excess connective tissue surrounding the CG was removed. A pulled glass micropipette attached to a picospritzer and filled with a mixture of 1 µl rAAV (Vector Biolabs, rAAV Testing Kit, cytomegalovirus (CMV) promoter driving expression of green florescent protein [GFP]), with titers ranging from $6.6\times10^{8}$ to $1\times10^{13}$ cg/ml, and 0.1 µl of 5mM fast green was advanced to a depth of 400 µm into CG via a micromanipulator. The glass micropipette was allowed to make a seal with the CG by waiting two minutes before injecting 25% of the viral mixture into the CG by activating the picospritzer as many times as needed. After 5 minutes, the glass micropipette was withdrawn and repositioned to a different location distant from the first injection site. This process was repeated until the total 1.1 µl volume was injected using four different injection sites. After completing injections the gut retractor was removed, the abdominal viscera were replaced, and the incision was closed. Animals were given antibiotics prior to the surgery (Baytril [5mg/kg]) and analgesic for three days post-surgery (Carprofen [5mg/kg]). Animals were housed for four weeks until viral expression was confirmed using immunohistochemistry.

*Application of rAAV to the mesenteric vasculature*

Animals were anesthetized with isoflurane (2%-3% during induction and surgery, 2% after surgical preparation) in 02 (0.75 l/min). Laparotomy was performed and the intestines revealed. Adjacently located secondary branches of superior mesenteric artery and vein 7 mm in length were secured with Hanks' balanced salt solution (HBSS, Gibco) soaked gauze onto a Plexiglas platform lined with Sylgard (Dow Inc.), cleared of surrounding fat, separated from each other, and encased in silicone tubing. During this

time, the blood vessels and surrounding tissues in the Plexiglas platform were constantly bathed with HBSS. Both ends of the silicone tubing were sealed with silicone sealant (Dow Inc.), small strips of sterile, absorbable, gelatin sponge (Gelfoam, Pharmacia and Upjohn Co.) were applied to the top of the blood vessels, and either 5 μl of rAAV1,6, or 9 were applied to the mesenteric artery (MA) and mesenteric vein (MV) with micropipettes pretreated with sigmacote (Sigma-Aldrich). After a one hour incubation, rAAVs were pipetted off of the mesenteric vasculature, the excised portion of gut was washed with HBSS, returned to the abdominal cavity, the abdominal incision sutured, and the rat recovered for 28-45 days. The animal was given antibiotic (Baytril [5mg/kg]) prior to surgical intervention and analgesic (Carprofen [5mg/kg]) for three days post-intervention. rAAVs used in this experiment were a kind gift from Dr. Manfredsson at the Van Andel Institute with viral titers ranging from $2X10^{12}$ to $6X10^{12}$ GC/ml. Each serotype uses a cytomegalovirus (CMV) promoter to drive expression of GFP.

*Tissue processing*

Four weeks after direct injection of rAAV into the CG, after rat were anesthetized with sodium pentobarbital (50 mg/kg, intraperitoneal) the heart was cut, the CG was harvested and submerged in 4% paraformaldehyde. Ganglionic tissue was post-fixed for one day at 4ºC, transferred to 30% sucrose for one day, and frozen at -80ºC in Tissue-Tek O.C.T. (Sakura). The CGs were cryostat sectioned [14-16 μm; Bright Model OTF cryostat (Hacker Instruments Inc.)] in a single series onto Superfrost plus micro slides.

Thirty eight or forty five days after mesenteric application of rAAV the CG was harvested and processed as described above with the following exceptions. Animals were perfusion fixed with 4% paraformaldehyde before any tissue was harvested, additionally,

ganglionic tissue was cut in a series of four instead of a single series. All of the mesenteric vasculature complete with the superior mesenteric artery and vein were harvested and post-fixed in 4% paraformaldehyde for three days at 4ºC, and then transferred to 70% EtOH until the vessels were processed for immunohistochemistry.

Location of the mesenteric vessels was cataloged and then mesenteric vessels were stripped of fat, and placed into a 1.5 ml eppendorf tube. Only segments from the 38-39 day group were washed 3×5mins in Tris buffered saline (TPBS), blocked with 10% NGS (30 mins), incubated with rabbit anti-GFP antibody (1:5,000, 1 day, Abcam), diluted in 10% NGS. Washed three times with TPBS and then incubated with goat-anti rabbit CY5 secondary antibody (1:100, 2 hrs, Jackson ImmunoResearch) diluted in 1% NGS. All vessels from the 38 and 45 day groups were coverslipped with ProLong Gold Antifade (Life Technologies) and stored at 4ºC until image acquisition.

The mesentery from the 38-39 day group was stored in 70% EtOH at 4°C for several weeks prior to immunohistochemical processing, which may have purged the GFP signal from the tissue. The experiment was repeated with a longer time course of 45 days to account for retrograde transport of the virus and anterograde transport of GFP. This group of animals was unknowingly subjected to constant light for an unknown period of time that did not exceed two weeks, which may have contributed to no transduction of mesenteric vascular-projecting neurons. Furthermore, the level of experimental difficulty could have resulted in any number of surgical errors to prevent successful uptake of the virus. For example, the vasculature proximal to the labeling apparatus could have dried out due to prolonged exposure to the environment, causing subsequent damage of axons and preventing retrograde transport of the virus

*Image acquisition*

PC12 cells were imaged on a (Nikon Eclipse TE200) with a 10x objective. A SPOT digital camera (Diagnostic Instruments, HRD06-NIK) with SPOT Advanced software was used to acquire digital micrographs. All cells were 90% confluent at the time of image acquisition. Sections of CG were visualized on an Axio Imager D1/D2 (Zeiss), with a 20x objective and AxioCamMR3 camera with Zen software, or on an inverted microscope with a MicroFIRE color camera (Optronics, Inc) and a 20x objective. Image Pro Plus (Media Cybernetics) software was used to acquire digital micrographs. Mesenteric vessels were visualized on a confocal microscope (Olympus Fluoview-F1000 confocal microscope) with a 20x objective. Photomultiplier tube voltage was optimized before collecting each series of z-stack images. Images were then processed by performing a max intensity projection of the images using FV10-ASW 3.1 viewer software (Olympus).

## Results

*In vitro infection of PC12 cells*

Tropisms of PC12 cells were investigated, because they have properties that closely resemble sympathetic neurons. PC12 cells expressing GFP varied greatly, five days after a one-hour exposure to four different serotypes of rAAVs (**Fig. 2.1**). Serotype 6 had the highest rate of GFP expression in PC-12 cells while rAAV serotype 1 and 5 had a comparable, but a lower expression profile. Serotype 2 had the lowest rate of transduction.

*In vivo transduction of the CG*

Based on the *in vitro* transduction of PC12 cells, serotypes 1 and 6 were selected for injection into the CG. The quality of the injection was tracked using fast green; based on the appearance of dye outside the ganglia, the virus diffused from the injection site during most injection procedures (**Fig. 2.2**). Transduction with rAAV6 was dependent on viral titer (**Fig 2.3**). No expression of GFP was observed in the CG of animal's receiving a titer less than $1x10^{10}$ GC/ml. Titers of $1x10^{10}$ GC/ml had rates of transduction similar to those ganglia treated with titers of $1x10^{13}$ GC/ml. Transduction with rAAV1 produced lower observable GFP expression in the CG as compared to those animals transduced with rAAV6. No noticeable adverse effects on the health of CG neurons or of the animal were observed at any point during the course of these experiments.

*In vivo transduction of mesenteric vascular-projecting prevertebral neurons*

The innervation patterns of vascular-projecting sympathetic neurons were examined by exposing mesenteric arteries and veins to rAAV for one hour. Thirty eight or thirty nine days after exposure of rAAV1 and rAAV6 to the mesenteric vasculature, GFP

expression was observed in the CG but not in the neuronal processes innervating the mesenteric vasculature (**Fig 2.4**). Mesenteric vessels harvested from these animals examined with confocal microscopy had no detectable GFP expression in the animals transduced with either rAAV1 or rAAV6. The experiment to produce an *in vivo* transduction of mesenteric vascular-projecting prevertebral neurons was repeated with a longer time course of 45 days to allow sufficient time for GFP to anterogradely fill neurites innervating the mesenteric vasculature. No GFP expression was observed in animals receiving rAAV6 or rAAV9 in neuronal cells bodies in the CG or in neurites innervating MA or MV (**Fig 2.5**).

## Figures

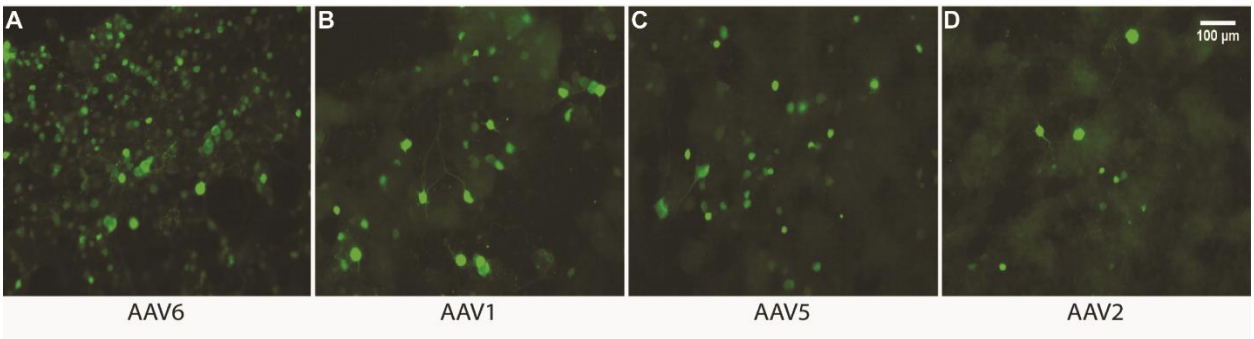


**Figure 2.1 Expression of GFP using different serotypes of rAVV in differentiated PC12 cells.** All serotypes express GFP driven by a CMV promoter. Different serotypes of rAAV were tested at a concentration of 1X $10^{10}$ GC/ml at an exposure time of 1 hour, followed by a 5 day expression period. All cultures were 90% confluent at the time of image acquisition. rAAV6 (**A**) had the highest infection rate, while rAAV2 (**D**) infected the least amount of cells. rAAV1 (**B**) and rAAV5 (**C**) had comparable expression, but did not reach the high levels of expression seen by rAAV6. Therefore, rAAV6 is the most efficient serotype when transducing differentiated PC12 cells.

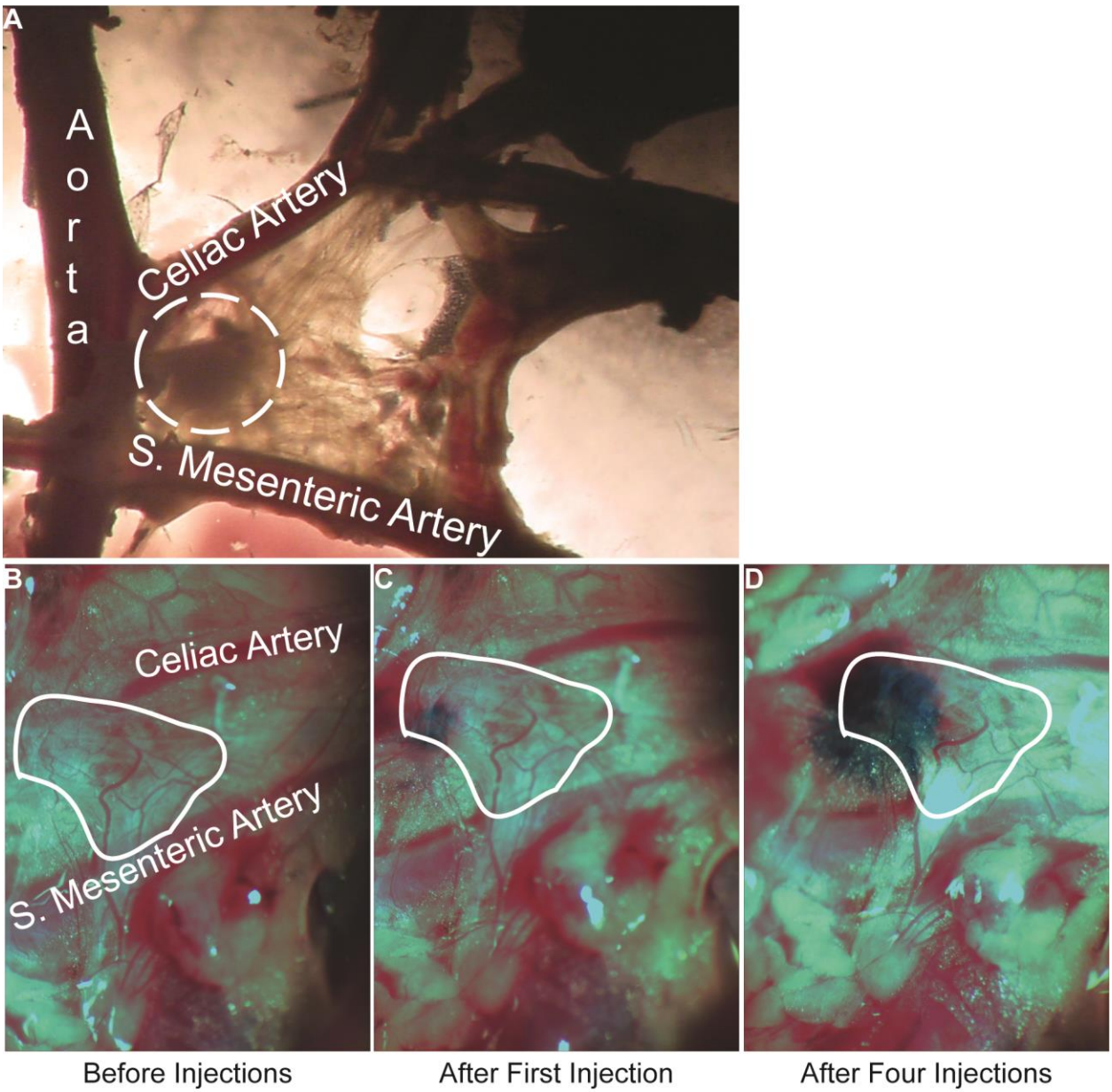


**Figure 2.2 Locating the CG *in vivo* and tracking microinjections with fast green.** An *ex vivo* image of the CG under a dissecting microscope after being cleared of connective tissue and fat. The CG is encircled by a dashed white line (**A**). *In vivo* images of the CG prior to rAAV injection (**B**), after the first injection (**C**), and after delivery of the entire viral load over several four injection sites (**D**). The CG is outlined by a white line.

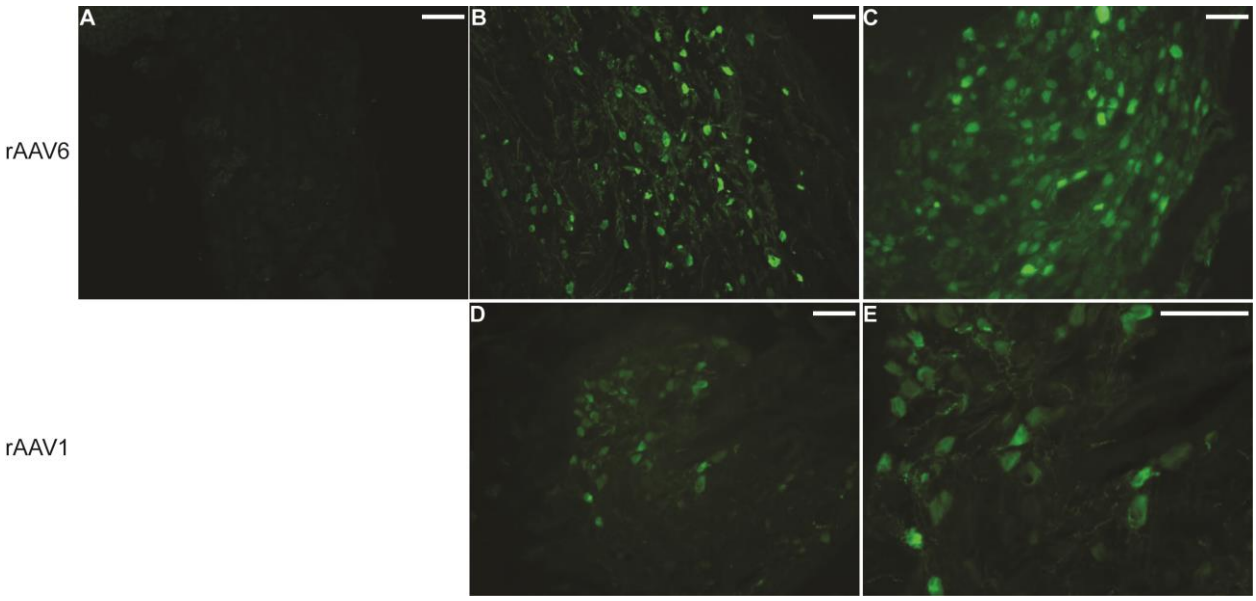


**Figure 2.3 Expression of GFP in the CG four weeks after direct injection of rAAV is dependent on titer and serotype.** Transduction of the CG with $6.6x10^{8}$ GC/ml (**A**), $1x10^{10}$ GC/ml (**B**), or $1x10^{13}$ GC/ml rAAV6 (**C**) demonstrates the effect of titer on observable GFP expression. Transduction of the CG with $1x10^{13}$GC/ml rAAV1 revealed expression of GFP in the CG four weeks post injection (**E**). A higher magnification of panel (**E**) reveals GFP expression in both the cell body and neurites of CG neurons (**F**). Photomicrographs were taken with a 10x or 20x objective and all scale bars represent 100 μm.

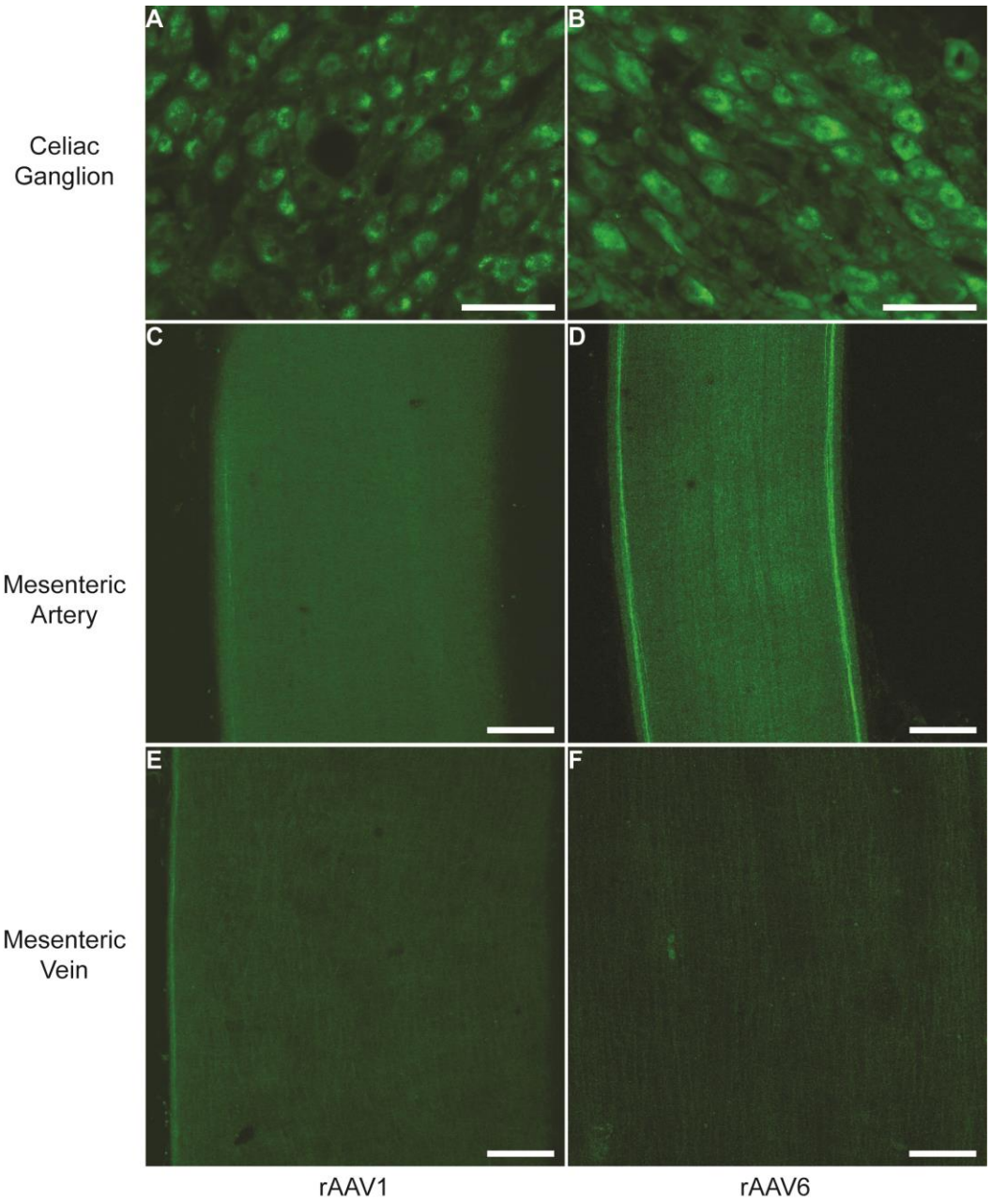


**Figure 2.4 GFP is expressed in the cell bodies, but not in the processes of neurons in the CG 38-39 days after rAAV application to the mesenteric vasculature.** Expression of GFP was present in the cell bodies of CG neurons 38-39 days after mesenteric application of rAAV1 (**A**) or rAAV6 (**B**). No GFP expression was present in perivascular nerves innervating MA (**C,D**) or MV (**E,F**) of animals treated with rAAV1 (**C, E**), or rAAV6 (**D, F**). All photomicrographs were taken with a 20x objective and all scale bars represent 100 μm.

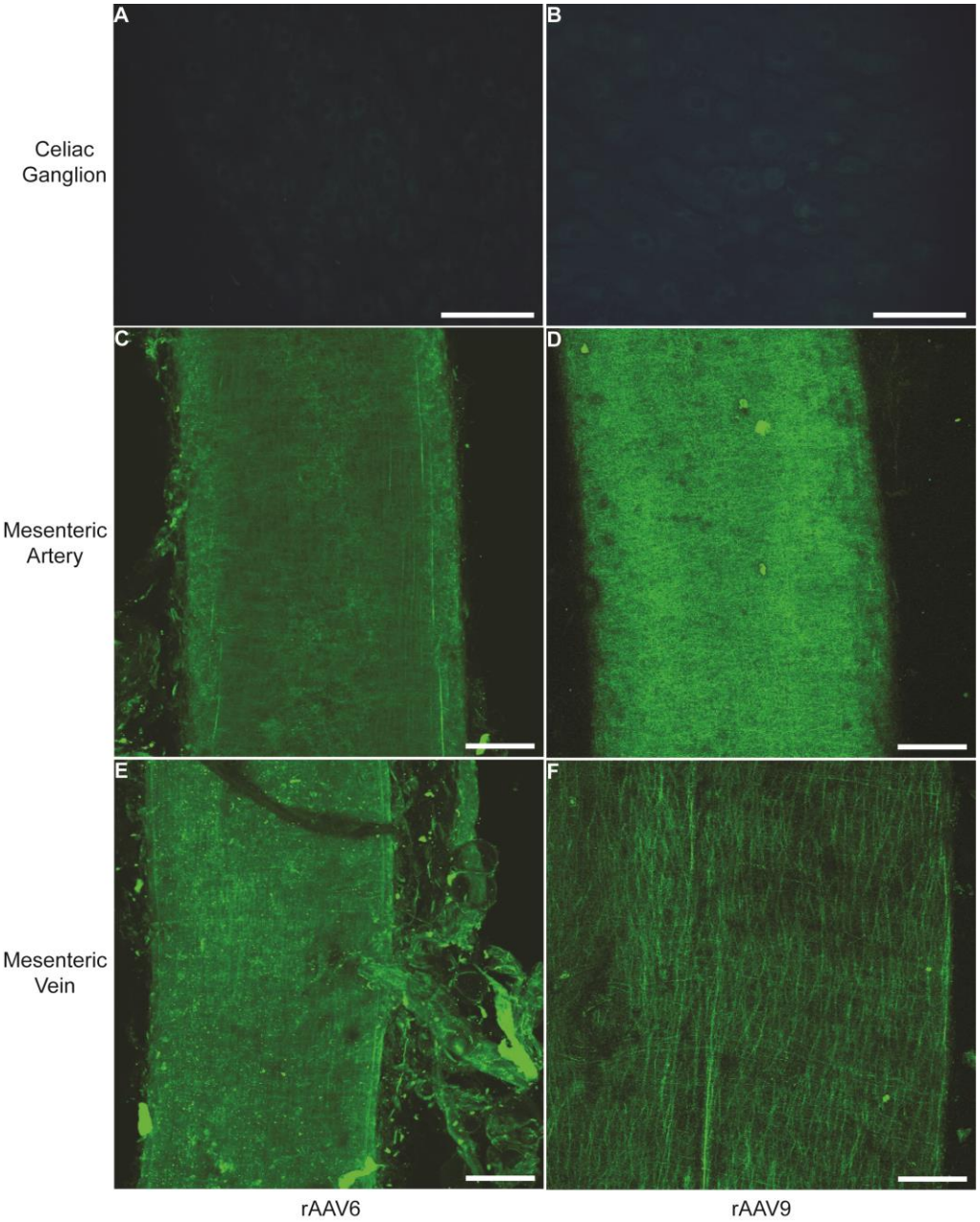


**Figure 2.5. GFP is not expressed in CG neurons 45 days after application of rAAV to the mesenteric vasculature.** No expression of GFP was present in the cell bodies of CG neurons 45 days after mesenteric application of rAAV6 (**A**) or rAAV9 (**B**). No GFP expression was present in perivascular nerves innervating MA (**C,D**) or MV (**E,F**) of animals treated with rAAV6 (**C, E**), or rAAV9 (**D, F**). All photomicrographs were taken with a 20x objective and all scale bars represent 100 μm.

## Discussion

Viral transduction of the CG revealed several key findings: 1) tropisms of PC12 cells dictate rAAV6 produces the most robust transduction of the serotypes tested; 2) direct injection of rAAV produced transduction of CG neurons; 3) vascular–application of rAAV produced no observable expression of GFP in perivascular nerve fibers, even 45 days after application of rAAV.

*Tissue tropisms of differentiated PC12 cells*

Tissue tropisms are specific for each rAAV serotype and contribute to expression of target genes in a tissue-specific manner; however, there is little data examining the transduction of peripheral neurons with rAAVs, let alone sympathetic neurons. Therefore, differentiated PC12 cells were selected to test tissue tropisms affecting transduction efficiency of different rAAV serotypes, because differentiated PC12 cells have properties resembling sympathetic neurons (Greene & Tischler, 1976). rAAV6 had the highest observable expression of GFP in differentiated PC12 cells, while rAAV2 had the lowest observable expression of GFP. The closest analog to sympathetic neurons that have been examined for tissue tropisms are sensory neurons, located in the dorsal root ganglion (DRG), where rAAV6 had the highest rates of transgene expression at four weeks, as compared to serotype 1 and 5 (Glatzel et al., 2000). In contrast, rAAV2 has been used to transduce various anatomical locations in the CNS, because of its robust ability to facilitate expression of a target gene in a wide variety of tissues (Kaplitt et al., 1994; Kirik et al., 2002). Incompatible tissue tropisms likely contributed to rAAV2's low transgene expression in PC12 cells. Differences in tissue tropism have been shown to greatly affect rAAV2 mediated transductions. For example, rAAV2 robustly transduces

neurons in the substantia nigra with great efficiency, but the number of neurons in DRGs are significantly reduced comported to serotype 5 (Bartlett, Samulski, & McCown, 1998; Mason et al., 2010). Based on the tissue tropisms of PC12 cells, rAAV6 likely produces the most efficient transductions of sympathetic neurons.

*Transduction of prevertebral neurons*

Viral transduction is dependent on tissue tropisms, while stable long-lasting gene expression is determined by its promoter. Serotype specific tropisms of PC12 cells correlated well with direct injections of rAAV into the CG, with rAAV6 demonstrating higher observable GFP expression in the CG as compared to rAAV1. Furthermore, rAAV6's transduction of the CG four weeks post injection, corresponded with peak transduction rates in DRGs, but expression levels of GFP in DRGs declined after four weeks (Glatzel et al., 2000). Declining transgene expression has been linked to methylation of the CMV promoter (Brooks et al., 2004; Löser, Jennings, Strauss, & Sandig, 1998); therefore GFP expression, driven by the CMV promoter, in CG neurons may not be stable past four weeks. This study demonstrates rAAV6 is the preferred serotype for transducing prevertebral neurons, but future studies requiring stable transgene expression past four weeks should utilize a cytomegalovirus early enhancer/chicken β-actin promoter which facilitates gene expression for months after successful transduction (Kim, Harada, Saito, & Miyamura, 1993; Kosuga et al., 2001).

Optimizing viral titer is essential for minimizing the volume required to produce viable transduction rates, while preventing damage to neural tissue from injecting large volumes. Titers ranging from $6.8 \times 10^8$ GC/ml in DRGs to $1\times10^{13}$ in the CNS have been used without seeing deleterious effects on neurons (Glatzel et al., 2000; Korecka, Ulusoy,

Verhaagen, & Bossers, 2011). Titers of $6.8 \times 10^8$ did not transduce the CG, but titers of $1 \times 10^{10}$ GC/ml or higher produced virally mediated expression of GFP in the CG. DRGs are easier to locate, are larger, and are thicker than the CG and do not move in concert with respiratory rhythm; therefore, DRG injections are more reliable when compared to CG injections. Fast green was used to track the spread of the viral load after injection into the CG, and was initially localized near the injection site, but quickly diffused away. Fast green did not diffuse when injected into DRGs. Viral diffusion limits the exposure of rAAVs to CG neurons; therefore, a higher titer is needed to transduce the CG as compared to low titers used to transduce the DRG.

*In vivo retrograde transduction of the CG*

The distinct innervation patterns of mesenteric vascular-projecting neurons are unknown; hence, a method was developed to investigate these innervation patterns. At nerve terminals rAAV is taken up and retrogradely transported to the cell body (Foust et al., 2007; Kaspar et al., 2003; Zheng et al., 2009) where the virus encodes expression of GFP and subsequent anterograde transport of GFP allowing tracing of neuronal networks by target (Chamberlin et al., 1998). Application of rAAV to the mesenteric vasculature mediated GFP expression in cell bodies of CG neurons, but did not label neurites with anterograde transport of GFP. Four weeks is sufficient time for expression of GFP after direct injection of rAAV into the CG, but 45 days may not be enough time for rAAV to be retrogradely transported back to the CG, and produce enough GFP to anterogradely fill vascular-projecting neurties. For example, injection of rAAV9 into the ventral tegmental area (VTA) resulted in lower transgene expression in projection areas, such as the amygdala after one month as compared to two months (Cearley & Wolfe, 2007). While,

rAAV is retrogradely transported from the VTA to its projection areas over a distance of mm, rAAV must cover a distance of cm back to the cell bodies of neurons in prevertebral ganglia. Longer time courses than 45 days may be required to visualize any expression of GFP in processes innervating the mesenteric vasculature. Alternatively, peripheral neurons may have difficulties retrogradely transporting rAAV, since motor neurons did not retrogradely transport rAAV after intramuscular injection (Ahluwalia & Vallance, 1997).

## Conclusions

This study employed two methods to transduce peripheral ganglia. The first method, direct microinjection of rAAV into the CG, mediated expression of GFP in CG neurons. Successful transduction of peripheral ganglia provides an avenue for the use of optognentics, manipulation of target genes, and anterograde track tracing in previously unexplored targets. The second method, rAAV application to the mesenteric vasculature, expressed GFP in cell bodies of CG neurons indicating successful retrograde transduction. Mesenteric application of rAAVs did not produce anterograde labeling of neurites, but optimization of mesenteric vascular rAAV application has the potential to elucidate the organization of the innervation supplied to different organs throughout the peritoneal cavity.

# CHAPTER THREE: ROLE OF PREVERTEBRAL VASCULAR-PROJECTING NEURONS IN THE SYSTEMIC PRESSOR RESPONSE ELICITED BY STIMULATING THE CELIAC GANGLION OR POSTGANGLIONIC NERVE FIBERS FROM THE SPLANCHNIC GANGLION

**Abstract**

Neurons located in prevertebral ganglia provide sympathetic innervation to the mesenteric vasculature. Although, the population of vascular-projecting neurons in the splanchnic ganglia (SG) has not been fully characterized, nor is it known whether activation of vascular-projecting neurons in the SG can elevate systemic arterial pressure. The greater splanchnic nerve (GSN) traverses the SG, terminates in the celiac ganglion (CG), and contains a mix of preganglionic fibers innervating sympathetic postganglionic neurons in the CG and postganglionic fibers from SG neurons. Retrograde tracers, pseudorabies virus-152 (PRV-152) and cholera toxin subunit B (CTB-555), were applied to the mesenteric vasculature and labeled a population of vascular-projecting SG neurons. Direct application of 200 mM nicotine to the CG elicited a 7.89 ± 1.53 mmHg systemic arterial pressure response via activation of prevertebral neurons in the CG. GSN stimulation elicited a 7.22 ± 0.92 mmHg systemic arterial pressure response, which could not be attenuated by blocking ganglionic transmission with intravenous administration of 30 mg/kg hexamethonium. However, the pressor response elicited by stimulating the GSN was attenuated after blockade of purinergic and adrenergic receptors by intravenous administration of 10 mg/kg pyridoxalphosphate-6-azophenyl-2',4'-disulfonic acid and 2 mg/kg phentolamine respectively. Furthermore, our pharmacological studies indicate that activation of postganglionic fibers from the SG was sufficient to elicit a systemic pressor response, indicating only a small number of vascular-projecting neurons are required to elicit a systemic pressor response. These studies demonstrate that the activation of postganglionic fibers of vascular-projecting neurons from the SG elevates systemic arterial pressure. Furthermore, this suggests that SG neurons have sufficient vascular projections to modulate constriction of the splanchnic circulation.

## Introduction

Prevertebral neurons are the final common path of the sympathetic nervous system innervating viscera, glands, and vasculature. The sympathetic nervous system is generally thought of as being a system of “mass action,” where the entirety of sympathetic outflow is recruited to produce a fight or flight response. Recent evidence, however, describes the sympathetic nervous system as separate neuronal subpopulations that are organized according to target with divisions of sympathetic neurons occurring centrally in the rostral ventrolateral medulla and peripherally in ganglia (Janig & McLachlan, 1992). Divisions of the sympathetic nervous system facilitate regional increases in sympathetic activity during pathophysiological conditions such as hypertension (Osborn et al., 2011).

A critical target for the sympathetic nervous system is the splanchnic circulation, because it accounts body’s largest volume of blood and the source of greatest vasculature resistance. Increased splanchnic sympathetic activity has been indicated in several animal models of hypertension (Kandlikar & Fink, 2011; King et al., 2007; Osborn et al., 2011). Each of these models involves altered long-term regulation of systemic arterial pressure by regional activation of the sympathetic nervous system. The innervation of the splanchnic circulation arises from neurons in para- and pre-vertebral ganglia that also contain neurons innervating the gastrointestinal tract, and its accessory organs (Browning et al., 1999; Hsieh, Liu, & Chen, 2000; Park et al., 2009; Quinson et al., 2001). While anatomical pathways of the celiac plexus are well defined, there is little evidence describing specific physiologic consequences of activating defined subsets of prevertebral neurons.

Sympathetically-mediated vasoconstriction of splanchnic arteries and veins actively increases splanchnic resistance and decreases splanchnic capacitance, thereby increasing systemic arterial pressure. Splanchnic capacitance is altered proportionally more than resistance by stimulating the greater splanchnic nerve (GSN), one primary source of vascular innervation, at a low frequency (1-2 Hz), although both responses peaked at higher frequencies (10-20 Hz; Karim & Hainsworth, 1976). Stimulating postganglionic splanchnic nerves at frequencies of 0.5-5 Hz constricts veins, but arteries require a much higher threshold (Hottenstein & Kreulen, 1987; Kreulen, 1986). Such differential responses between arteries and veins may be mediated by P2X receptors, which mediate vasoconstriction and are found on mesenteric arteries (MA) but not veins (MV). Alternatively, these differential responses may be due to greater inhibition of norepinephrine (NE) release onto arteries via prejunctional $\alpha$-2 adrenergic receptors (Gitterman & Evans, 2001b; 2001a; Park et al., 2009). The delineation of arterial and venous function is further expounded by distinct populations of prevertebral neurons that innervate arteries and veins (Browning et al., 1999). The importance of separate innervation and regulation of arteries and veins in the splanchnic circulation is unknown, but separate control of arteries and veins is crucial in other vasculature beds and likely plays an essential role in the regulation of blood flow and volume in the splanchnic circulation.

The sympathetic nervous system is not the only source of innervation to the splanchnic circulation, the sensory system provides extensive innervation to the splanchnic circulation and is in close association with sympathetic fibers. Sensory fibers provide a source of vasodilation mediated by nitric oxide or calcitonin gene related peptide

(Holzer, 1992; Zheng et al., 1998) and repetitive stimulation of periarterial nerves, at low frequencies or in combination with sympathetic blockade, results in vasodilation (Hukkanen et al., 1992; Kreulen & Peters, 1986; Park et al., 2009; Pucovský et al., 2002). Therefore, sensory and sympathetic systems interact to generate opposing effects on splanchnic vasculature.

The purpose of this study is to develop an *in vivo* method to activate neurons in the celiac plexus either by direct application of nicotine to the celiac ganglion (CG) or by stimulating the GSN. These preparations allow for regional activation of the splanchnic circulation without systemic activation of the sympathetic nervous system by specifically activating neurons or fibers projecting to the splanchnic region. This is an important development that will allow investigation of the acute effects of constricting splanchnic arteries and veins on systemic arterial pressure. Furthermore, these methods allow the delineation of the physiological relevance of different neuronal subpopulations in the celiac plexus, by granting a means to acutely test the effect of modulating different neuronal subpopulations on acute rises in systemic arterial pressure.

## Materials and Methods

*Animals*

Male Sprague Dawley rats (Charles River Laboratories, Inc., Portage, MI) weighing 225-380g were used in this study and were housed in a temperature- and humidity-controled (22-24°C) room with a 12 hour light/dark cycle. All rats had *ad libitum* access to standard rat chow and water. Rats treated with pseudorabies virus were housed in a biosafety level 2 room, under the same conditions listed above. All experimental procedures in this study were approved by Michigan State University's Institutional Animal Care and Use Committee.

*Catheter implantation and drug infusion*

All animals that underwent drug infusion were prepared with an arterial and venous femoral catheter for direct measurements of arterial pressure and intravenous (IV) administration of drugs. Arterial pressure was measured with PowerLab (ADInstruments) via a pressure transducer (ADInstruments), which was calibrated on the day of the experiment with a sphygmomanometer.

*In vivo modulation of arterial pressure using nicotine*

After anesthetizing rats with 1.5-2% isoflurane, they were laparotomized and the intestines, spleen, and stomach were retracted to expose the CG (**Fig 3.1A**). Excess connective tissue was removed from the top and surrounding areas of the CG. A silicone sealant (Dow Corning Corp.) dam was placed around the CG to prevent nicotine from diffusing into surrounding tissue. To check the integrity of the seal, saline was pipetted into the silicone barrier, compromised seals were reinforced with a parafilm lining outside the edge of the silicone. Nicotine (10μl; 200mM; Sigma-Aldridge) or vehicle (PBS) was

carefully pipetted into the circle of silicone sealant surrounding the CG using a P-10 pipette. Four animals received 30 mg/kg hexamethonium IV prior to administration of nicotine. In a separate surgery, three animals received celiac ganglionectomy (CGx) two weeks prior to administration of the nicotine protocol. Care was taken to locate the former location of the CG and replicate the addition of nicotine in animals receiving CGx. A final group of 4 animals were treated with an intraperitoneal (IP) injection of 5 mg/kg nicotine.

*Stimulation of the GSN*

After anesthetizing rats with 1.5-2% isoflurane, they were positioned on their right side and a left flank incision was made just above the kidney. Fat was cleared using two flame polished glass pipettes, until the GSN was revealed (**Fig 3.1B**). The nerve was carefully separated from the underlying fat and connective tissue, at which point, a bipolar electrode was placed underneath the nerve. The nerve was decentralized by tying off a piece of 5-0 suture proximal to the electrode. The nerve was then stimulated for 20s at 3 Hz, 5 V, 1 ms to generate a baseline pressor response for each animal. Voltage and pulse duration were set constant at 5V and 1ms, respectively. The nerve was stimulated several more times at frequencies ranging from 1 Hz to 5 Hz, with at least four minutes separating each stimulation of the nerve. Drugs were administered sequentially via an IV catheter with a 3 Hz stimulation separating each infusion. First, 30 mg/kg hexamethonium was administered, followed by 2 mg/kg phentolamine (Sigma-Aldrich); and then 10 mg/kg pyridoxalphosphate-6-azophenyl-2',4'-disulfonic acid (PPADs, Sigma-Aldrich). An equal number of animals received an infusion of PPADs followed by phentolamine.

*Labeling with retrograde tracers*

As previously described, a large percentage of sympathetic postganglionic neurons were labeled by injecting fluorogold (1mL of 0.5%, IP) one week prior to surgical intervention (Tang, Mitchell, Espy, Smith, & Persing, 1999). In this study, pseudorabies virus (PRV) Bartha vaccine strain expressing enhanced green fluorescent protein (PRV 152, $8.6X10^8$ pfu/mL) and cholera toxin subunit B conjugated to Alexa Fluor 555 (0.5% CTB-555, Life Technologies) were used as retrograde tracers. PRV tracers were generously provided by Dr. Lynn Enquist (Princeton Neuroscience Institute).

After rats were anesthetized with isoflurane, a loop of the small intestine was exteriorized through a laparotomy and secured to a Sylgard (Dow Corning) platform by draping hanks' balanced salt solution (HBSS, Gibco) soaked gauze over the small intestine. Secondary branches of mesenteric vasculature were isolated by carefully clearing the perivascular fat from the vessels. Two pieces of silicone tubing were cut longitudinally to form a ¾ semicircle and each one was placed under either an artery or vein. Both pieces of tubing were sealed with silicone sealant (Dow Corning) and saline was pipetted into the sealed tubing to check the integrity of the seals. After observing the saline for 5 minutes, to verify the integrity of the silicone seals, the saline was pipetted out of the sealed tubing. 5 μl of PRV-152 or CTB-555 were then pipetted into the sealed tubes. Gelfoam (Pharmacia and Upjohn Co.) was then added to each sealed piece of tubing, and then the entire apparatus was encased in a silicone elastomer (World Precision Instruments). After allowing the elastomer to cure, the entire apparatus was replaced into the animal, the intestines were moistened with 1 ml of warm sterile HBSS

and then the incision was closed. Each animal was given antibiotic (Baytril [5mg/kg]) and analgesic (Carprofen [5mg/kg]) for three days post-intervention.

*Tissue collection, sectioning, and visualization*

Animals were sacrificed 4 days after application of retrograde tracers. The CG and both SG were harvested and drop-fixed in 4% paraformaldehyde. Ganglia were post-fixed for 24-48 hours, cryoprotected for 24 hours in a 20% sucrose, flash frozen in optimal cutting temperature mounting medium (VWR International) cooled by liquid nitrogen, and stored at -80°C until they were cryostat sectioned on a Bright Model OTF cryostat (Hacker Instruments Inc.) into five series of 16 μm thick sections. One series of sections was rinsed in tris-buffered saline three times for 10 mins, and coverslipped with ProLong Gold Antifade (ThermoFisher). Sections were visualized on a confocal microscope (Olympus Fluoview-F1000 Spectral confocal microscope). Photomultiplier tube voltage was optimized before collecting each series of z-stack images. Images were then assessed after performing a maximum intensity projection of the images.

*Data analysis*

Analysis of hemodynamic responses were performed using LabChart 8 (ADInstruments), where Δ arterial pressure and Δ heart rate were measured as the largest change from baseline after adding nicotine or electrically stimulating the GSN. Area under the curve was calculated by taking the integral of the arterial pressure response from the start of the stimulus until arterial pressure returned to baseline. Time to peak was calculated as the time from the start of the stimulus until peak change in pressure was observed.

Mean values of all data sets were compared using a one-way analysis of variance paired with a Tukey's post-hoc test where appropriate. All data is expressed as mean ± the SEM with n values notating the amount of animals contained in each group.

## Results

*Retrograde labeling of vascular-projecting neurons in the SG*

Despite successful retrograde labeling with both PRV-152 and CTB-555 in only 1 out of 10 animals, we were able to detect vein-projecting neurons, artery-projecting neurons, and neurons projecting to both veins and arteries within the SG. Retrograde tracers were applied to MA and MV to identify vascular-projecting neurons. Many PRV-152 labeled neurons were seen in the SG, indicating the presence of vein-projecting neurons (**Fig 3.2B, F**). In addition, many CTB-555 labeled neurons were seen in the SG, indicating the presence of artery-projecting neurons (**Fig 3.2C, G**). Moreover, a subpopulation of SG neurons were colabeled with PRV-152 and CTB-555, indicating that they project to both MA and MV (**Fig 3.2D, H**).

*In vivo application of nicotine*

Injecting nicotine IP served as a positive control for activating all nicotinic acetylcholine receptors (nAchRs) in the splanchnic region. IP injection of 5 mg/kg nicotine increased arterial pressure by 14.38 ± 1.67 mmHg and area under the curve for the arterial pressure response was 4190.09 ± 919.89 mmHg*s. Time to peak response was 173.75 ± 48.74 s, and peak change in heart rate was -79.23 ± 15.34 BPM (Beats per minute, **Fig 3.4A-D**). In a separate set of animals, nicotine was applied to the CG to investigate the effects of specifically activing nAchRs in CG neurons. CG–applied nicotine increased arterial pressure by 7.89 ± 1.53 mmHg and area under the curve for the arterial pressure response was 1647.08 ± 535.42 mmHg*s. Time to peak response was 69.5 ± 15.18 s, and peak change in heart rate was -41.42 ± 13.49 BPM (**Fig. 3.4 A-D**).

To confirm that the effect of CG–applied nicotine was mediated by nAchRs within the CG, animals either received IV administration of hexamethonium or underwent CGx. CGx-ing animals caused a peak change in arterial pressure of 4.17±0.90 mmHg. The latency to peak response was 49.33 ± 14.62 s and the area under the curve for the arterial pressure response was 1154.17 ± 274.59 mmHg*s. Applying nicotine to the CG reduced ∆ heart rate by -6.10 ± 3.51 BPM (**Fig 3.4A-D**). Administering hexamethonium IV decreased arterial pressure by -33.42 ± 5.19 mmHg ($p \leq 0.05$) indicating successful ganglionic blockade. After administering hexamethonium, nicotine was applied to the CG. The peak change in arterial pressure was 16.4 ± 2.9 mmHg, and area under the curve for the arterial pressure response was 2922.63 ± 1051.29 mmHg*s. Time to peak response was 34 ± 3.18 s, and the peak change in heart rate was -6.08 ± 6.04 BPM (**Fig 3.4A-D**).

*In vivo stimulation of the GSN*

The GSN was stimulated to examine the acute effects of activating splanchnic sympathetic neurons on systemic arterial pressure. Stimulating the GSN elicited a systemic pressor response (**Fig. 3.6A**) at frequencies ranging from 1-5 Hz. Stimulating at 1 Hz was significantly different from stimulating at 5 Hz in both peak pressor response and area under the curve ($p \leq 0.05$, **Fig 3.6A, C**). The preganglionic component of the systemic arterial pressure response to GSN stimulation was investigated by administering hexamethonium IV, which decreased arterial pressure by 21.98 ± 12.65 mmHg, indicating successful ganglionic blockade. Stimulating the GSN after administration of hexamethonium increased arterial pressure by 7.79 ± 5.68 mmHg, which was not significantly different from the baseline 3 Hz stimulation of 7.22 ± 0.92 mmHg (**Fig 3.6A**).

Neither blockade of purinergic postganglionic transmission by infusing PPADS IV nor blockade of adrenergic postganglionic transmission by infusing phentolamine IV blocked the pressor response to GSN stimulation (**Fig 3.5A**). However, blocking both purinergic and adrenergic transmission did attenuate the pressor response to stimulating the GSN with reductions in peak pressure response and area under the curve ($p \leq 0.05$, **Fig 3.6A, C**). Changes in heart rate were small and not significant in any experimental parameter (**Fig 3.6B**).

## Figures

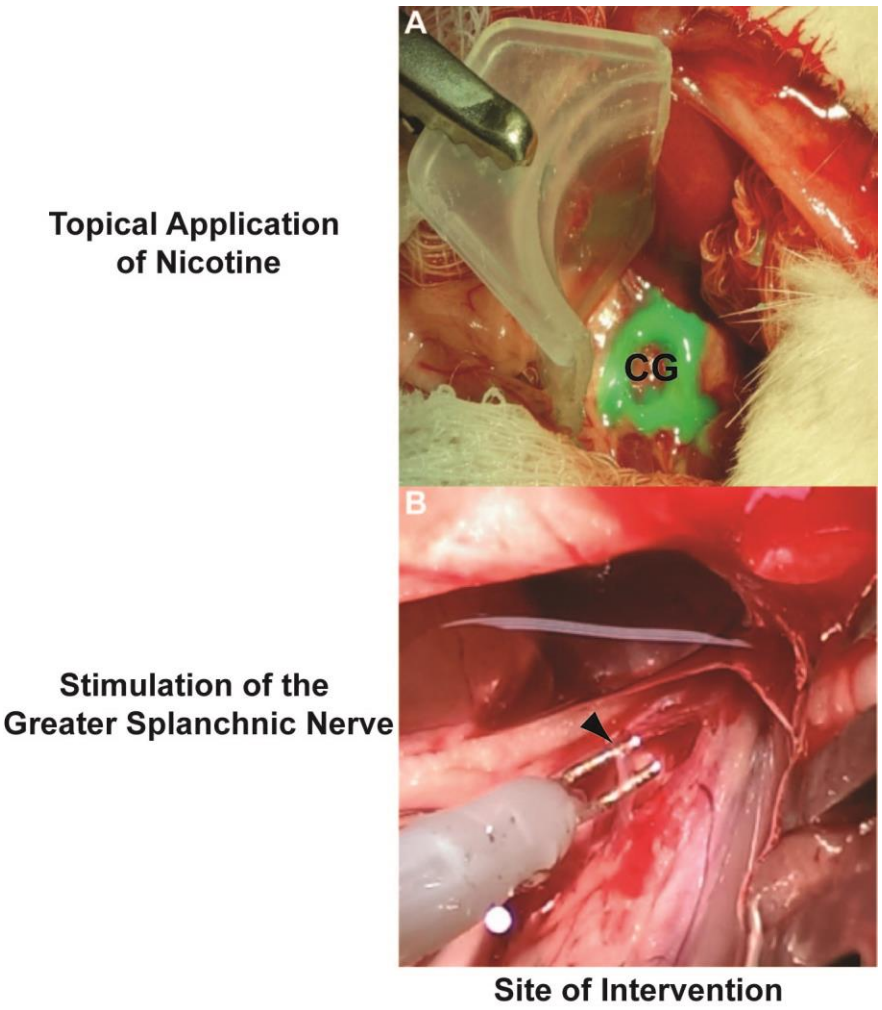


**Figure 3.1 Stimulating the GSN is less invasive to the mesenteric circulation than applying nicotine to the CG.** The mesentery is exteriorized through a midline incision to gain access to the CG. Silicone sealant (green) is used to localize application of nicotine to the CG (**A**). The GSN is accessed via a flank incision, leaving the mesentery intact. A bipolar electrode is positioned under the GSN, which is indicated by a black arrow (**B**).

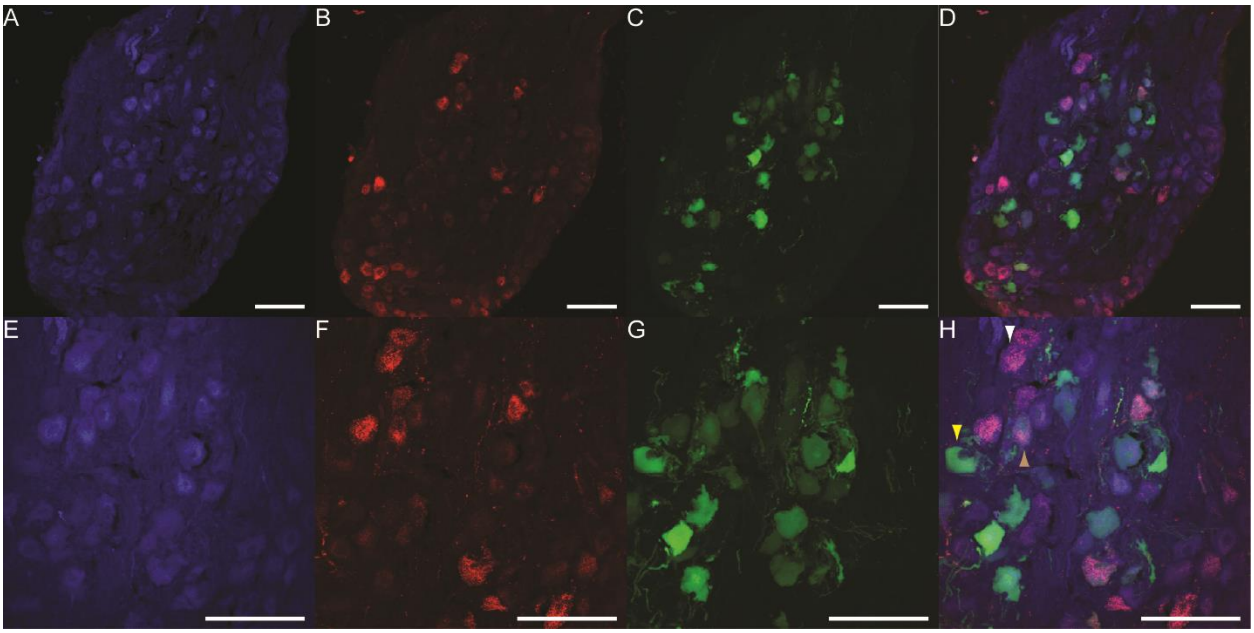


**Figure 3.2 The SG contains neurons projecting to the mesenteric vasculature.** Photomicrographs of neurons in the SG labeled from injecting Fluorogold IP taken with a 20x (**A**), or 40x (**E**) objective. Visualizing CTB-555 in the SG 4 days after application of the tracer to a MA with a 20x (**B**), or 40x (**F**) objective. Visualization of PRV-152 in the SG 4 days after application of the tracer to a MV with a 20x (**C**), or 40x (**G**) objective. CTB-555 or PRV-152 singly labeled SG neurons (white or yellow arrow respectively), and double labeled SG neurons (**D, H,** brown arrows). Singly labeled neurons project to either arteries or veins, while double labeled neurons project to arteries and veins. All scale bars represent 100 μm.

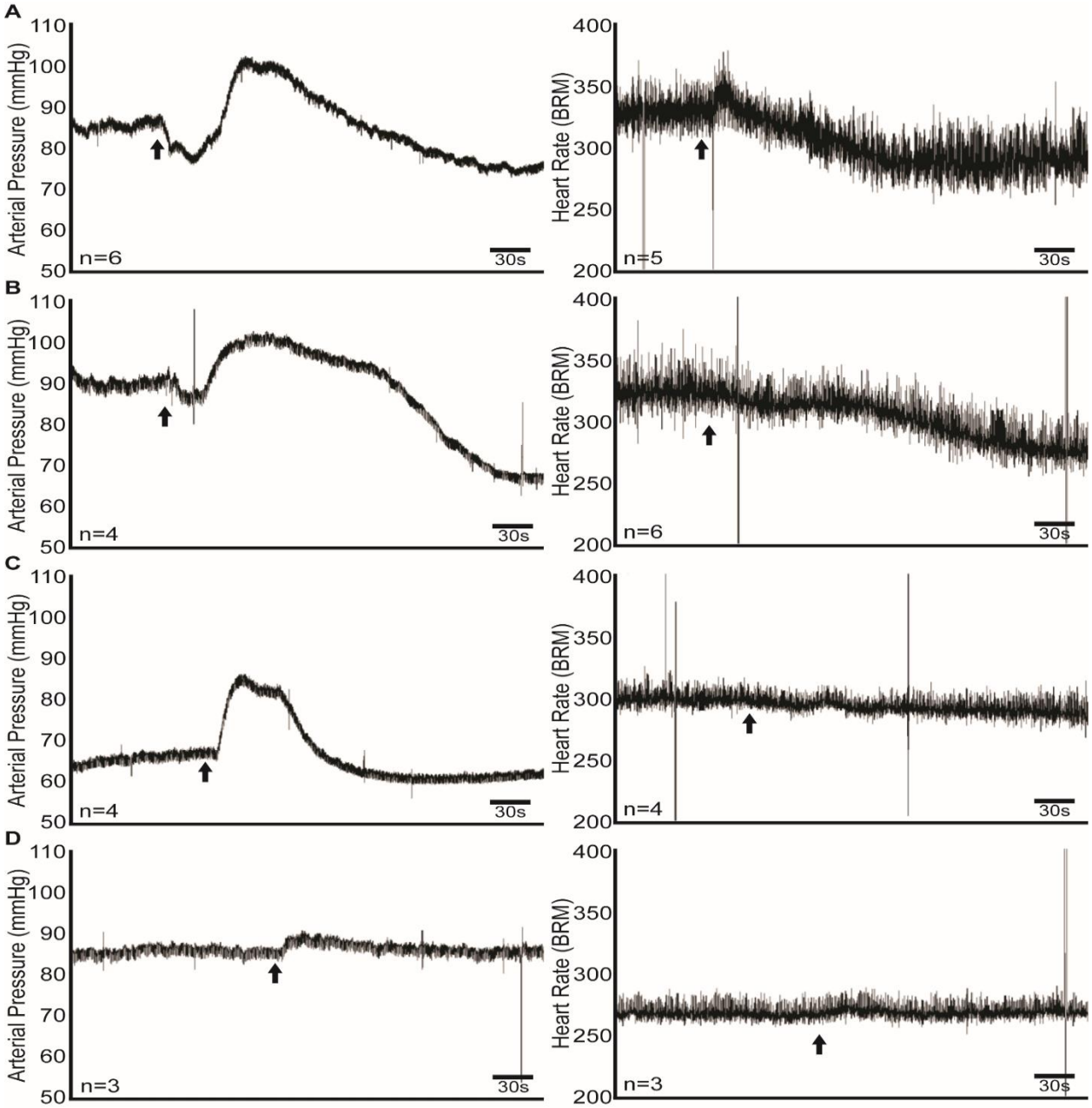


**Figure 3.3 Hexamethonium does not block the systemic arterial pressure response to applying nicotine topically and a component of the systemic arterial pressure response is not mediated by the CG.** Representative traces of systemic arterial pressure and heart rate responses to directly applying nicotine to the CG (**A**), when nicotine is injected IP (**B**), when applying nicotine to the CG after IV infusion of hexamethonium (**C**), or applying nicotine to the area previously occupied by the CG after CGx. Arrows indicate nicotine application.

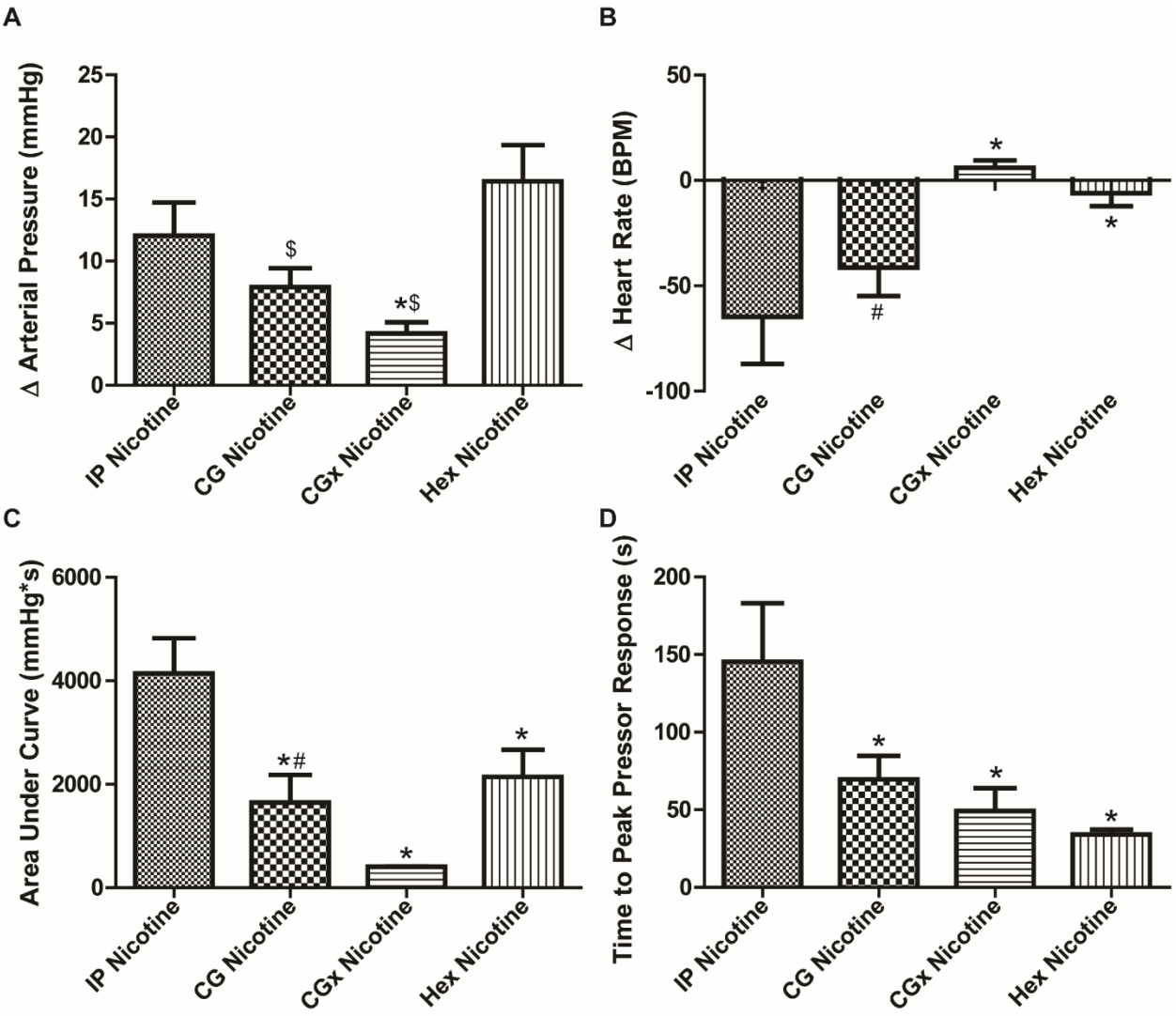


**Figure 3.4 The hemodynamic response to applying nicotine topically is not blocked by hexamethonium or entirely mediated by the CG.** Quantification of peak changes in systemic arterial pressor (**A**), peak change in heart rate (**B**), area under the curve of the arterial pressor response (**C**), and time to peak pressor response (**D**) to nicotine injected IP (IP nicotine), or applying nicotine topically to the CG (CG nicotine). Some animals had their CG removed 2 weeks prior to nicotine administration (CGx nicotine) or recieved hexamethonium (Hex nicotine) prior to CG nicotine. Data expressed as mean ± SE; n = 3-6. *, $, # indicates $p \leq 0.05$ when compared to IP, Hex, or CGx nicotine respectively.

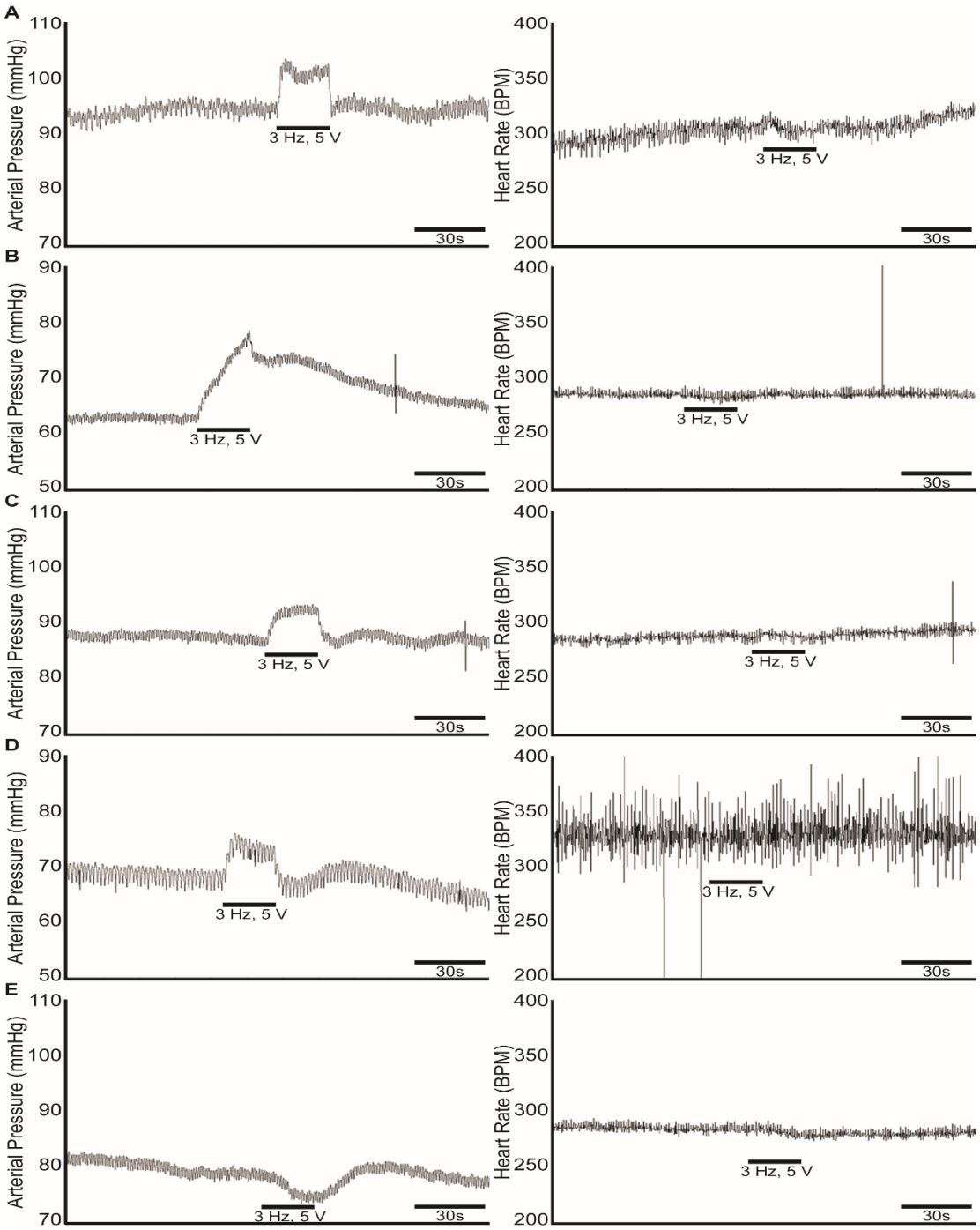


**Figure 3.5 Stimulating the GSN elicits a systemic arterial pressor response that is not blocked by hexamethonium, but is blocked by a combination of phentolamine and PPADs.** Representative arterial pressure and heart rate traces of a typical arterial pressure response to a 20s duration 3 Hz, 5 V stimulation (**A**), which was not blocked by hexamethonium (**B**), PPADs (**C**), or phentolamine (**D**). A combination of both PPADs and phentolamine did block the response to stimulating the GSN (**E**).

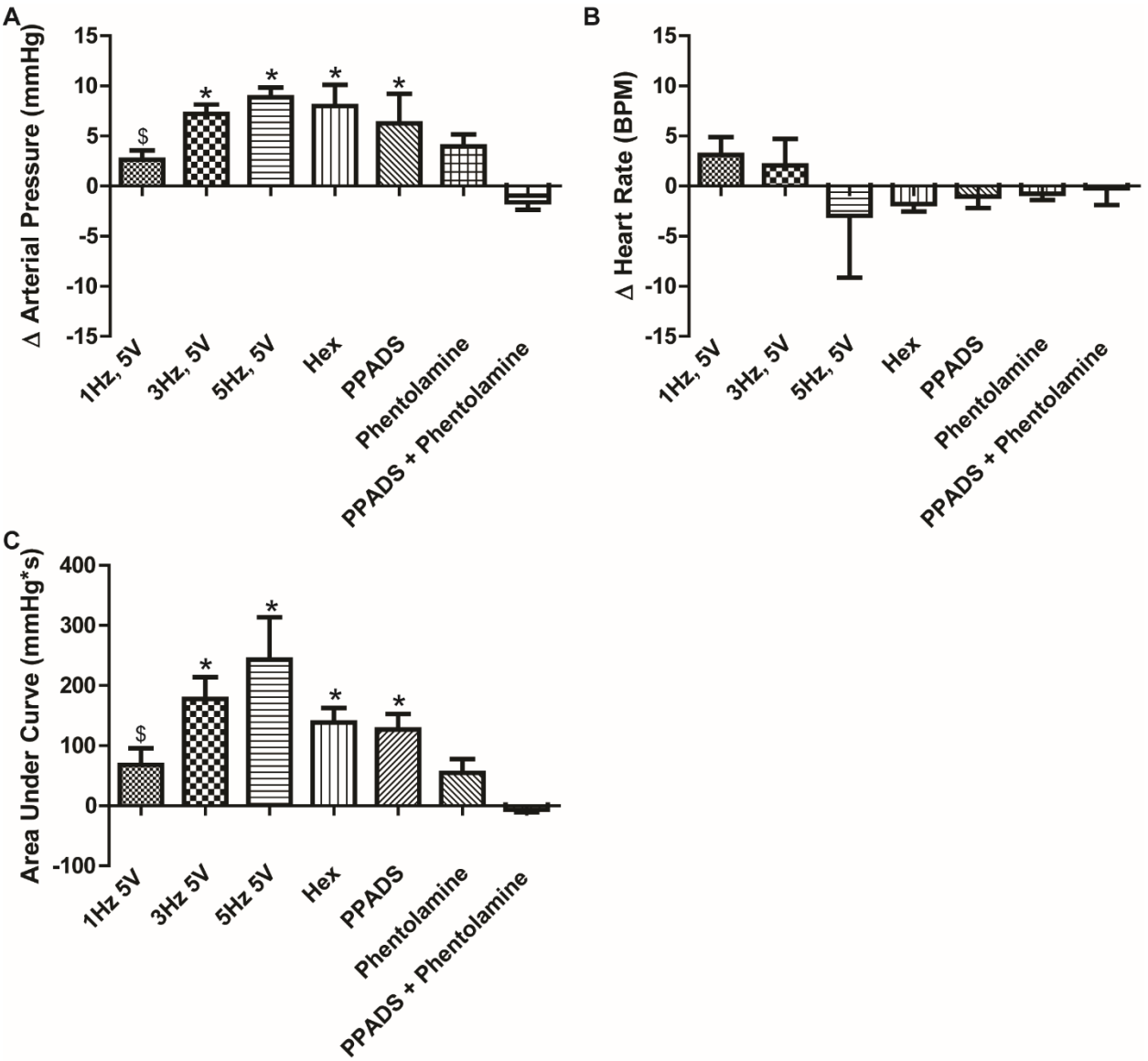


**Figure 3.6 Pretreatment with PPADs and phentolamine blocks the systemic pressor response to stimulating the GSN.** The arterial pressure response to stimulating the GSN was frequency dependent with significant differences between 1 Hz and 5 Hz in both peak arterial pressor response (**A**), and area under the curve (**C**). Pretreatment with PPADS and phentolamine significantly reduced peak arterial pressure response (**A**) and area under the response (**C**) to stimulating the GSN. Heart rate was not significantly different among any of the stimulation parameters tested (**B**). Data expressed as mean ± SE; n = 3-7. $,* indicates $p \leq 0.05$ when compared to 5 Hz, or PPADs + phentolamine respectively.

## Discussion

This study examines the effects of selectively stimulating the GSN on systemic arterial pressure. The key findings of this study were: 1) the SG contained a population of mesenteric vascular–projecting neurons; 2) hexamethonium did not block the arterial pressor response to nicotine applied to the CG; 3) the action of nicotine is not localized to the CG 4) hexamethonium did not block the arterial pressor response to GSN stimulation; 5) post junctional blockade by a combination of phentolamine and PPADS blocked the arterial pressor response to stimulating the GSN; 6) stimulating postganglionic nerve fibers from neurons in the SG elicited a systemic arterial pressor response.

*The SG contained vascular-projecting neurons*

Neurons in the SG project to splanchnic viscera and vasculature (Sawchenko & Swanson, 1981). Previous reports were inconclusive, however, because the paravascular nerves were not removed during tracer application and previously used tracers are taken up by fibers of passage (Sawchenko & Swanson, 1981). Therefore, tracers applied to the vasculature may have been taken up by paravascular nerves that contain fibers projecting to the small intestine (Brunsden, Brookes, Bardhan, & Grundy, 2007), and this would be problematic because labeled neurons would not be specific for vascular-projecting neurons. In this study, unique retrograde tracers were applied to perivascular nerves on MA or MV such that singly labeled neurons were either MA- or MV-projecting whereas doubly labeled neurons projected to both MAs and the MVs. Neurons projecting to MA, MV, or both have been similarly observed in other prevertebral ganglia (Browning et al., 1999; Hsieh, Liu, & Chen, 2000). Due to the inability to consistently label the SG with two

tracers, vascular-projecting neurons in SG were not characterized, and future studies are required to fully describe the population of vascular-projecting SG neurons.

*In vivo application of nicotine*

A component of the systemic pressor response from applying nicotine to the CG is a result of nicotine activating nAChRs located outside the CG. In addition to the CG, nAChRs are located on sympathetic post ganglionic neurons and adrenal chromaffin cells and administering nicotine systemically elevates arterial pressure (Aceto et al., 1979; Ikushima et al., 1982). Applying nicotine to the CG elicited a peak systemic arterial pressor response that was not different from peak pressor responses elicited by injecting nicotine IP, however the size of the pressor response was significantly smaller after infusing nicotine onto the CG compared to injecting nicotine IP. Thus, nAChRs outside of the CG likely play a role in mediating larger pressor responses. To investigate the action of nicotine activating nAChRs outside of the CG, a group of animals underwent CGx and nicotine was applied to the area formerly occupied by the CG. CGx animals responded to nicotine infusion, most likely because nicotine diffused away from the former location of the CG and stimulated release of NE and epinephrine from the adrenal glands (Armitage, 1965).

To confirm the pressor response to nicotine was mediated by activation of nAChRs, hexamethonium was applied to block nAChRs. Interestingly, infusing hexamethonium IV enhanced peak pressor responses. While hexamethonium has been routinely used in this dose to block transmission of the sympathetic nervous system to the splanchnic circulation (Adams, Bevan, & Terrar, 1991), hexamethonium requires activation of nAChRs to infiltrate and block it's ion channel (Gurney & Rang, 1997).

Therefore the large dose of nicotine used in this study (200 mM) could have initially activated a large number of nAChRs before hexamethonium was able to block the ionic channels located in nAChRs.

Acute rises in arterial pressure activate the baroreceptor reflex resulting in a compensatory decrease in heart rate, thus stabilizing blood pressure (Barman et al., 2001). Applying nicotine topically to the CG reduced heart rate and increased arterial pressure. Interestingly, even in the presence of increased arterial pressure, heart rate did not decrease in CGx animals, suggesting that systemic pressure response elicited in CGx treated animals was likely not large enough to elicit a significant reduction in heart rate. As reported previously, hexamethonium can prevent baroreceptor mediated decreases in heart rate during increases in systemic arterial pressure (Uechi et al., 1998). Interestingly, we saw this effect even at doses that may have been insufficient to block nAChRs from our supraphysiological levels of nicotine. Blocking nAChRs outside of the splanchnic region with IV hexamethonium, while constricting the splanchnic circulation could have attenuated decreases in cardiac output despite increases in arterial pressure.

*In vivo GSN stimulation*

Stimulating the GSN of dogs has well-characterized effects on splanchnic capacitance and resistance (Sapru et al., 1982) and GSN nerve activity has been characterized in rats (Bratton et al., 2010; Lundin, Ricksten, & Thorén, 1984; Nilsson, Ljung, Sjöblom, & Wallin, 1985). To date, there are few published reports specifically characterizing the effects of stimulating the GSN on systemic arterial pressure in rats. Therefore, the systemic arterial pressure response to stimulating the GSN was optimized starting with frequencies designed to mimic frequencies at the upper end of endogenous

nerve activity, 3 Hz (Hottenstein & Kreulen, 1987). Although maximal constriction of MA and MV occurs at frequencies higher than 3 Hz (Kreulen, 1984), stimulating the GSN at 5 Hz did not have a significant effect on the peak pressor response or size of the response as compared to 3 Hz, but lower frequencies (1 Hz) did not elicit a robust pressor response. Therefore, 3 Hz was chosen to test all pharmacological agents, because it is a physiologically relevant frequency and elicited a robust pressor response.

Ganglia are not simple relays of preganglionic fibers to postganglionic neurons, rather they are sites of integration (Kreulen, 1984). Prevertebral ganglia receive input from preganglionic fibers (Langley, 1893), spinal sensory fibers (Crowcroft & Szurszewski, 1971), intestinofugal afferent neurons (Kreulen & Szurszewski, 1979), and projections from the vagus nerve (Rosas-Ballina et al., 2008), summation of these inputs are important for determining sympathetic outflow to end organs (Kreulen, 1984). Intracellular recordings of prevertebral neurons in the third lumbar sympathetic ganglion demonstrated one strong preganglionic input was responsible for propagation of only 32% of all recorded action potentials in postganglionic neurons (Bratton et al., 2010). Even so, blocking preganglionic inputs with hexamethonium did not affect the peak pressure response to stimulating the GSN. In previous reports, stimulating the preganglionic nerves innervating the inferior mesenteric ganglion elicited smaller amplitude excitatory junction potentials in mesentery arteries cells than stimulating postganglionic nerves (Kreulen, 1986). Moreover, postjunctional blockade of the neuroeffector junction with purinergic and adrenergic antagonists attenuated the pressor response to stimulating the GSN, indicating activation of postganglionic nerve fibers in the GSN is sufficient to impact systemic arterial pressure. In the rat, the GSN contains a mix of pre– and post–ganglionic

nerve fibers (Sapru et al., 1982); therefore, it is likely that the pressor response from stimulating the GSN is primarily influenced by postganglionic fibers whereas presynaptic input from activated preganglionic fibers is integrated in the CG, but not relayed to end organs.

Stimulating postganglionic nerve fibers arising from a relatively small population of SG neurons elevated systemic arterial pressure. In order to increase systemic arterial pressure SG neurons must innervate a significant portion of splanchnic vasculature, suggesting SG neurons project widely to many segments of MA and MV. There is considerable evidence indicating vascular neurons have divergent innervation fields. For example, anterograde tracing of human perivascular nerve fibers revealed extensive branching patterns innervating substantial portions (> 4.3 mm) of blood vessels (De Fontgalland et al., 2008). Single neurons innervate even greater lengths of blood vessels (7 mm) of cutaneous blood vessels in the ears of guinea pigs. Conversely, 50-100 neurons converged to the same portion (1 $mm^2$) of these cutaneous blood vessels indicating extensive branching to several segments of vasculature (Gibbins et al., 1998). The same extensive branching pattern could be present in SG neurons, granting innervation fields large enough to vasoconstrict a sufficient portion of the splanchnic circulation to impact systemic arterial pressure.

Blocking the systemic pressure response to stimulating the GSN requires concomitant application of purinergic and adrenergic antagonists, suggesting that there is both an arterial and venous component to the systemic arterial pressure responses. Adenosine triphosphate (ATP) and NE are co-released and actively constrict MA and MV via P2X receptors and $\alpha$-1 adrenergic receptor (AR) respectively (Gitterman & Evans,

2001a; 2001b; Luo et al., 2003). MV do not contain P2X receptors, but can still be constricted by ATP via P2Y receptors (Galligan et al., 2001). However, constrictions of MV by perivascular stimulation are primarily blocked by $\alpha$-1 AR antagonists indicating MV are primarily constricted by NE (Galligan et al., 2001) In contrast, MA are primarily constricted by ATP as instanced by constriction of MA being blocked by P2X receptor antagonists (Gitterman & Evans, 2001a; Luo et al., 2003; Park et al., 2009). Furthermore, NE can still constrict MA, but the response is left-shift compared to MV (Sporkova et al., 2010). The remaining pressor response during $\alpha$-1 AR blockade suggests ATP-mediated constriction of MA is sufficient to elevate arterial pressure. Similarly, blocking P2X receptors did not completely abolish the systemic pressor response to stimulating the GSN, suggesting NE mediated vasoconstriction of the MV is sufficient to elicit systemic rises in arterial pressure. Taken together, this suggests MA and MV both significantly contribute to the pressor response when stimulating the GSN at a low frequency (3 Hz).

During postganglionic blockade the pressor response was reversed suggesting a vasodilatory response when stimulating the GSN in the absence of sympathetic transmission. Vasodilation is probably caused by activating primary sensory afferents that send projections to the mesenteric vasculature, which release nitric oxide and calcitonin gene related peptide onto mesenteric vasculature causing vasodilation (Holzer, 1992; Zheng et al., 1998). Furthermore, vasodilation would not be inhibited by any of the pharmacological agents used in this study and demonstrates the ability of splanchnic primary sensory neurons to modulate systemic arterial pressure in the absence of sympathetic transmission.

## Conclusions

In this study, we developed a method to selectively activate the splanchnic circulation via electrically stimulating the GSN. In the process, we discovered that applying nicotine to the CG overwhelmed hexamethonium blockade, and that removal of the CG did not prevent the systemic arterial pressor response indicating nicotine was acting at sites extraneous to the CG. Stimulating the GSN provoked an arterial pressor response even in the presence of hexamethonium, but post-junctional blockade of the neuroeffector junction with phentolamine and PPADs together did block the arterial pressor response to stimulating the GSN. Taken together, the inability of ganglionic blockade but the success of neuroeffector junction blockade to attenuate acute rises in systemic arterial pressure suggested that there was population of vascular-projecting post ganglionic nerve fibers in the GSN. The origin of vascular-projecting post ganglionic nerve fibers in the GSN arose from the SG and when stimulated, were sufficient to elevate systemic arterial pressure. In order for a relatively small population of neurons to have an effect on systemic arterial pressure, splanchnic vascular-projecting neurons must have wide fields of innervation, suggests a novel mechanism for the neural control of the splanchnic circulation.

# CHAPTER FOUR: ORGAN-SPECIFIC IMMUNOLESIONS OF PREVERTEBRAL GANGLIA

**Abstract**

Prevertebral ganglia are sympathetic ganglia located in the splanchnic region that innervate splanchnic viscera, vasculature, and glands. Removing a prevertebral ganglion (e.g. the celiac ganglion; CG) removes sympathetic innervation to the splanchnic region and thereby attenuates rises is systemic arterial pressure. The CG contains many different populations of neurons as well as fibers of passage, but effects of CG removal (CGx) are hypothesized to be mediated by one specific population of neurons: those projecting to the splanchnic vasculature. To test this hypothesis, we applied a neurotoxin, saporin, conjugated to an antibody against dopamine beta hydroxylase (DβH-sap), to two adjacent ~7 mm segments of mesenteric artery and vein. Applying DβH-sap to both veins and arteries reduced the depressor response evoked by stimulating the greater splanchnic nerve to -1.59 ± 1.53 mmHg from 6.22 ± 0.65 mmHg in controls. These effects depended on CG input to both veins and arteries because DβH-sap applied only to either mesenteric arteries or veins did not attenuate the response to the same degree (reduced to 4.10 ± 1.78 mmHg, and 3.80 ± 1.59 mmHg respectively). The vast ablation of tyrosine hydroxylase immunoreactive (TH-IR) fibers generated by applying DβH-sap on both mesenteric artery and vein (arteries by 72.1% and veins by 91.0%) compared to the smaller reduction by singular application to either artery (arteries by 50.9% and veins by 61.5%) or vein (arteries by 33.7% and veins by 62.6%) suggested that some vascular-projecting neurons in prevertebral ganglia projecting widely to many segments of mesenteric vasculature, while others project regionally to only a few segments of mesenteric vasculature.

## Introduction

The sympathetic nervous system plays an important role in maintaining the homeostasis of cardiovascular hemodynamics by controlling vascular resistance and capacitance during physiological conditions (Brooksby & Donald, 1972; Rowell et al., 1984). The splanchnic circulation significantly contributes to cardiovascular hemodynamics, because splanchnic veins contain the body's single largest volume of blood (capacitance), and splanchnic arteries confer the largest source of vascular resistance (Greenway & Lister, 1974). As a result, the splanchnic vasculature is densely innervated by the sympathetic nervous system (Furness & Costa, 1974), with the majority of sympathetic innervation arising from neurons with cell bodies located in three prevertebral ganglia: the celiac ganglion (CG), superior mesenteric ganglion, and splanchnic ganglion (SG; Hsieh, Liu, & Chen, 2000; Quinson et al., 2001; Trudrung, Furness, Pompolo, & Messenger, 1994). The CG and superior mesenteric ganglia lie in close proximity along the aorta just caudal to the celiac artery to form the celiac plexus, and will be henceforth referred to as the CG. The SG is a bilateral structure that resides just proximal to the CG along the greater splanchnic nerve (GSN).

The regulation of cardiovascular hemodynamics can be studied by removing sympathetic innervation to the splanchnic region. Celiac ganglionectomy (CGx) removes innervation to the splanchnic viscera and vasculature (Li et al., 2010) and has been performed in rats, dogs, humans (Grimson & Orgain, 1949; Kandlikar & Fink, 2011; King et al., 2007; Li et al., 2010; Marlett & Code, 1979). A beneficial effect of CGx is attenuating increases in arterial pressure, as seen in multiple models of hypertension (Kandlikar & Fink, 2011; King et al., 2007). In addition to neurons that innervate the vasculature of the

splanchnic region, the CG contains viscera-projecting neurons and fibers of passage that are a mix of sensory nerves (Lindh, Hökfelt, & Elfvin, 1988) and postganglionic nerve fibers (Sapru et al., 1982), so it is unknown which component of the CG, when removed, is responsible for attenuating arterial pressure. Increased sympathetic tone to splanchnic vasculature mediates long-term rises in systemic arterial pressure indicating removing sympathetic innervation to the vasculature may be responsible for attenuating increases in systemic arterial pressure. In support of this proposal, ganglionic blockade with hexamethonium or CGx both alleviate rises in systemic arterial pressure, and splanchnic venous tone (Fink et al., 2000; King et al., 2007). Similarly, ganglionic blockade with hexamethonium alleviates rises in splanchnic arterial tone in hypertension (Fink et al., 2000; Kuroki et al., 2011). Therefore, we hypothesized that CGx mediated removal of vein-projecting and artery-projecting neurons is responsible for attenuating long-term increases in systemic arterial pressure. In this study, we used the immunotoxin anti dopamine-β-hydroxylase (DβH)-saporin (DβH-sap) to target sympathetic neurons. The anti-DβH antibody recognizes membrane bound DβH presented to the synaptic milieu during neurotransmitter release to facilitate endocytosis of the immunotoxin by sympathetic neurons. The immunotoxin is then retrogradely transported back to the cell body, where saporin inactivates ribosomes causing the cell to undergo apoptosis (Jacobowitz, Ziegler, & Thomas, 1975; Wiley & Lappi, 1994; Ziegler et al., 1976). DβH-sap injected intravenously ablates sympathetic neurons in the superior cervical ganglia, while sparing sensory neurons in the dorsal root ganglia and nodose ganglia (Picklo et al., 1995). Similarly, DβH-sap injected intraperitoneally (IP) produces sympathectomy of the spleen and duodenum, but not viscera outside of the abdominal cavity such as the

heart (Worlicek et al., 2010). Taken together, DβH-sap is a tool to selectively target sympathetic neurons projecting to a desired tissue. Applying it to mesenteric arteries (MA) and veins (MV), as done here, provides insight into the hemodynamic consequences of selectively removing vascular innervation to MA and MV.

## Materials and methods

*Animals*

Adult male Sprague Dawley rats (Charles River Laboratories, Inc., Portage, MI) weighing 225-300g were used in these studies. Rats were housed in a room with a 12:12 light dark cycle and temperature control (22-24°C) and had *ad libitum* access to standard rat chow and distilled water. All experimental procedures conformed to the National Institutes of Health and Michigan State University guidelines for animal care and use.

*Application of DβH-sap to MA and MV*

Animals were anesthetized with isoflurane (2%-3% during induction and surgery, 2% after surgical preparation) in $0_2$ (0.75 l/min). Laparotomy was performed, the intestines excised, adjacently located secondary branches of superior mesenteric artery and vein 7 mm in length were secured with hanks' balanced salt solution (HBSS, Gibco) soaked gauze onto a Plexiglas platform lined with Sylgard (Dow Inc., **Fig. 4.1A**), cleared of surrounding fat (**Fig. 4.1B**), separated from each other, and encased in silicone tubing (**Fig. 4.1C**). Depending on the group, either MA, MV, or both were placed into the silicone tubing. Both ends of the silicone tubing were sealed with silicone sealant (Dow Inc.) and silastic glue (World Precision Instruments), 2.5-20 μg DβH-sap (Advanced Targeting Systems) was applied to the vessels with micropipettes (**Fig. 4.1D**), and small strips of a sterile, absorbable, gelatin sponge (Gelfoam, Pharmacia and Upjohn Co.) were placed in the silicone tubing (**Fig. 4.1E**). In some animals. IgG-saporin was substituted for DβH-sap as a negative control. Gelfoam absorbed the saporin conjugates ensuring minimal leakage. Then, silastic glue was applied to the top of the apparatus and given 5 mins to cure (**Fig. 4.1F**). The whole preparation was returned to the abdominal cavity, the

abdominal incision sutured, and the rat was left to recover for 21-23 days prior to stimulating the GSN. While the mesentery was excised, the blood vessels and surrounding tissues in the Plexiglas platform were constantly bathed with HBSS. The animal was given analgesic (Carprofen® [5mg/kg]) and antibiotics (Baytril® [5mg/kg]) for three days post-surgery.

*Stimulating the GSN*

The GSN was isolated, decentralized and stimulated as described in chapter 3. The peak increase in systemic arterial pressure was measured in response to stimuli at 1, 3 and 5 Hz. After performing the frequency-response curve, the peripheral end of the GSN was cut distal to the site of stimulation and the nerve was stimulated a final time at 3 Hz. A lack of a response confirmed the absence of current spread to surrounding structures. Animals with pressor responses after nerve section were omitted from the study. Analysis of hemodynamic responses were performed using LabChart 8 (ADInstruments), where arterial pressure and heart rate were measured as the largest change from baseline when electrically stimulating the GSN.

*Tissue collection*

After the conclusion of stimulating the GSN, the diaphragm and heart of each animal were cut. The CG and both SG ganglia were rapidly harvested and drop-fixed into ice-cold 4% paraformaldehyde. The duodenum, and the capsule of the spleen were harvested and placed into ice cold 0.1 N perchloric acid (Sigma-Aldrich). The mesentery was exorcised from the animal and placed onto a petri dish and soaked in HBSS. The superior mesenteric artery was cannulated with a 30 ml syringe and flushed with HBSS, until devoid of blood. Two sets of secondary branches of mesenteric vessels adjacent to

the encased vessels were harvested and drop-fixed into ice cold 4% paraformaldehyde. A third set of vessels were taken from the distal ileum and placed into ice cold 0.1 N perchloric acid. All samples placed into perchloric acid were frozen at -80°C and stored until analysis for NE content. All samples drop-fixed into 4% paraformaldehyde were stored at 4ºC until processed for immunohistochemistry.

*Processing ganglionic tissue*

Ganglia were processed by the Histopathology Laboratory at Michigan State University. In brief, ganglia were vacuum infiltrated with paraffin on a VIP tissue processor (Sakura); then embedded with a HistoCentre III™ (ThermoFisher) embedding station. Blocks were sectioned on rotary microtome (Reichert Jung) at 4 μm in a series of 4. Sections were then dried at 56°C in a slide incubator for 2-24 hours. One series underwent a nissl stain and was coverslipped with Flo-Texx (Richard-Allan Scientific).

A second series underwent immunodetection for glial fibrillary acidic protein (GFAP) using the following protocol. Slides were incubated in 2 changes of xylene, then hydrated through descending grades of ethanol to distilled water. Rinsed in several changes of $dH_2O$ and incubated in tris-phosphate buffered saline (TPBS) for 5 minutes. The series then underwent antigen retrieval in 0.03% Pronase E (Sigma-Aldrich) in TPBS for 10 minutes at 37°C. After antigen retrieval, samples were rinsed in running tap water for 5 mins, and then rinsed times in $dH_2O$ for 5 minutes each. Endogenous peroxidase was blocked with 3% $H_2O_2$ in methanol for 20 minutes at room temperature (RT). Slides were then rinsed with running tap water for 5 minutes and washed in $dH_2O$ three times. Slides were then placed in TPBS with Tween 20 for 5 minutes, blocked for 30 minutes with normal goat serum incubated with a Rabbit anti GFAP antibody at 1:250 (DAKO, lot

# 00015316) for 60 mins, incubated with a goat anti Rabbit at 1:136 for 30 mins, then incubated with an ABC kit (Vector), and finally visualized with 3,3'-Diaminobenzidine for 10 minutes. Slides were dehydrated with ascending grades of ethanol, cleared in several changes of Xylene, and cover slipped with Flo-Texx (Thermo Scientific) mounting media. GFAP stained tissue sections were visualized on an inverted microscope with a MicroFIRE color camera (Optronics, Inc) and a 20x objective. Image Pro Plus (Media Cybernetics) software was used to acquire digital micrographs.

*Mesenteric vasculature immunohistochemistry*

Secondary branches of mesenteric vasculature were post-fixed in paraformaldehyde for at least 48 hours, perivascular fat was stripped off of the vessels. vessels were then permeabilized in TPBS with 0.3% triton (IB), blocked in 10% NGS in IB solution, and incubated for 24-48 hours with either an antibody against tyrosine hydroxylase (TH, 1:500 in 10% NGS IB solution, Enzo) or calcitonin gene related peptide (CGRP, 1:600 in 10% NGS IB solution, Sigma-Aldrich). After incubation with primary antibody, vessels were then washed in TBPS, incubated with a goat anti-rabbit Cy5 secondary antibody diluted in 1% NGS in IB (1:100, Jackson ImmunoResearch), washed three times in TPBS, and then cover slipped on superfrost slides (VWR) with ProLong Gold Antifade (Life Technologies). Samples were then visualized on a confocal microscope (Olympus Fluoview-F1000) by optimizing the photomultiplier tube voltage before collection of each series of Z-stack images.

*Quantification of prevertebral neurons and tyrosine hydroxylase immunoreactive (TH-IR) fibers*

Ganglia previously cut in a series of four had images of every other section acquired from the Nissl stained series and blinded to the observer. Ganglionic tissue was traced in each image and the area recorded using ImageJ software (National Institutes of Health). Neurons completely within the traced area exhibiting a completely defined cytoplasm or nucleus were counted using the cell counter plugin in ImageJ. The strict counting parameters and imaging of every 8$^{th}$ section made double counting a rare event.

Z-stacks of secondary vessels stained for TH were converted to max intensity projections, saved, and re-opened in ImageJ. A 45° line transecting the image of the vessel was drawn as described previously (De Fontgalland et al., 2008). In brief, TH positive fibers intersecting the line were counted and normalized to the length of the line.

*NE content*

Duodenums were thawed on ice, weighed, and homogenized in 250 μl 0.1 N perchloric acid using a Bead Ruptor (Omni Bead) with a disruption time of 45 s for two cycles. Splenic capsules were thawed on ice, weighed, and sonicated three times for one second using a cup horn sonicator. Doudenum, and splenic samples were spun down twice at 18,000 RCF at 4°C while collecting the supernatant after each centrifugation.

Secondary branches of mesenteric vessels were thawed on ice, stripped of fat, and homogenized using a Powergen 125 (Thermo Fisher) tissue homogenizer at high speeds for bursts no longer than 3 seconds until the sample was completely disrupted. Samples were then centrifuged at 16,000 RCF for 5 minutes, the supernatant was collected and queued up to 100 μl with 0.1 N perchloric acid. All pellets were stored at -

80°C in 100 μl NaOH for later analysis with a bovine serum albumin protein assay (Bio-Rad).

All supernatants were analyzed for NE content using high-performance liquid chromatography by electrochemical detection as previously described (Li et al., 2010). Duodenal and splenic NE content were normalized to tissue weight and expressed as NE (ng)/protein (g). NE content of mesenteric vessels were normalized to protein content as measure by bovine serum albumin protein assay and expressed as NE (ng)/protein (mg).

*Data analysis*

Mean values of arterial pressure and heart rate responses were analyzed using a mixed two-way ANOVA with and posthoc testing using a bonferroni's procedure (Graphpad Prism 5). Mean values from neuronal counts, TH-IR fiber analysis and NE content analysis were compared using a two-tailed Student's t-test. $P \leq 0.05$ was considered statistically significant. All data are expressed as mean ± SEM.

## Results

*Neuronal ablation mediated by DβH-sap is dose-dependent*

CG and SG were visualized via a Nissl stain to investigate the size of the lesion generated by 2.5-20 μg vessel-applied DβH-sap (**Fig. 4.2**). Infusing DβH-sap 20 μg significantly reduced prevertebral neuronal number by 94% in both the CG and SG ($p \leq 0.05$, **Fig. 4.3A**), but total area of either ganglion was not reduced (**Fig. 4.3B**). Ablation of prevertebral neurons with 20 μg DβH-sap increased observable GFAP-IR in both the CG and SG (**Fig. 4.4B, D**). The sympathetic innervation of the vasculature was also affected by vessel-applied DβH-sap, which dose-dependently reduced tyrosine hydroxylase immunoreactivite (TH-IR) fibers on MAs and MVs (**Fig. 4.5A-J**). The number of TH-IR fibers on MA was significantly reduced in animals receiving 20 μg DβH-sap ($p \leq 0.05$, **Fig 4.5K**), while the number TH-IR fibers on MV was significantly reduced in animals receiving 5, 10, or 20 μg DβH-sap ($p \leq 0.05$ **Fig 4.5K)**. Another marker for sympathetic innervation, NE content, was used to analyze sympathetic innervation to viscera and vasculature. No dose of DβH-sap reduced NE content in the duodenum, spleen, or mesenteric vasculature. Animals treated with 20 μg DβH-sap were not analyzed (**Fig. 4.6**).

The effect of sympathectomy on systemic arterial pressure was examined by stimulating the GSN. DβH-sap (2.5-10 μg) did not reduce the arterial pressor response to stimulating the GSN at any frequency as compared to frequency matched controls (**Fig. 4.7B-D**). However, stimulating the GSN evoked an arterial depressor response in animals receiving 20 μg DβH-sap that increased throughout the stimulation period, reached its maximum at the end of stimulation and persisted for several seconds after stimulation

ceased ($p \leq 0.05$, **Fig 4.7E**). Depressor responses from stimulating the GSN at 3 Hz and 5 Hz were significantly different from controls in animals receiving 20 μg DβH-sap ($p \leq 0.05$, **Fig 4.8A**). Pressor responses were frequency-dependent in control animals (**Fig 4.8A**). Stimulating the GSN did not significantly impact heart rate in any parameter tested (**Fig. 4.8B**).

Animals were weighted at the beginning and end of the 21-23 day time course as a marker for disruptions in whole-body metabolism. DβH-sap (20 μg) significantly attenuated weight gain, while doses of 2.5-10 μg DβH-sap did not experience any attenuations in weight gain during the course of the experiment ($p \leq 0.05$, **Fig. 4.9**).

*DβH-sap mediated lesions require access to innervated mesenteric vasculature*

Because DβH-sap mediated ablations were widespread, the site of DβH-sap uptake by prevertebral neurons was investigated to rule out endocytosis of DβH-sap by nerve terminals not contained in the encasement apparatus. IP injection of 20 μg DβH-sap ablated 85% of neurons in both the CG and SG ($p \leq 0.05$, **Fig. 4.10A**), but total area was not reduced (**Fig. 4.10B**). TH-IR fibers on MA and MV were significantly reduced in animals receiving 20 μg DβH-sap via IP injection or via application to the MA and MV ($p \leq 0.05$, **Fig. 4.11I**). However, suturing the segment of vasculature proximal to DβH-sap application prevented significant reductions in TH-IR fibers on MA and MV (**Fig. 4.11I**). Innervation to the viscera and vasculature was assessed by analyzing whole tissue NE content. IP injection of 20 μg DβH-sap significantly reduced duodenal, splenic, and mesenteric vasculature NE content ($p \leq 0.05$, **Fig 4.12A-B**). Suture pretreatment significantly reduced splenic NE content, but duodenal and mesenteric vasculature NE content was not reduced ($p \leq 0.05$, **Fig 4.12C-D**). Furthermore, DβH-sap was not

endocytosed by sensory neurons, because IP injection of DβH-sap had no effect on sensory innervation to the mesenteric vasculature. IP injection of DβH-sap did not significantly reduce CGRP-IR in MA (**Fig. 4.13B**) or MV (**Fig. 4.13D**) as compared to controls (**Fig. 4.13A, C**).

The effect of DβH-sap mediated lesions on systemic arterial pressure was examined by stimulating the GSN. IP injection or mesenteric application of DβH-sap attenuated and reversed the pressor response to stimulation of the GSN at 3 Hz and 5 Hz as compared to frequency matched controls ($p \leq 0.05$, **Fig. 4.14, Fig. 4.15**). Suture pretreated animals had pressor responses similar to IgG-sap treated controls (**Fig. 4.14, Fig. 4.15**). Heart rate was not significantly impacted by GSN stimulation after any method of DβH-sap application.

*DβH-sap applied to MA or MV*

DβH-sap (20 μg) was applied on either two segments of MA or MV, henceforth, referred to as DβH-MA and DβH-MV respectively, to selectively ablate innervation to arteries or veins. The sympathetic innervation to the splanchnic region was investigated with TH immunohistochemistry and the analysis of whole tissue NE content. DβH-MA and DBH-MV significantly reduced TH-IR fibers on MA and MV ($p \leq 0.05$, **Fig 4.16I**). DβH-MA significantly reduced duodenal, splenic, and venous NE content, while DβH-MV significantly reduced splenic and venous NE content ($p \leq 0.05$, **Fig. 4.17**).

The effect of the lesion generated by DβH-MA and -MV on systemic arterial pressure was examined by stimulating the GSN. DβH-MA and -MV visibly (**Fig. 4.18**) and statistically ($p \leq 0.05$, **Fig. 19A**) reduced the arterial pressor responses to stimulation of the GSN. Heart rate was not significantly different between any groups during the

stimulation period (**Fig. 19B**). Weight gain was significantly attenuated in the DBH-MA group, but not the DBH-MV group ($p \leq 0.05$, **Fig. 4.20**).

## Figures

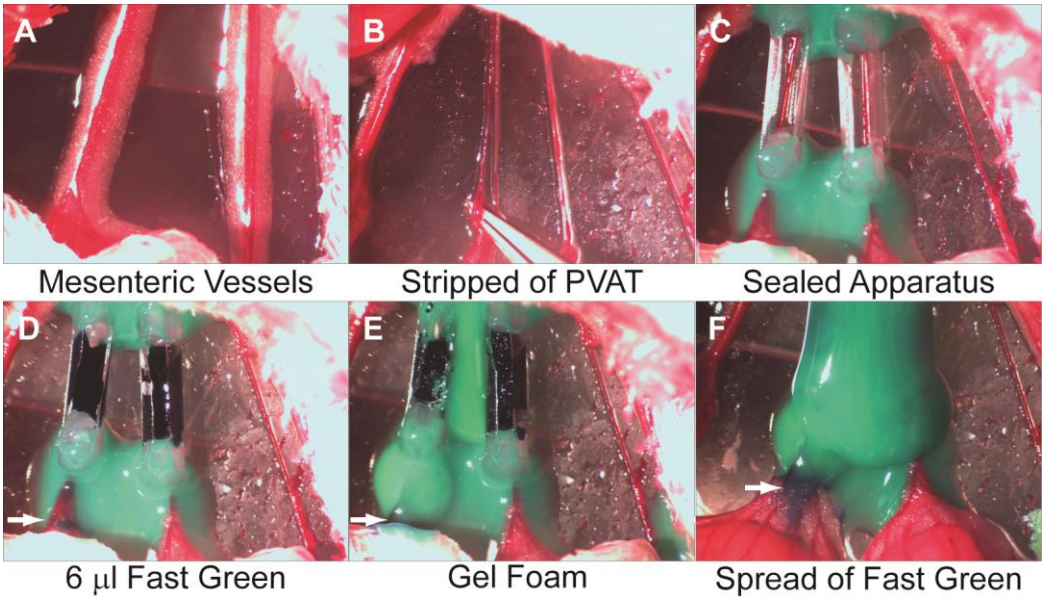


**Figure 4.1 Photomicrographs of the technique used to isolate segments of mesenteric vasculature.** Two branches of MA and MV prior to removal of perivascular adipose tissue (PVAT) (**A**) and after removal of PVAT (**B**). The bottom portion of the encasement apparatus before addition of fast green (**C**). Fast green solution (6 μl) was added to the apparatus (**D**), followed by a pledget of gel foam to each apparatus (**E**), and the top of the apparatus was sealed with silicone elastomer (**F**). By design, one seal was compromised on the left apparatus to demonstrate the ability to track solutions leaving the apparatus as indicated by the white arrows.

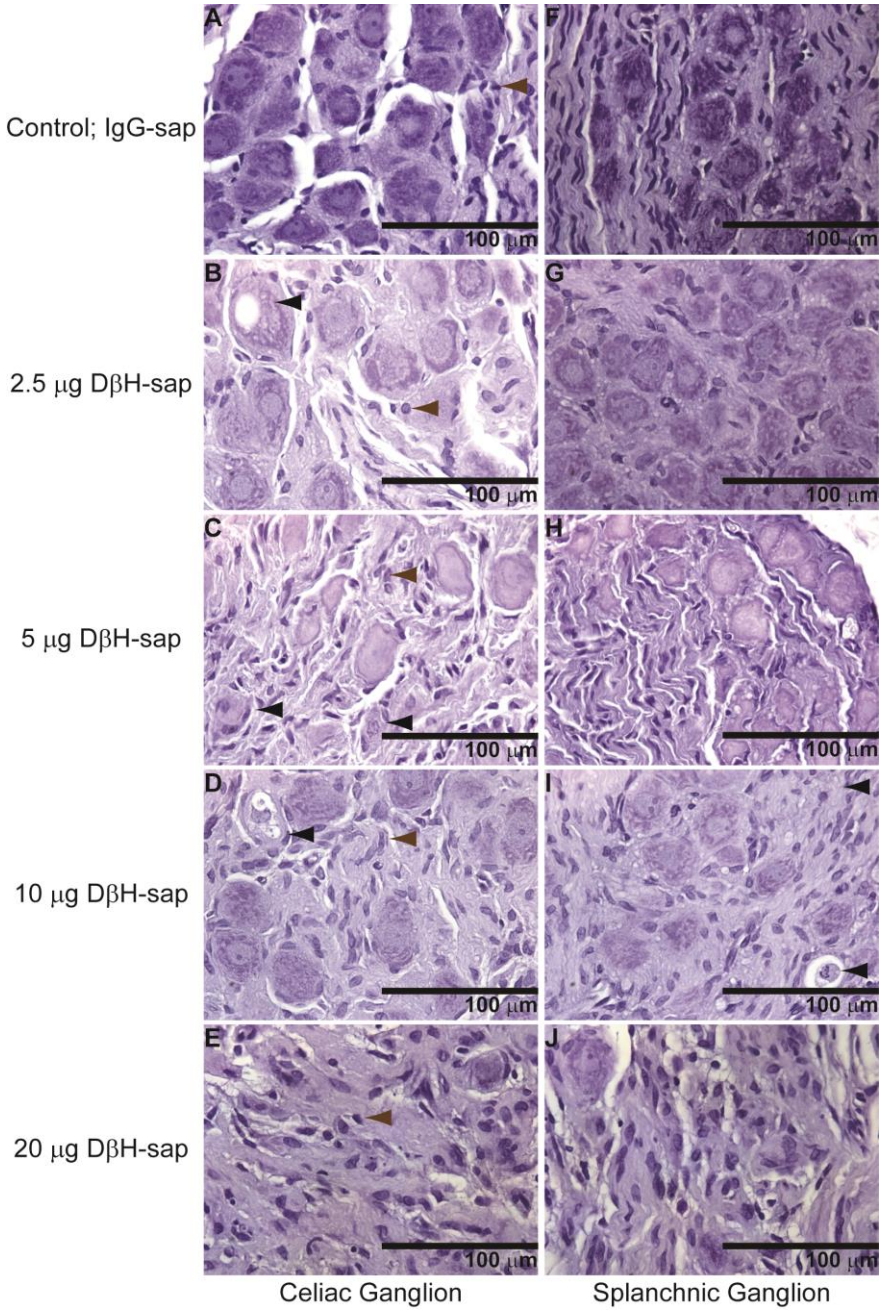


**Figure 4.2 Vessel-applied DβH-sap had a dose-dependent effect on neurons in prevertebral ganglia.** Vessel-applied IgG-sap had no adverse effects on neurons in the CG (**A**) and SG (**F**). Vessel-applied 2.5-10 μg DβH-sap sparsely ablated neurons in the CG (**B, C, D**) and SG (**G, H, I**). Vessel-applied 20 μg DβH-sap ablated vast quantities of neurons in the CG (**E**) and SG (**J**). Black arrows indicate neurons showing signs of cell death. Brown arrows indicate satellite cells. All slices were visualized via Nissl stain, and photomicrographs were taken with a 40x objective.

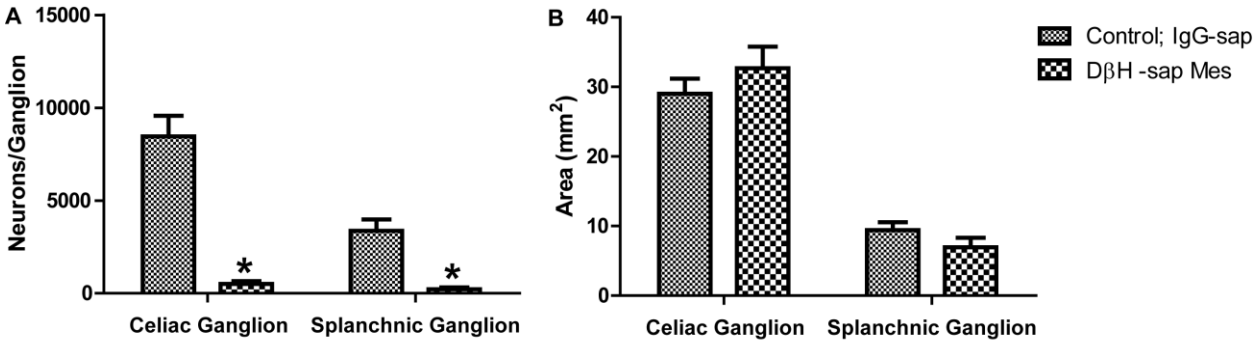


**Figure 4.3 Vessel-applied DβH-sap reduced neuronal number but not total area of prevertebral ganglia.** DβH-sap applied to MA and MV significantly reduced neuronal number in the CG and SG (**A**), but did not reduce the total area of either ganglion (**B**). Data expressed as means ± SEM, * $p \leq 0.05$ as compared to controls.

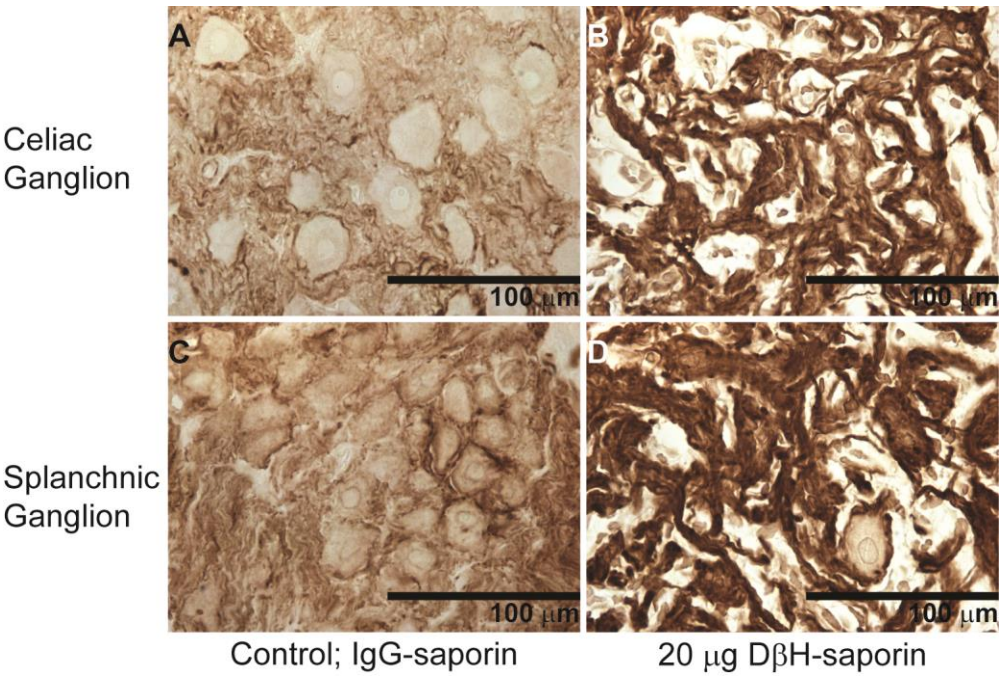


**Figure 4.4 Vessel-applied DβH-sap increased GFAP immunoreactivity in prevertebral ganglia.** IgG-sap applied to the mesenteric vasculature illustrates endogenous GFAP-IR in the CG (**A**) and SG (**C**). DβH-sap applied to the MA and MV increases GFAP-IR in the CG (**B**) and SG (**D**).

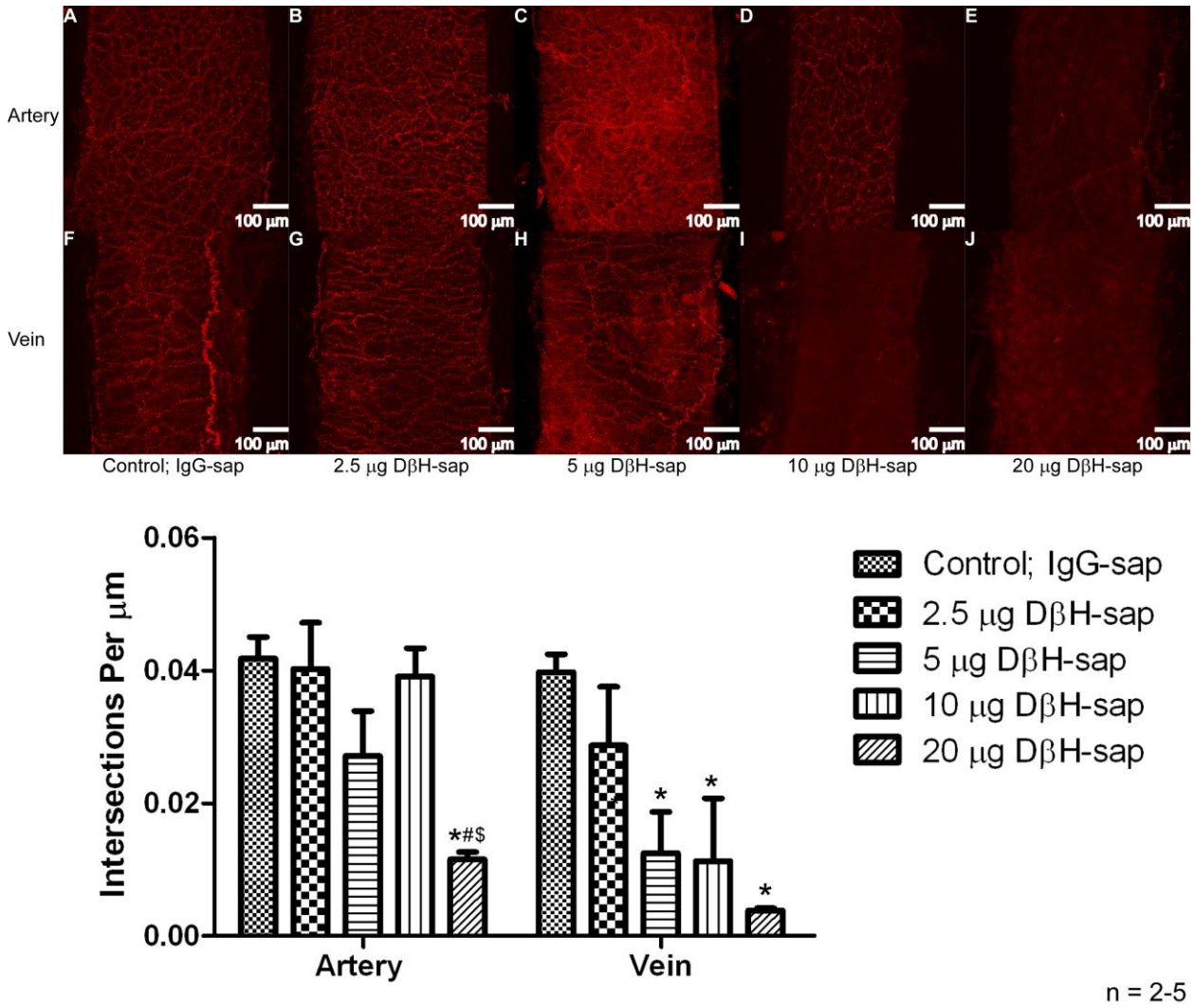


**Figure 4.5 Vessel-applied DβH-sap had a dose-dependent effect on the disruption of sympathetic innervation to MA and MV.** Vessel applied IgG-sap did not visibly affect TH-IR fibers on MA or MV (**A, F**). Photomicrographs of MA (**B**, **C, D, E**) and MV (**G, H, I, J**) after application of 2.5, 5, 10, or 20 µg DβH-sap to the mesenteric vasculature. Quantification of TH-IR fibers on arteries were significantly reduced in animals receiving 20 µg DβH-sap (**K**). TH-IR fibers on veins were significantly reduced in animals receiving 5, 10, or 20 µg DβH-sap as compared to controls (**K**). Data expressed as mean ± SEM. $^{*,\#,\$}$ $p \leq 0.05$ as compared to Control; IgG-sap, 5 µg, and 10 µg respectively.

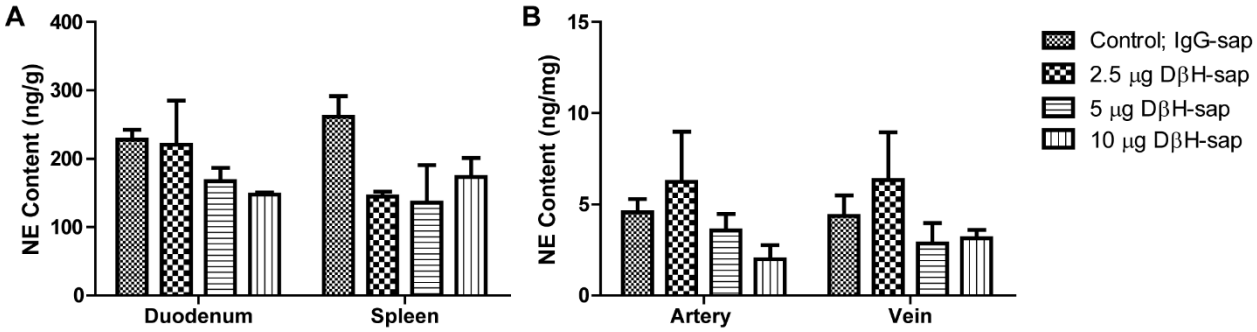


**Figure 4.6 NE content was not reduced in the duodenum, the spleen, or the mesenteric vasculature in animals receiving 2.5-10 μg DβH-sap.** NE content in the duodenum and spleen was not significantly different in animals receiving 2.5, 5, or 10 μg DβH-sap (**A**). NE content in MAs and MVs was not significantly different in animals receiving 2.5, 5, or 10 μg DβH-sap (**B**). Data expressed as means ± SEM, n = 2-9.

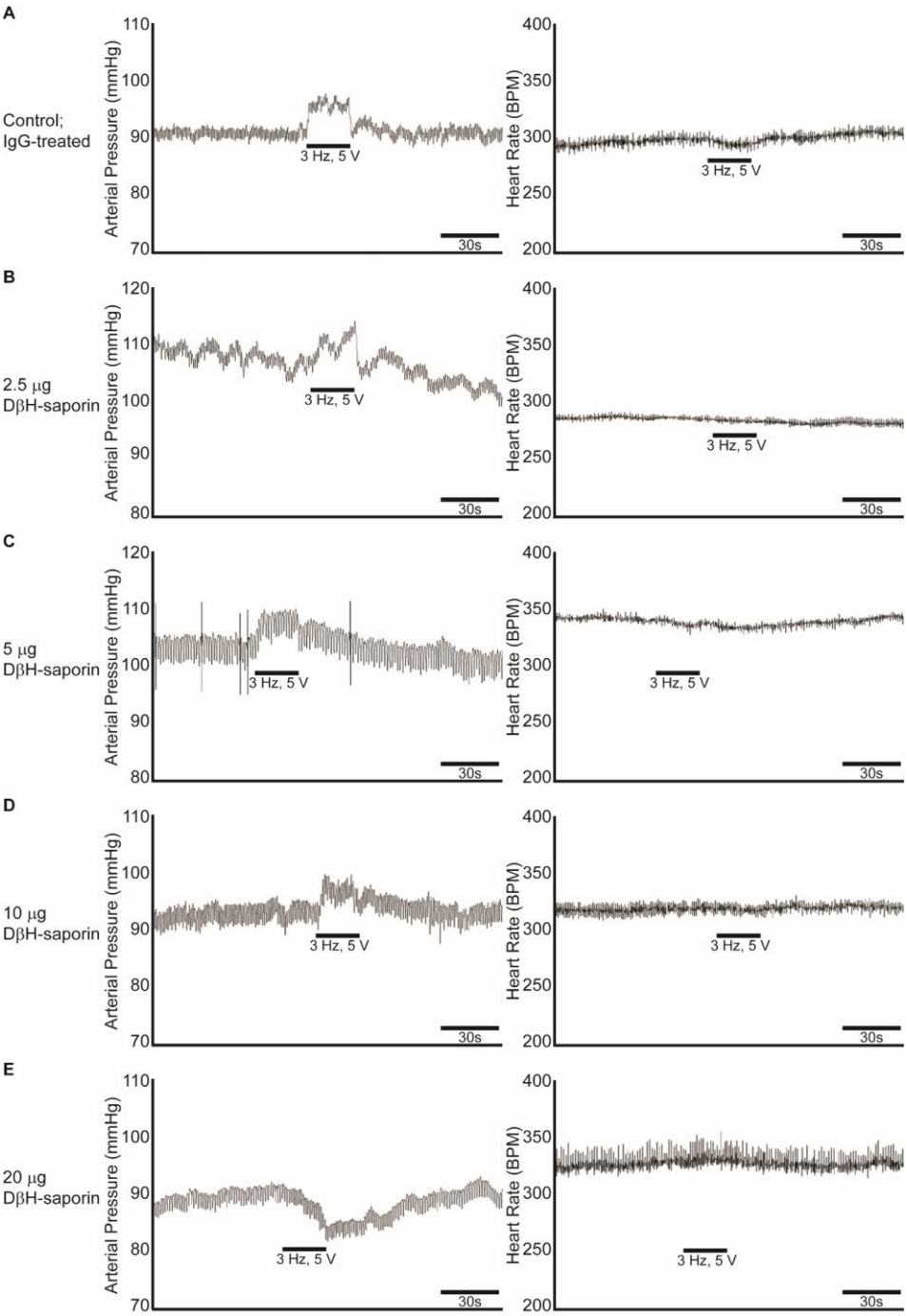


**Figure 4.7 Arterial blood pressure and heart rate responses to stimulation of the GSN 21-23 days after application of vessel-applied DβH-sap.** IgG-saporin applied to the mesenteric vasculature demonstrates the control pressor and heart rate response to stimulation of the GSN at 3 Hz, 5 V, 1 ms, 20 s (**A**). Vasculature application of 2.5, 5, or 10 μg DβH-sap did not attenuate the pressor response to GSN stimulation (**B-D**). Vessel-applied 20μg DβH-sap reversed the pressor response to GSN stimulation (**E**). Stimulation of the GSN had minimal impact on heart rate throughout the course of the study (**A-E**).

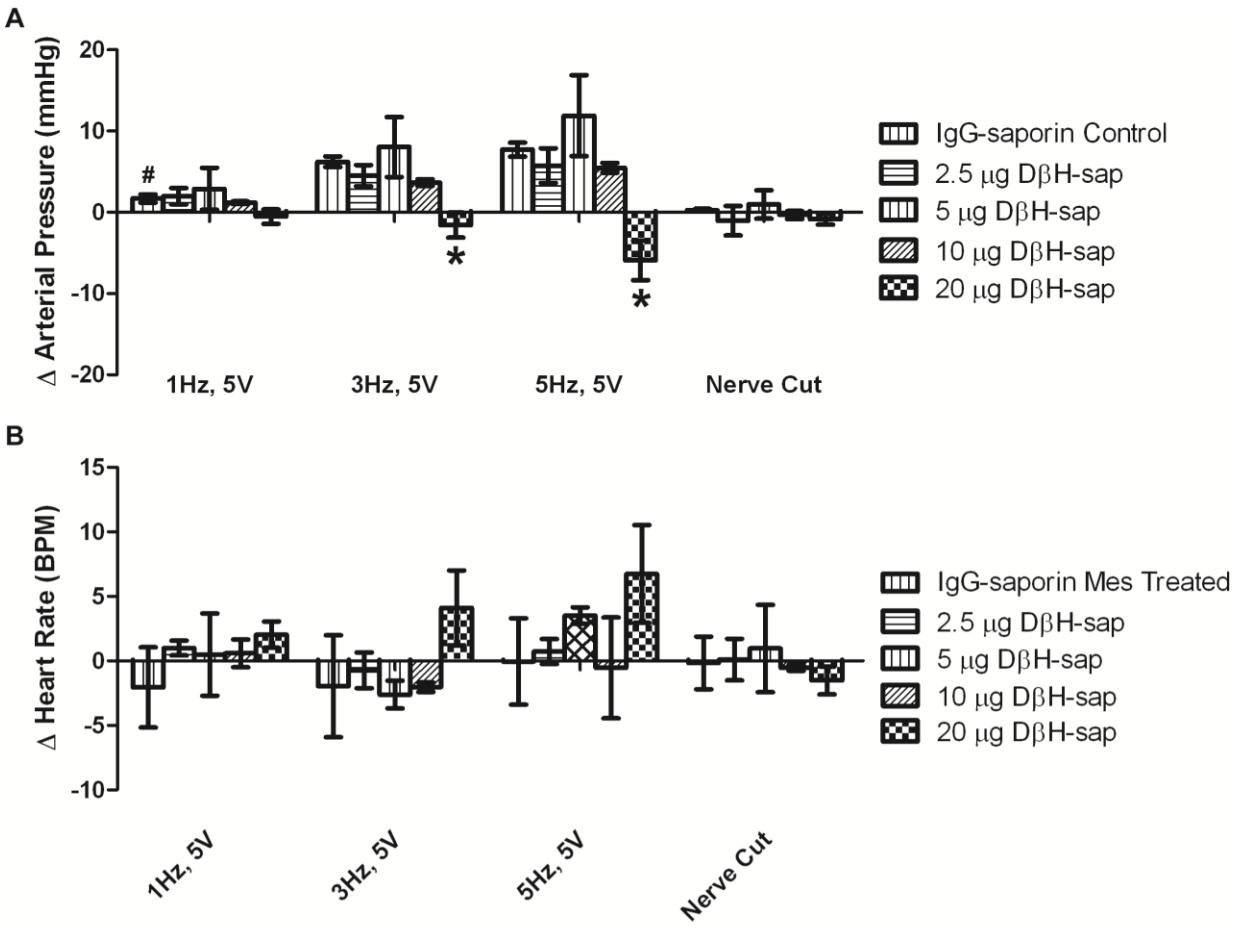


**Figure 4.8 Vessel-applied 20 μg DβH-sap reversed the pressor response to stimulation of the GSN, but did not significantly alter heart rate.** Vessel-applied 20 μg DβH-sap reversed the arterial pressor response at 3 Hz and 5 Hz (**A**). Smaller doses did not have a significant effect on arterial pressure. Quantification of heart rate to stimulation of the GSN revealed no effect of any experiment condition (**B**). Data expressed at mean ± SEM. $^{*,\#}$ $p \leq 0.05$ as compared to controls, or 5 Hz respectively.

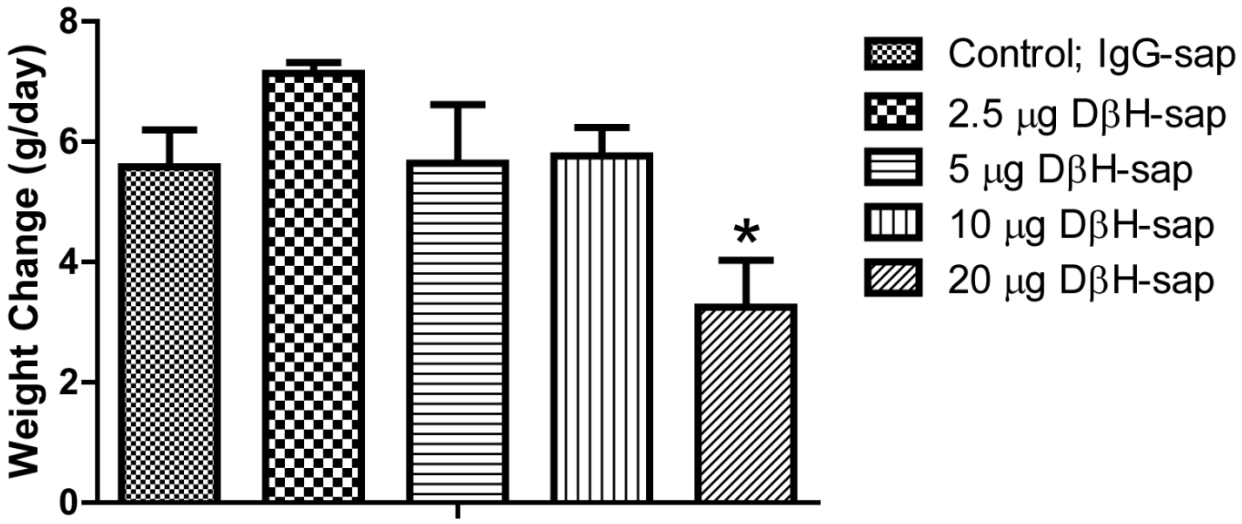


**Figure 4.9 Weight gain is significantly attenuated in animals receiving 20 μg DβH-sap.** Vessel-applied 2.5-10 μg DβH-sap did not significantly alter weight gain during the course of the experiment. Vessel-applied 20 μg DβH-sap significantly reduced weight gain during the course of the experiment. Data expressed as mean ± SEM, * $p \leq 0.05$ as compared to controls.

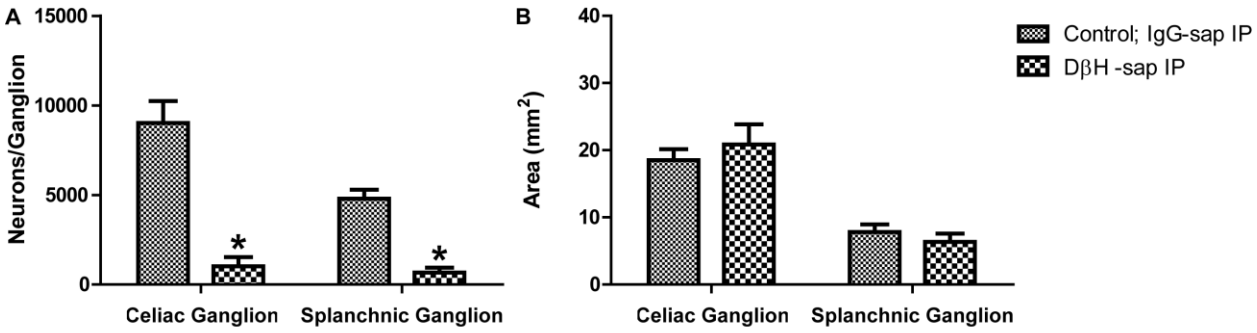


**Figure 4.10 DβH-sap injected IP reduces neuronal number, but not total area of prevertebral ganglia.** DβH-sap injected IP significantly reduced neuronal number in the CG and SG (**A**), but did not reduce the total area of either ganglion (**B**). Data expressed as mean ± SEM, * $p \leq 0.05$ as compared to controls.

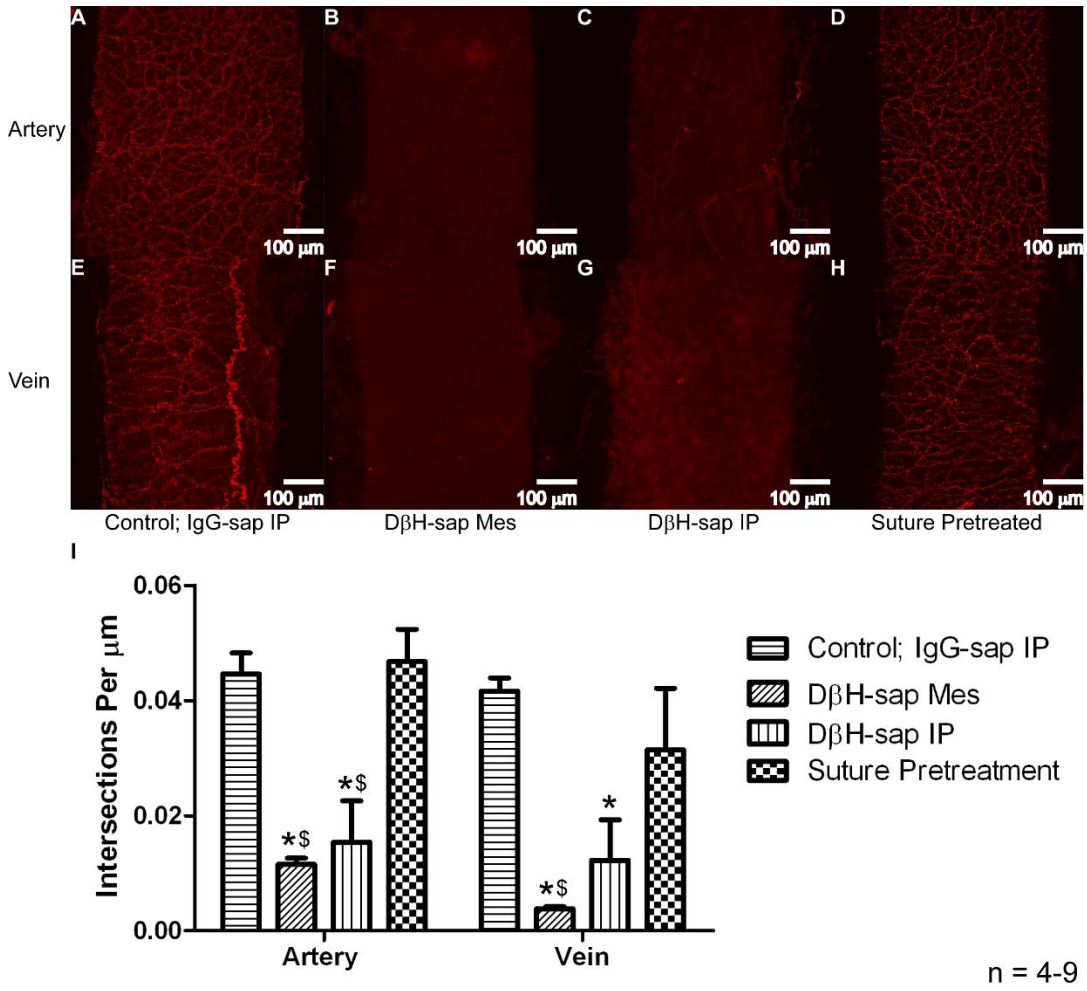


**Figure 4.11 DβH-sap mediated disruption of sympathetic innervation to MA and MV is dependent on retrograde transport of DβH-sap from perivascular nerves.** TH-IR on MA and MV of IgG-sap controls (**A, E**). DβH-sap applied to mesenteric vasculature (**B, F**) or injected IP (**C, G**) significantly reduced TH-IR fibers on MA and MV (**I**). Sutures placed proximal to the DβH-sap application site attenuated significant reductions in TH-IR fibers on MA (**D, I**) and MV (**H, I**). Data expressed at mean ± SEM. $^{*,\$}$ $p \leq 0.05$ as compared to control and suture pretreatment groups respectively.

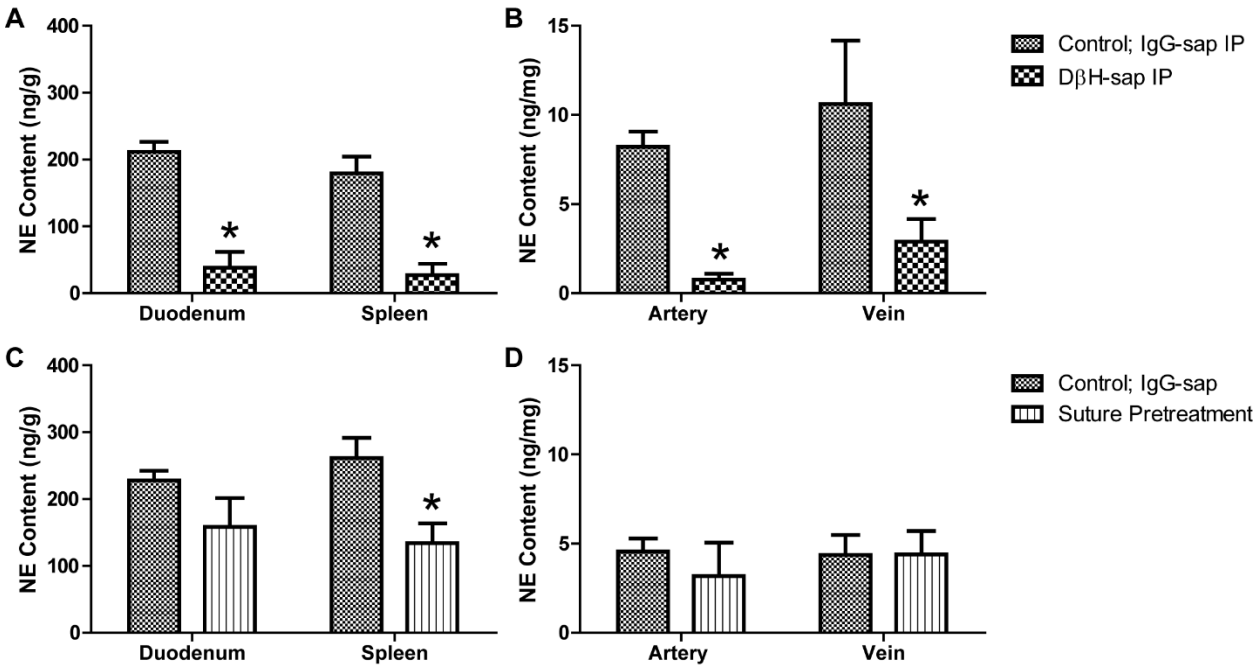


**Figure 4.12 Access to perivascular nerve fibers is required to reduce NE content in splanchnic viscera and vasculature.** DβH-sap injected IP significantly reduced NE content in the duodenum, spleen (**A**), and mesenteric vasculature (**B**). DβH-sap applied to a segment of mesenteric vasculature, ligated with sutures proximal to the application site, significantly reduced NE content in the spleen (**C**), but not in the duodenum (**C**) or mesenteric vasculature (**D**). Data are expressed as mean ± SEM, * = $p \leq 0.05$ as compared to similarly treated controls, n = 4-11.

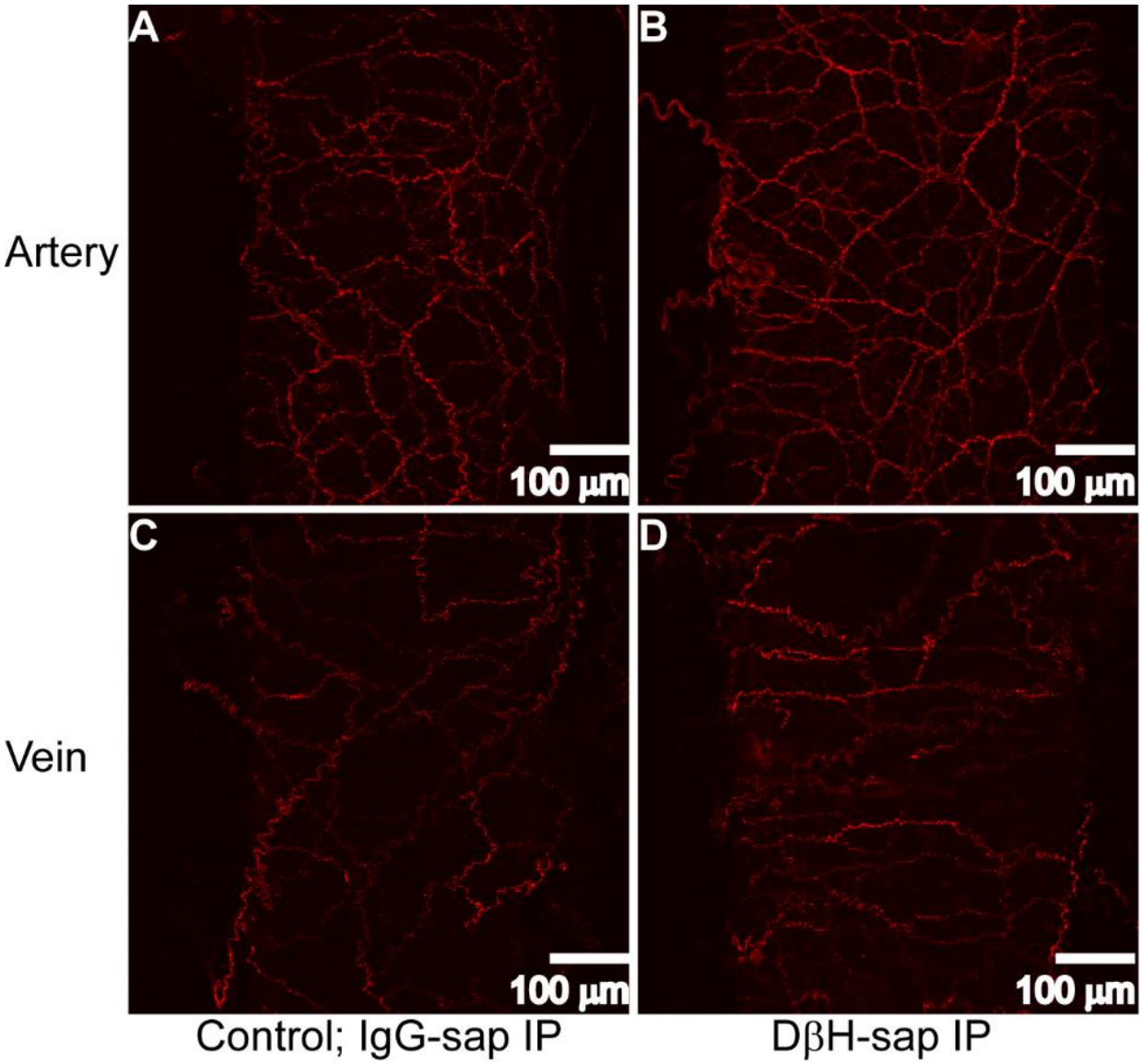


**Figure 4.13 DβH-sap injected IP did not reduce CGRP-IR fibers on MA or MV.** Photomicrographs taken with a 20X objective of control rats injected with IgG-saporin revealed endogenous CGRP positive fibers innervating MA (**A**) and MV (**C**). Photomicrographs taken with a 20X objective of rats injected with 20 µg DβH-sap revealed CGRP positive nerve fibers on MA (**B**) and MV (**D**).

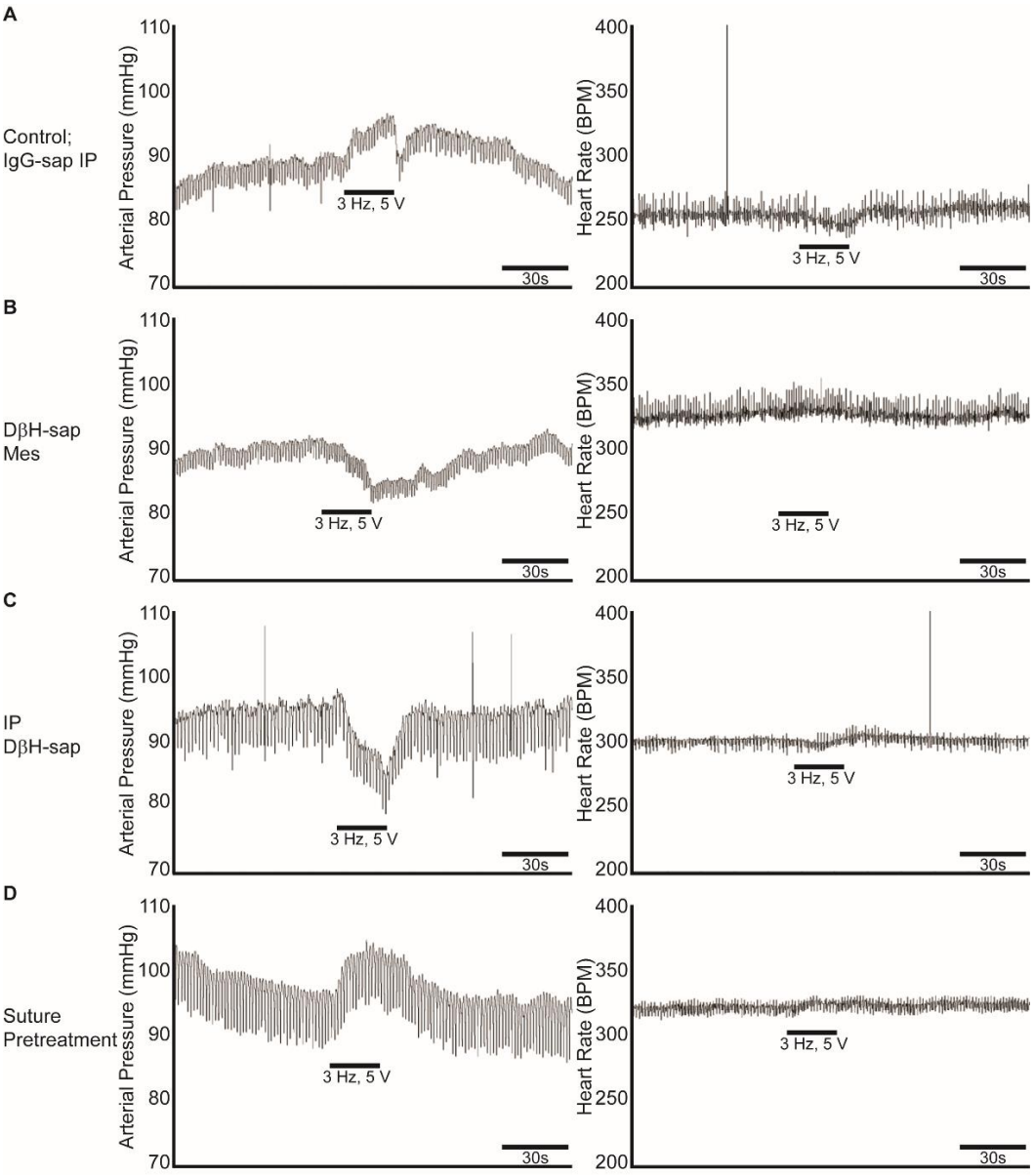


**Figure 4.14 Blockade of DβH-sap uptake at perivascular nerve terminals with suture pretreatment attenuated the action of DβH-sap on arterial pressure.** IgG-saporin injected IP demonstrates the control pressor and heart rate response to GSN stimulation (**A**). Vessel-applied DβH-sap to the MA and MV (**B**) reversed the pressor response to GSN stimulation with minimal impact on heart rate. IP injection of DβH-saporin reversed the pressor response to GSN stimulation with minimal impact on heart rate (**C**). Sutures placed proximal to the DβH-sap application site attenuated significant reductions in arterial pressor responses to GSN stimulation (**D**).

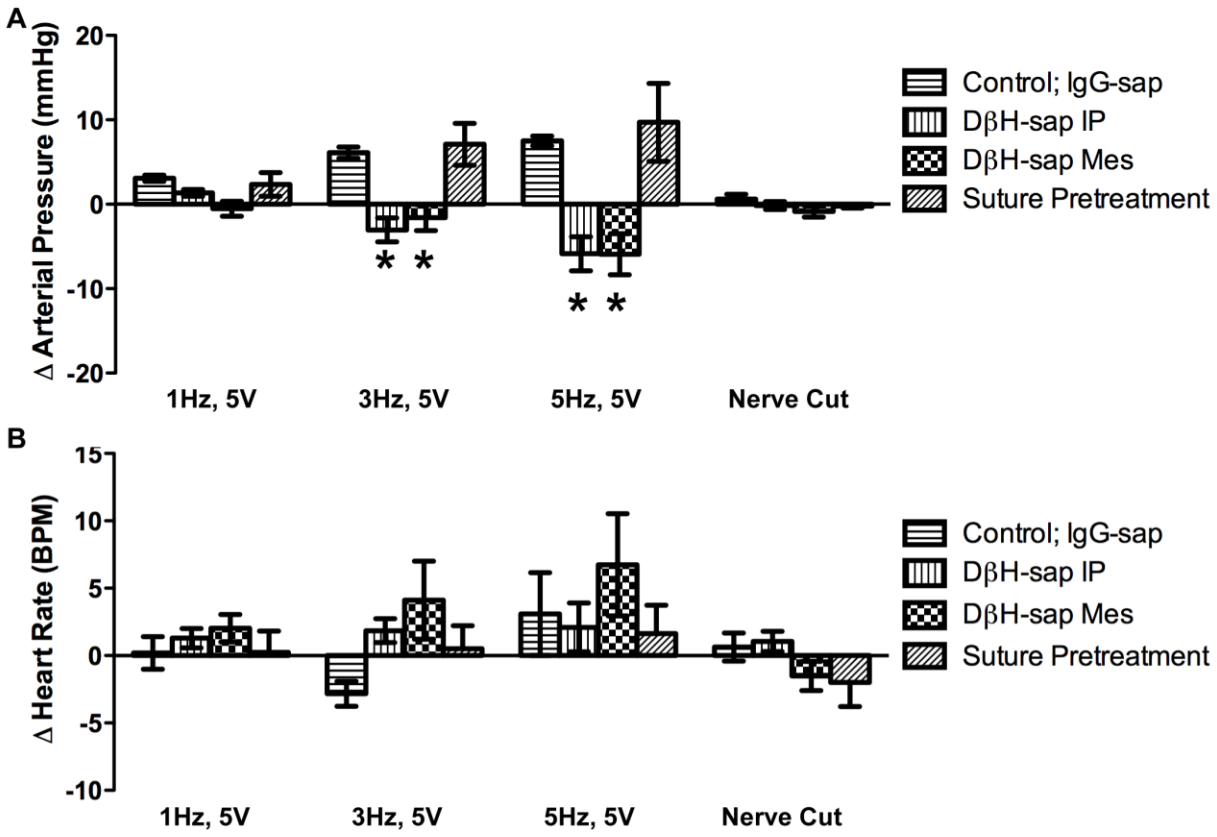


**Figure 4.15 Suture pretreatment blocks the action of DβH-sap on arterial pressure.** DβH-sap injected IP or applied to the mesenteric vasculature reversed the arterial pressor response at 3 Hz and 5 Hz (**A**). Suture pretreatment blocked the reversal of the arterial pressure response to DβH-sap applied to MA and MV at 3 Hz and 5 Hz. No experimental condition had any significant effect on heart rate (**B**). Data expressed at mean ± SEM. * $p \leq 0.05$ as compared to IgG-saporin, n = 3-7.

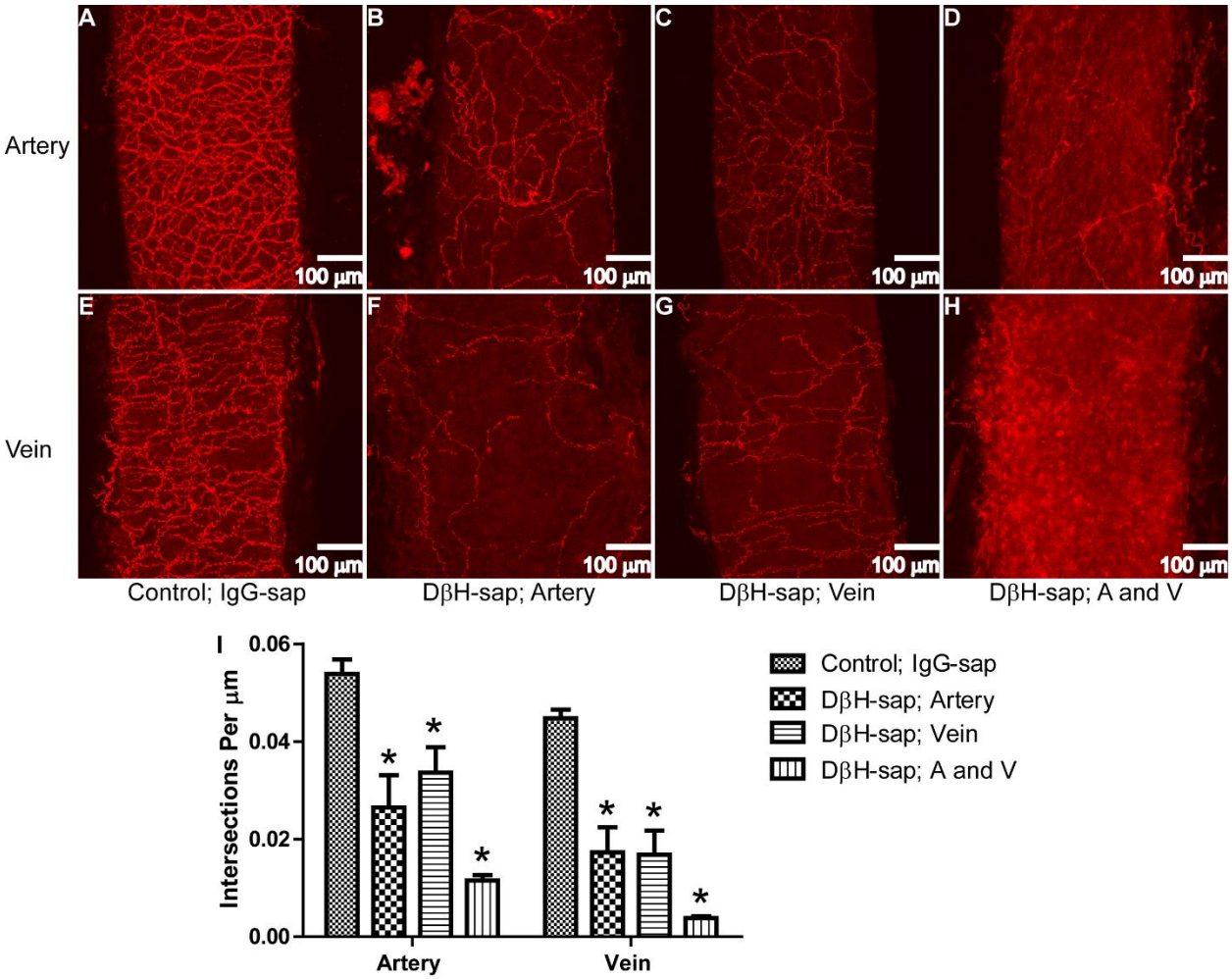


**Figure 4.16 TH-IR fibers are reduced when DβH-sap is applied to arteries, veins, or both.** IgG-sap applied to MA and MV demonstrate control levels of TH-IR fibers (**A, E**). DβH-sap applied to the MA (**B, F**) or MV (**C, G**) significantly reduced TH-IR fibers on MA and MV (**I**). DβH-sap applied to MA and MV (**D, H**) significantly reduced TH-IR fibers on MA and MV (**I**). Data expressed at mean ± SEM. * $p \leq 0.05$ as compared to controls, n = 5-11.

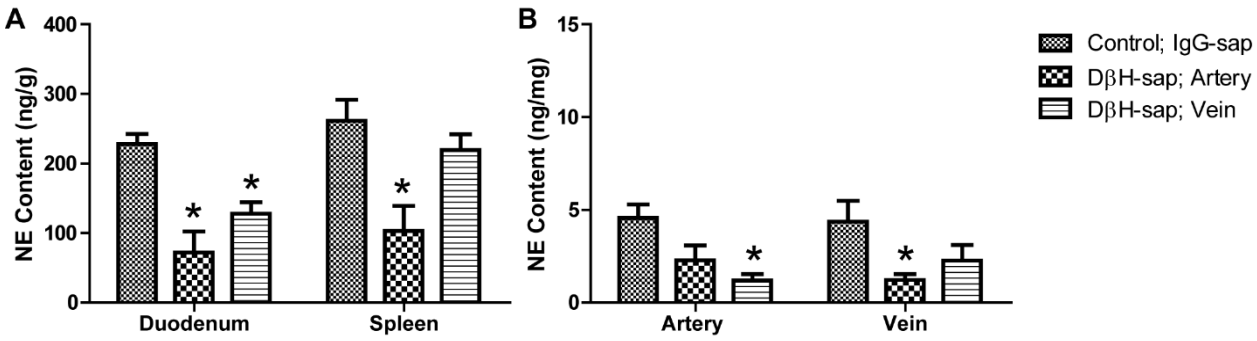


**Figure 4.17 DβH-MA and DβH-MV have differential effects on NE content in splenic and vascular tissue.** DβH-MA significantly reduced NE content in the duodenum, spleen (**A**), and MV (**B**). DβH-MV significantly reduced NE content in the duodenum (**A**), and MA (**B**). Data expressed as means ± SEM, * = $p \leq 0.05$ as compared to controls, n = 9-11.

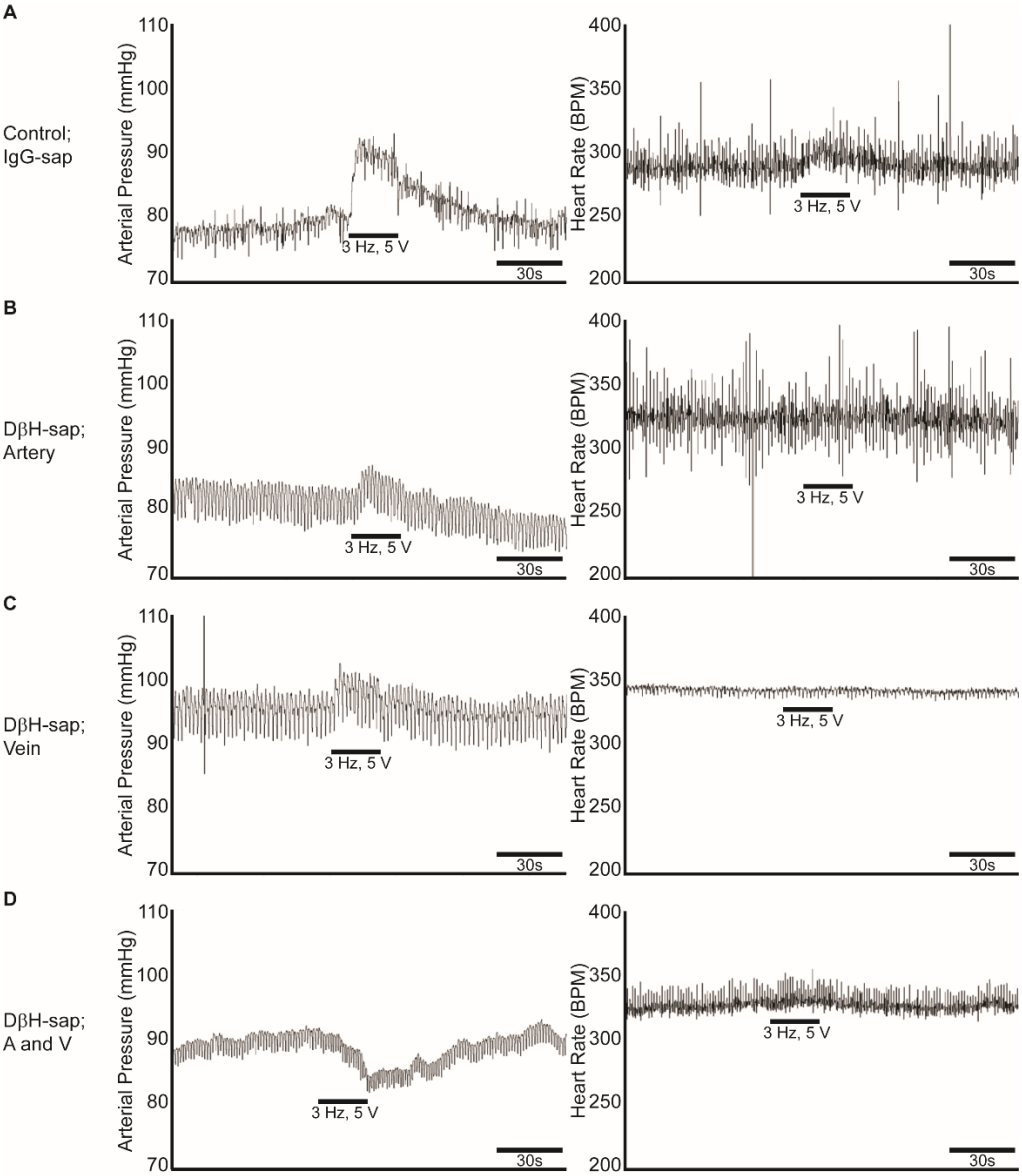


**Figure 4.18 DβH-MA and –MV reduced, but did not block the arterial pressure response to stimulation of the GSN.** The control pressor and heart rate response to stimulation of the GSN at 3 Hz (**A**). DβH-MA and -MV attenuated the pressor response to GSN stimulation with minimal impact on heart rate (**B, C**). Vessel-applied DβH-sap reversed the pressor response to GSN stimulation with minimal impact on heart rate (**D**).

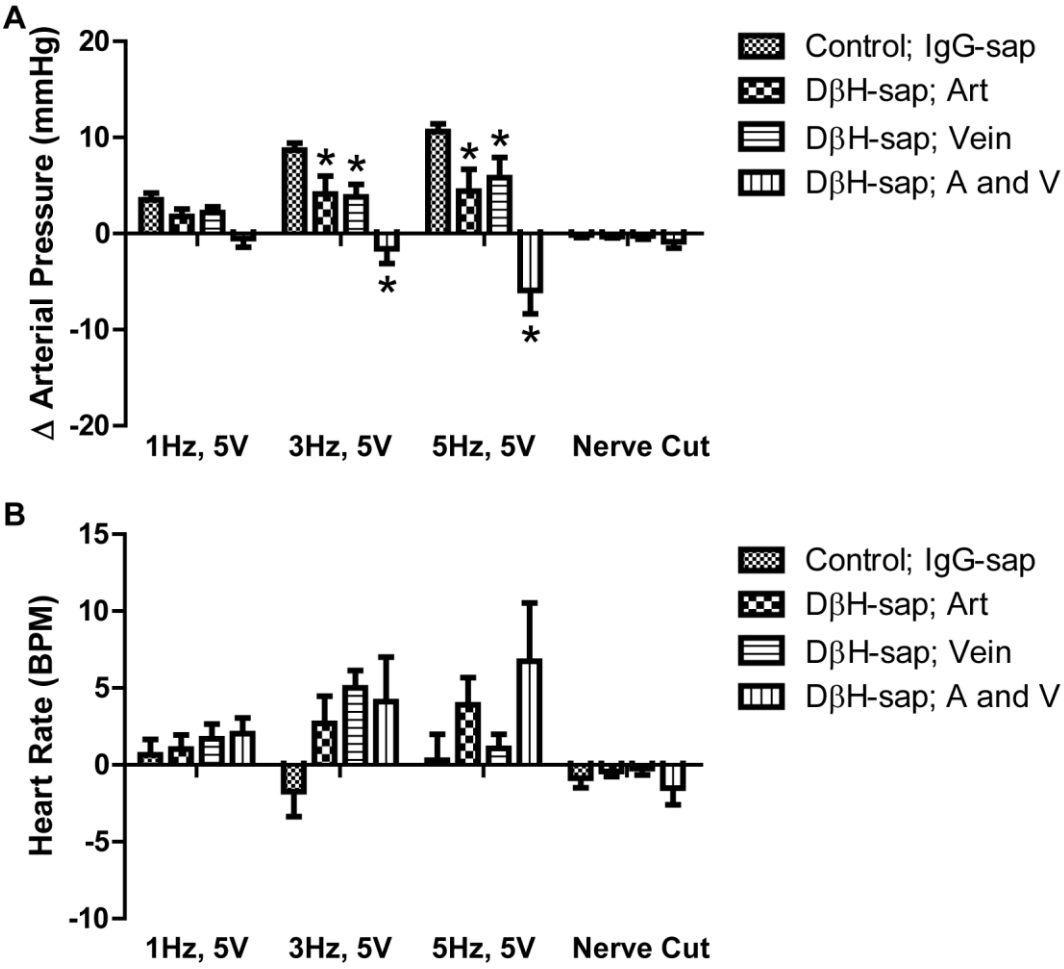


**Figure 4.19 DβH-sap application to MA, MV, or both attenuated or reversed the arterial pressor response to stimulation of the GSN.** DβH-sap applied to MA, MV, or both on attenuated or reversed arterial pressor response at to GSN stimulation at 3 Hz and 5 Hz (**A**). DβH-sap application had no effects on heart rate. (**B**). Data expressed at mean ± SEM. * $p \leq 0.05$ as compared to IgG-saporin, n = 4-11.

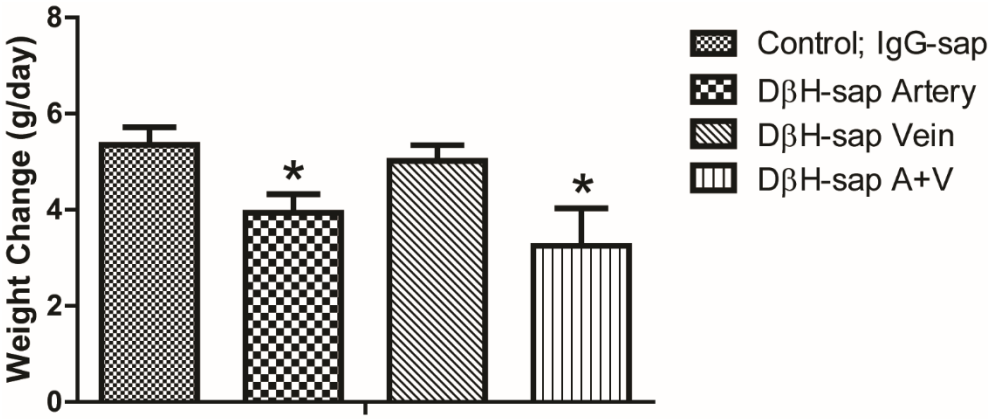


**Figure 4.20 Weight gain was differentially affected based on method of DβH-sap application to the mesenteric vasculature.** DβH-MA significantly attenuated weight gain, however application of DβH-MV did not significantly affect weight gain. Application of DβH-sap to both MA and MV significantly reduced weight gain. Data expressed at mean ± SEM. * $p \leq 0.05$ as compared to IgG-saporin, n = 5-11.

## Discussion

This study reports the impact of target-specific lesions of abdominal prevertebral neurons on systemic arterial pressure. The key findings in this study are: 1) applying DβH-sap to small segments of MA and MV produced a dose-dependent ablation of prevertebral sympathetic neurons; 2) lesions generated by applying DβH-sap to MA and MV required retrograde transport by perivascular nerves; 3) applying DβH-sap to MA and MV reversed rises in systemic arterial pressure evoked by stimulating the GSN; 4) applying DβH-sap to discrete vascular targets revealed that prevertebral neurons project widely and regionally; 5) removing sympathetic innervation to MA or MV both contributed to attenuating rises in systemic arterial pressure; 6) injecting DβH-sap IP did not reduce vascular CGRP-IR fibers on MA or MV; 7) DβH-sap applied to MA or both MA and MV, significantly attenuated weight gain over the course of the experiment.

*The ablation of mesenteric vascular-projecting neurons with Dβ H-sap was dose-dependent*

In this study, a 20 μg dose of DβH-sap produced widespread sympathectomy of splanchnic viscera and vasculature, and reversed the systemic arterial pressure response evoked by stimulating the GSN. Intravenous infusion of 87.5 μg/kg DβH-sap (19.68 μg in a 225g rat) produces a similar dose-dependent DβH-sap mediated reduction in superior cervical ganglion neuronal number (Picklo et al., 1995). Similarly, IP injection of 15 μg DβH-sap reduces sympathetic innervation to the intestine (Worlicek et al., 2010). In the current study, MV TH-IR fibers were reduced in animals receiving 5 and 10 μg doses of DβH-sap to MA and MV without reductions in MA TH-IR fibers; suggesting perivascular nerves innervating veins are more susceptible to DβH-sap. Alternatively, it is possible that

venous innervation is less dense than arterial innervation and this facilitated detection of reduced sympathetic innervation of veins at levels that are undetectable in arteries. We found more evidence for the former explanation because secondary branches of MV are similarly innervated compared to similar sized arteries (Furness, 1971) and TH-IR fibers on secondary branches of MA and MV harvested from control animals were not significantly different. Applying 20 μg DβH-sap to both MA and MV also increased observable GFAP-IR, indicating neuronal death and subsequent gliosis. Taken together, applying 20 μg DβH-sap to MA and MV produced maximal ablation of sympathetic prevertebral neurons.

*DβH-sap mediated lesions require retrograde transport by perivascular nerves*

Two methods of ablating CG neurons, applying DβH-sap to MA and MV or injecting it IP, were similarly effective, suggesting DβH-sap applied to MA and MV was taken up by sympathetic nerve terminals located outside of the 14 mm segment of MA and MV exposed to DβH-sap. To test this hypothesis, we used nerve crush mediated by suture-based ligation to block the retrograde transport of DβH-sap by perivascular nerves innervating the site exposed to DβH-sap. Suture-based crush of perivascular nerves attenuated the effects of DβH-sap applied to MA and MV on TH-IR fibers, and systemic arterial pressure responses to stimulating the left GSN. In contrast, splenic NE content was still significantly reduced in animals that underwent suture-based ligations of perivascular nerves. These results indicated perivascular nerves on the small segments of MA and MV where DβH-sap is applied, are the primary group of sympathetic nerve terminals endocytosing DβH-sap.

*Prevertebral neurons project widely and regionally*

Retrograde tracing studies have shown that vascular-projecting neurons in the CG are a distinct subpopulation of prevertebral neurons (Browning et al., 1999; Hsieh, Liu, & Chen, 2000). If this were the case, applying DβH-sap to MA and MV would ablate a subset of prevertebral neurons. Instead, DβH-sap applied to a small 14 mm area of MA and MV ablated 94% of prevertebral neurons, indicating prevertebral neurons project widely to many segments of MA and MV. Vascular-projecting neurons in other vascular beds and species also project widely. Human mesenteric perivascular nerve fibers are highly branched and innervate distances separated by up to ~4 mm (De Fontgalland et al., 2008). Rodent vasomotor neurons are able to innervate even larger areas (7 mm) of cutaneous vasculature (Gibbins et al., 1998). Meanwhile, a 1 $mm^2$ area of skin was innervated by 50-100 neurons (Gibbins et al., 1998). Taken together, these studies suggest prevertebral neurons project widely, with many collaterals innervating different vascular targets throughout the splanchnic region, while also extensively converging to small areas of MA and MV.

Given that singular application of DβH-sap to either MA or MV did not replicate the prolific effects of applying DβH-sap to MA and MV, we concluded that not all prevertebral neurons project widely. Applying DβH-sap to both MA and MV reduced TH-IR fibers by 72% on MA and 91% on MV, DβH-MA reduced MA and MV TH-IR fibers by only 50.9% and 61.5% and DβH-MV reduced MA and MV TH-IR fibers by only 33.7% and 62.6%. Reductions in MA TH-IR fibers when DβH-MV and in MV TH-IR fibers when DβH-MA support the existence of widely-projecting neurons. Neurons projecting solely to MA or MV cannot account for reductions in vascular TH-IR fibers in the opposing vessel type

distant to the segment of vasculature (i.e. the vessels examined for TH-IR) exposed to DβH-sap. The preverbal neurons that don't project widely, regionally-projecting neurons, innervate one or two primary branches of MA or MV and their corresponding tributaries. Most regionally-projecting neurons were not ablated by DβH-MA or -MV, because DβH-sap was only applied to small segments of vasculature. Therefore, regionally-projecting neurons still provided sympathetic innervation to MA and MV distant to the site of DβH-sap application. In summary, these data provide evidence for three populations of vascular-projecting neurons, one that projects widely to all vascular segments, and two that project regionally to MA or MV. This proposal corroborates retrograde tracer studies of prevertebral neurons that show vascular-projecting neurons innervating MA, MV, or both (Hsieh, Liu, & Chen, 2000)

*Contribution of MA and MV to acute rises in systemic arterial pressure*

To date the only studies that have provided insight into the contribution of MA and MV to rises in systemic arterial pressure has been the observation that neurally mediated constrictions of splanchnic arteries and veins both contribute to long-term increases in systemic arterial pressure in angiotensin II-salt hypertension (King et al., 2007). The present study furthers this understanding by demonstrating that applying DβH-sap to MA and MV reversed the pressor response to stimulating the GSN by removing innervation to both MA and MV. Indicating sympathetic innervation to both MA and MV mediates acute rises in systemic arterial pressure.

Singular application of DβH-sap to MA or MV attenuated, but did not reverse responses in systemic arterial pressure to stimulating the GSN, suggesting sympathetic innervation to either MA or MV is sufficient for mediating attenuated rises in systemic

arterial pressure. Interestingly, NE content of MV, but not MA was significantly reduced by applying DβH-sap to MA and vice-versa, indicating ablation of sympathetic neurons projecting to MA or MV reduced sympathetic innervation of the opposing vessel type. Removing sympathetic innervation to MV by applying DβH–MA attenuated arterial pressure responses to stimulating the GSN. Similarly, removing sympathetic innervation to MA by applying DβH–MV attenuated arterial pressure responses to stimulating the GSN. Taken together innervation to MA and MV both comprise a portion of the acute rises in systemic arterial pressure generated by stimulating the GSN, and alone are capable of producing, albeit attenuated, rises in systemic arterial pressure. Alternatively, DβH-MA or -MV did not remove all sympathetic innervation to MA or MV as indicated by the, albeit significantly reduced, presence of TH-IR fibers in MA and MV and this could explain the small attenuation in the acute rises of systemic arterial pressure relative to DβH-sap applied to MA or MV.

*DβH-sap does not eliminate perivascular sensory nerves and reveals a sensory nerve-mediated depressor response*

DβH-sap either injected IP or applied to the MA and MV reversed the arterial pressor response to either 3 Hz or 5 Hz stimulation. Sensory fibers are abundant in the GSN (Neuhuber, Sandoz, & Fryscak, 1986) and intravenous infusion of DβH-sap does not ablate sensory neurons in the dorsal root or nodose ganglia (Picklo et al., 1995). In this study, mesenteric vasculature had intact CGRP fibers after IP injection of DβH-sap indicating intact sensory innervation to MA and MV. Stimulating perivascular nerves releases CGRP which mediates dilation of MA (Fujimori et al., 1989; Han, Naes, & Westfall, 1990; van Eijndhoven et al., 2003). Therefore, stimulating the GSN released

CGRP onto MA and MV, which initiated vasodilation of the mesenteric circulation, and ultimately decreased systemic arterial pressure.

*DβH-sap reduces weight gain*

Groups receiving IP injection of DβH-sap, or application on MA or on both MA and MV, had gained less body weight over the course of the experiment and had reduced duodenal NE content than control animals. While several reports have indicated an absence of adverse effects of CGx on whole-body metabolism (Furness et al., 2001; King et al., 2007), sympathetic neurons in prevertebral ganglia send projections to myenteric ganglia, and submucosal ganglia (Quinson et al., 2001), and inhibit gut motility by activating enteric neurons (Furness & Costa, 1974). Furthermore, impaired sympathetic activity has been correlated with impaired colonic transit (Emmanuel & Kamm, 2000) and may contribute to the pathology of the diarrhea-predominant subgroup of irritable bowel syndrome patients (Aggarwal et al., 1994). Similarly, others have reported diarrhea in dogs after removal of the CG (Freedman et al., 1952; Lillehei & Wangensteen, 1948), but no diarrhea was observed in any animals receiving DβH-sap. Widespread denervation of the sympathetic nervous system in the gut by DβH-sap application may have led to disruptions in gut motility by interrupting sympathetic innervation or blood flow to the gut; thereby, influencing water and nutrient absorption causing attenuations in weight gain.

## Conclusions

The present study was the first to investigate target specific immunolesions of the celiac and splanchnic ganglia using a toxin specific to sympathetic neurons. Applying 20 μg DβH-sap to a small area of mesenteric vasculature ablated 94% of prevertebral neurons, suggesting sympathetic prevertebral neurons project widely to many segments of MA and MV throughout the gut. Singular application of DβH-sap to MA or MV produced a smaller lesion compared to DβH-sap applied to MA and MV, suggesting populations of vascular-projecting neurons that don't project widely. Instead vascular-projecting neurons project widely to all vascular targets or regionally to MA or MV. The attenuation or reversal of rises in systemic arterial pressure after DβH-sap immunolesions of innervation to MA, MV, or both suggested MA and MV both contribute to acute rises in systemic arterial pressure. The present study suggested novel fields of innervation for prevertebral neurons, which has large implications for how the splanchnic circulation is recruited to influence cardiovascular hemodynamics.

# CHAPTER 5: GENERAL DISCUSSION

## Major Findings

The sympathetic nervous system directly modulates the function of peripheral vasculature and viscera. Sympathetic prevertebral ganglia that innervate the splanchnic region are thought to be organized into organ-specific neural pathways (Browning et al., 1999; Hsieh, Liu, & Chen, 2000; Quinson et al., 2001). No study has isolated the physiological consequences of activating or removing a single organ-specific pathway. Rather, sympathetic innervation to the splanchnic region has only been studied by non–selectively activating or removing large populations of sympathetic efferent neurons (Kandlikar & Fink, 2011; Karim & Hainsworth, 1976; King et al., 2007). Neurons projecting to the splanchnic vasculature are of particular interest, because the splanchnic region is the body's largest vascular bed. Splanchnic sympathetic efferent neurons control the diameter of splanchnic arteries and veins. Reducing the diameter of arteries primarily increases the resistance of the splanchnic vascular bed, while reducing the diameter of veins primarily decreases the volume of blood contained (capacitance) within the splanchnic circulation. The relative contribution from reducing the diameter of splanchnic arteries and veins to increases in systemic arterial pressure is unknown, therefore the current study set out to isolate and examine the impacts of removing the sympathetic innervation from splanchnic arteries, veins, or both on systemic arterial pressure.

The current study examined organ–specific pathways in preverbal ganglia by utilizing several distinct approaches. In chapter 2, recombinant adeno-associated virus (rAAV) was applied to the mesenteric vasculature to overexpress green fluorescent protein (GFP) in the neurites of vascular-projecting neurons to identify their innervation fields. Additionally, rAAV was directly injected into prevertebral ganglia to develop a

technique that selectively targets vascular–projecting neurons. In chapter 3, the impacts of activating prevertebral neurons on systemic arterial pressure were examined by applying nicotine to the CG or by stimulating the left greater splanchnic nerve (GSN). In chapter 4, the effects of ablating prevertebral vascular-projecting neurons on systemic arterial pressure were investigated by applying an antibody against dopamine beta hydroxylase conjugated to saporin (DβH-sap) to the mesenteric vasculature. The major findings of these works are: 1) GFP was observed in the cell body of prevertebral neurons after applying rAAV to the mesenteric vasculature, but GFP was not observed in the neurites of prevertebral neurons; 2) rAAV directly injected into the CG was able to transduce the cell bodies of prevertebral ganglia; 3) retrograde tracers labelled three populations of vascular-projecting neurons in the splanchnic ganglia (SG); 4) electrically stimulating postganglionic nerve fibers in the left GSN were sufficient to elicit rises in systemic arterial pressure; 5) DβH-sap applied on two 7 mm segments of mesenteric arteries (MA) and veins (MV) ablated 94% of neurons in prevertebral ganglia; 6) DβH-sap applied to MA and MV reversed the systemic arterial pressure response evoked by stimulating the left GSN; 7) DβH-sap applied to MA (DβH-MA) or MV (DβH-MV) produced a significant ablation of the sympathetic innervation to the spleen, the duodenum, and the mesenteric vasculature; 8) DβH-MA and –MV significantly attenuated the systemic arterial pressure response to stimulating the left GSN 9) DβH-sap did not ablate sensory fibers innervating the mesenteric circulation.

The current study provides insight into the innervation fields of prevertebral neurons that are essential to understanding how the sympathetic nervous system modulates splanchnic hemodynamics during physiological states like exercise,

hemorrhage, and digestion. The individual contributions of splanchnic arteries and veins to increases in systemic arterial pressure were elucidated by acutely activating or removing splanchnic sympathetic efferents and indicated that both arteries and veins significantly impact systemic arterial pressure. Ablating prevertebral neurons with immunotoxins indicated that they are not tightly organized into organ-specific pathways, rather innervation fields of prevertebral neurons may project widely, and innervate multiple targets like splanchnic viscera as well as vasculature.

**Relative contribution of MA, MV, and sensory fibers to acute rises or reductions in systemic arterial pressure**

Stimulating the left GSN elicited acute rises in systemic arterial pressure mediated by constricting the splanchnic vasculature, and isolates the contribution of the splanchnic region by excluding the recruitment of other vascular beds seen during *en masse* activation of the sympathetic nervous system. Phentolamine, an $\alpha_1$ adrenergic receptor (AR) antagonist, or pyridoxalphosphate-6-azophenyl-2',4'-disulfonic acid (PPADs), a P2X receptor antagonist, was used to investigate the relative contribution of MA and MV to acute rises in systemic arterial pressure evoked by stimulating the GSN. Rises is systemic arterial pressure were not blocked by intravenously injecting phentolamine or PPADs, but intravenously injecting both phentolamine and PPADs blocked acute rises in systemic arterial pressure. Adenosine triphosphate (ATP) is the primary neurotransmitter constricting MA via P2X receptors (Gitterman & Evans, 2001a; Luo et al., 2003; Park et al., 2009), while MV do not express P2X receptors, they express P2Y and constrict in the presence of ATP (Galligan et al., 2001). However, norepinephrine (NE) is the primary neurotransmitter constricting veins via $\alpha_1$ and $\alpha_2$ ARs (Park et al., 2009; Sporkova et al.,

2010). Differences in neurotransmitters mediating constriction of arteries and veins is illustrated when stimulating perivascular nerves, where constricting arteries is largely blocked by PPADS and constricting veins is largely blocked by an $\alpha_1$ AR antagonist (Luo et al., 2003; Park et al., 2009). In my work, constricting MA must account for a large portion of the systemic arterial pressure response to stimulating the GSN during blockade of $\alpha_1$ AR. Similarly, constricting MV must significantly contribute to acute rises in systemic arterial pressure after stimulating the GSN during blockade of P2X receptors with PPADS. Therefore, acute rises in arterial pressure to stimulating the GSN has an arterial and venous component, that replicates responses of the splanchnic circulation to acute physiological conditions such as exercise (Perko, Nielsen, Skak, Clemmesen, Schroeder, & Secher, 1998) or prevention of orthostatic hypotension during standing where increases in splanchnic resistance and decreases in splanchnic capacitance are both observed (Smit, Halliwill, Low, & Wieling, 1999).

Removing sympathetic innervation to the splanchnic region via celiac ganglionectomy (CGx), attenuates elevations in systemic arterial pressure during hypertension (Kandlikar & Fink, 2011; King et al., 2007), but the population of neurons or fibers responsible for the effects of CGx has yet to be identified. Evidence put forth by DβH-sap ablating vascular-projecting neurons suggested that sympathetic innervation to splanchnic arteries and veins both play a critical role in elevating systemic arterial pressure. Removing innervation to the MA and MV by applying DβH-sap to both MA and MV reversed the pressor response to stimulating the left GSN. The lesions generated by DβH-sap were similar to those generated by CGx, with reductions in sympathetic innervation to mesenteric vasculature (vascular TH-IR fibers) and destruction of 94% of

CG neurons (compared to removal of 100% neurons from CGx). An important distinction between the two methods of sympathectomy was the presence of sensory fibers after applying DβH-sap, but not after CGx (Li et al., 2010). Removing the CG disrupts sensory fibers coursing through the CG that provide innervation to the vasculature (Lindh et al., 1988), while sensory neurons are unaffected by DβH-sap (Picklo et al., 1995). Intact sensory innervation, without corresponding sympathetic innervation, to the mesenteric vasculature likely contributed to the reversal of the pressor response while stimulating the GSN. Repetitive nerve stimulation is known to produce inhibitory junction potentials in MA resulting in vasodilation when sympathetic transmission is diminished with guanethidine (Kreulen & Peters, 1986; Meehan, Hottenstein, & Kreulen, 1991). This vasodilation is capsaicin-sensitive and is therefore mediated by sensory nerve fibers. The absence of intact sympathetic innervation to the splanchnic region revealed a previously unknown role of sensory afferents neurons to directly decrease systemic arterial pressure via vasodilation of the splanchnic vasculature. Sensory afferents may play an important role in physiological states that experience increases in splanchnic blood flow such as postprandial hyperemia (Chou, 1983; Gallavan et al., 1980; Gallavan & Chou, 1985; Granger et al., 2011) and will be explored more in depth later in this discussion.

The relative contributions of MA and MV to acute rises in systemic arterial pressure were investigated by applying DβH-sap to mesenteric arteries (DβH-MA) or mesenteric veins (DβH-MV). Interestingly, DβH-MA nor -MV produced a complete reduction in MA or MV TH-IR fibers. This indicated that sympathetic innervation to arteries and veins was still present despite targeted ablation of artery-projecting or vein-projecting neurons. Although, another marker of sympathetic innervation, NE content, was significantly

reduced in MA from DβH-MV, while DβH-MA significantly reduced MV NE content. Significant knockdown, as indicated by NE content, of sympathetic innervation to MA or MV produced a significantly attenuated, but not abolished systemic pressure response to stimulating the GSN. This indicated MA and MV both contribute, but neither are critical, to acute rises in systemic arterial pressure. In support of this proposal, increases in arterial tone, and decreases in venous tone have both been shown to mediate increases in systemic arterial pressure in angiotensin (Ang) II–salt hypertension (King et al., 2007; Kuroki et al., 2011). Increases in splanchnic arterial and venous tone are attenuated by blocking ganglionic neurotransmission with hexamethonium, suggesting increases in systemic arterial pressure are neurogenically driven in Ang II–salt hypertension (King et al., 2007; Kuroki et al., 2011). These studies have demonstrated both MA and MV contribute to acute rises in systemic arterial pressure, but incomplete removal of all venous or arterial sympathetic innervation limited the development of robust conclusions about the individual contributions of MA and MV to acute rises in systemic arterial pressure.

**Innervation fields of vascular–projecting neurons**

*Using viral techniques to determine innervation fields of prevertebral neurons*

To determine if vascular-projecting neurons innervate distinct targets, rAAV was applied to the mesenteric vasculature, where rAAV can be taken up and retrogradely transported to the cell body (Foust et al., 2007; Kaspar et al., 2003; Zheng et al., 2009). The virus encodes expression of a fluorescent protein, which undergoes anterograde transport, thereby tracing neurites of the transduced neuron (Chamberlin et al., 1998). By isolating the vasculature, rAAV only labels the innervation fields of vascular-projecting

neurons. Green florescent protein (GFP) was observed in the cell bodies of prevertebral neurons 38 days after applying rAAV1 or 6 to the mesenteric vasculature indicating successful retrograde transport of rAAV. However, neurites of prevertebral neurons were not filled with GFP 38-45 days after applying rAAV1, 6, or 9 to the mesenteric vasculature. One possible explanation for the lack of GFP in neurites is an insufficient length of time from exposure of prevertebral neurons to rAAV to examination of prevertebral ganglia. For example, retrograde transport mediated expression of transgenes in the amygdala, which sends projections to the ventral tegmental area (VTA), occurred 2 months after injection of rAAV9 into the VTA (Cearley & Wolfe, 2007). The distance from the VTA to the amygdala is several mm, while the distance from the mesenteric vasculature to the CG is several cm, so a 45 day time course may have not been sufficient to fill neurites of prevertebral neurons with GFP produced by viral transduction. Anterograde labeling of neuronal neurites innervating the splanchnic circulation would be a powerful tool to elucidate the innervation patterns of vascular-projecting neurons in the splanchnic circulation, but further investigation into the time course of anterograde labelling is needed.

Prevertebral neurons were transduced for the first time by directly injecting rAAV into the CG and this technique could be used to elucidate innervation patterns of prevertebral neurons by injecting a helper virus-free herpes simplex virus (HSV) vector expressing a Brainbow cassette into the CG. This technique would eschew issues that arose from the retrograde transport of rAAV by directly transducing the cell bodies of prevertebral neurons. Furthermore, HSV-Brainbow creates hundreds of unique hues allowing an observer to match neuronal cell bodies to corresponding axons (Zhang et al.,

2014). HSV-Brainbow would allow investigation into innervation fields of prevertebral neurons by observing the sympathetic innervation of multiple end organs and comparing the unique hues of neurites at each end organ, thereby elucidating the innervation fields of preverbal neurons.

V*ascular-projecting neurons in the SG suggest redundant sympathetic innervation to the mesenteric vasculature*

I hypothesized the innervation fields of separate populations of vascular-projecting SG and CG neurons innervate the same segments of vasculature to produce a graded pressor response correlated to the number of activated vascular-projecting neurons. Prevertebral neurons in rats a do not have a viscerotopic organization (Shah et al., unpublished data), and in the current study applying distinct retrograde tracers to separate segments of MA or MV labeled neurons in both the CG and SG projecting to MA or MV, or both (CG data not shown), suggesting there is overlap in sympathetic innervation to the mesenteric vasculature that arises from separate neuronal populations located in distinct ganglia. Stimulating the GSN activates postganglionic fibers from vascular-projecting neurons in the SG and preganglionic fibers innervating vascular-projecting neurons in the CG, but during ganglionic blockade transmission from preganglionic fibers is disrupted (Sapru et al., 1982). Interestingly, stimulating the GSN during ganglionic blockade is sufficient to elicit rises in systemic arterial pressure, indicating SG neurons innervate enough splanchnic vasculature to increase systemic arterial pressure. From this, I hypothesized populations of vascular-projecting neurons in each ganglion are sufficient to elicit rises is systemic arterial pressure. Therefore, activating vascular-projecting neurons in multiple ganglia could produce an additive effect

on the constriction of vascular targets. Recruiting more prevertebral vascular-projecting neurons would then increase the frequency of nerve activity, thereby constricting splanchnic vascular targets to a greater degree. In support of this proposal, the frequency of nerve stimulation is positively correlated to the number of varicosities releasing neurotransmitters at the vascular neuroeffector junction, which theoretically accounts for the larger responses in splanchnic resistance and splanchnic capacitance at higher frequencies (Karim & Hainsworth, 1976; Stjärne & Stjärne, 1995). Therefore, the sympathetic innervation to the splanchnic circulation may be organized in a fashion that permits graded control over splanchnic hemodynamics.

*Removal of the innervation to the splanchnic circulation suggested that prevertebral neurons project widely*

DβH-sap applied on two ~7 mm segments of MA and MV ablated 94% of neurons in prevertebral ganglia, reduced the number of tyrosine hydroxylase immunoreactive (TH-IR) fibers by 72.1% on MA and 91% on MV and reversed the systemic arterial pressure response to stimulating the GSN. Interestingly, the lesion generated by DβH-sap indicated a much larger population of neurons than that examined by retrograde tracers. The total population of vascular-projecting neurons elucidated by retrograde tracers was 22.5% (Shah et al., unpublished). Differences between uptake mechanisms and labeling efficiency may account for the discrepancy in the number of prevertebral neurons ablated versus the number retrogradely traced. Cholera toxin subunit B (CTB) and pseudorabies virus (PRV) have labeled the greatest percentage of prevertebral vascular-projecting neurons (Shah et al., unpublished), but reach maximal labeling at different time points (Chen, Yang, Miselis, & Aston-Jones, 1999). During a shorter time course (26-30 hours

after injection into the cerebral ventricles), CTB labeled up to 24 times more cells than PRV, while at longer time courses PRV labeled up to 2 times more cells than CTB (Chen et al., 1999). Similarly, PRV applied to mesenteric vasculature labeled a maximal number of prevertebral neurons in 4-5 days, while the number of neurons labeled with CTB started to decline after 3 days (Shah et al., unpublished). Therefore, a mixture of PRV/CTB underestimates the number of neurons projecting to the mesenteric vasculature, due to the different time courses of each tracer. Alternatively, saporin is a very potent immunotoxin that requires only a few molecules to initiate cell death within 4 hours of the initial exposure (Polito et al., 2008; Wiley & Lappi, 1994). The three week time course allotted for the experiments with saporin conjugates allowed for sufficient time for the uptake, transport, and ablation of the maximal amount of neurons. Therefore, unlike retrograde tracers, saporin was allowed to reach maximal efficiency and did not underestimate the number of neurons ablated.

The size of the DβH-sap mediated ablation suggested that prevertebral neurons project widely to innervate multiple targets throughout the splanchnic region (**Fig 5.1A**). In previous experiments from our lab, 46.8 ± 4.2% of artery-projecting and 49.8 ± 5.0% of vein-projecting prevertebral neurons innervated segments of vessels supplying the ileum and jejunum (Shah et al., unpublished data). In other studies, human mesenteric perivascular nerve fibers are highly branched and can cover spans of 4.32 mm (De Fontgalland et al., 2008). Vascular-projecting neurons innervate portions of cutaneous blood vessels up to 7 mm apart, while ~100 vascular-projecting neurons innervated a small 1 $mm^2$ area of vasculature in the guinea pig ear (Gibbins et al., 1998). Therefore, it is conceivable that prevertebral neurons have wide fields of innervation, while densely

innervating individual branches of mesenteric vessels leading to widespread ablation of prevertebral neurons when DβH-sap was applied to a 14 mm length of mesenteric vasculature.

DβH-sap mediated ablations of prevertebral neurons suggested that single neurons innervate vast portions of vasculature via a large number of collaterals; this proposal is supported by the development of sympathetic innervation to vascular targets. Vascular innervation is not present until postnatal day 2 and is not fully developed until postnatal day 10 (Brunet et al., 2014). Vascular innervation is completed in a distal to proximal fashion mediated by netrin, vascular endothelial growth factor, and semaphorin3A signaling (Brunet et al., 2014; Hill et al., 1983; Long et al., 2009). Netrin is of particular importance because it promotes the dynamic addition and retraction of axonal branches (Manitt, Nikolakopoulou, Almario, Nguyen, & Cohen-Cory, 2009). Distal to proximal vascular innervation suggested two possible mechanisms for development of sympathetic vascular innervation. In the first mechanism, nerve fibers innervate distal portions of vasculature and netrin promotes axon collaterals to sprout from proximal portions of the nerve fibers to complete innervation to the mesenteric vasculature. In the second mechanism, axons continually sprout from ganglia over postnatal day 2 to postnatal day 10 and a carefully regulated milieu of guidance cues are expressed to facilitate distal to proximal innervation. The first mechanism suggested single neurons branch significantly and innervate many vascular targets, and explains how applying DβH-sap to a small 14 mm segment of mesenteric vasculature ablated 94% of prevertebral neurons.

*Vascular-projecting neurons could also project to viscera*

Prevertebral neurons have been shown to project to multiple targets, such as arteries and veins, but no study has examined if prevertebral neurons project to viscera and vasculature. This dearth of knowledge exists because labeling viscera-projecting neurons with retrograde tracers also labels perivascular nerve fibers within viscera. For example, sympathetic nerves innervate the vasculature and lymphocytes of the spleen (Felten & Olschowka, 1987). Therefore, injecting a tracer into the spleen would label vascular-projecting neurons and lymphocyte-projecting neurons, meaning retrograde tracers cannot be used to examine neurons projecting to splanchnic viscera and vasculature. The existence of prevertebral neurons projecting to viscera and vasculature were implied by a 94% percent ablation of prevertebral neurons after vessel–applied DβH-sap. It is highly improbable for only 6% of prevertebral neurons to exert sympathetic control over the entirety of splanchnic viscera, so a portion of vascular–projecting neurons may also project to viscera. Furthermore, application of DβH-sap to MA or MV reduced NE in splenic and duodenal tissue indicating neurons possibly project to vasculature and viscera. Alternatively, DβH-sap could remove perivascular innervation contained within the viscera to account for reductions in NE content.

*Applying DβH-sap to MA and MV suggested prevertebral neurons project regionally*

In contrast to the near total destruction of prevertebral neurons when DβH-sap was applied to both MA and MV, applying DβH-MA, or MV produced a smaller lesion that suggested multiple populations of vascular-projecting neurons. DβH-MA produced a 50.9% reduction in arterial and a 61.5% reduction in venous TH-IR fibers, while DβH-MV

produced a 33.7% reduction in arterial and a 62.6% reduction in venous TH-IR fibers. The resistance of MA and MV TH-IR fibers to complete reduction suggested there are multiple populations of vascular-projecting neurons. If only one population of widely-projecting neurons existed, as suggested by applying DβH-sap to MA and MV, the entirety of vascular TH-IR fibers would be removed regardless of which vessel type was exposed to DβH-sap. That was not the case, indicating widely-projecting neurons account for a smaller portion of vascular-projecting neurons than indicated by the much larger reduction in vascular TH-IR fibers produced by applying DβH-sap to MA and MV. The remaining vascular TH-IR fibers can be explained by two populations of regionally-projecting neurons that innervate only a few adjacent secondary branches of either MA or MV and their corresponding tributaries. Therefore, regionally-projecting neurons not innervating the site where DβH-sap was exposed would provide innervation to primary branches of mesenteric vessels distant to the exposure (i.e, the vessels examined for TH-IR) and confer resistance to reductions in vascular TH-IR fibers. In support of this, 46.8 ± 4.2% of artery-projecting and 49.8 ± 5.0% of vein-projecting prevertebral neurons project widely to segments of mesenteric vasculature supplying the ileum and jejunum, while 46.4 ± 11.1% of artery-projecting and 43.8 ± 13.9% of vein-projecting project to adjacent secondary branches of mesenteric vasculature (Shah et al., unpublished). According to this data, there is likely a mix of prevertebral neurons projecting regionally and widely. Taken together, I hypothesized regionally–projecting neurons innervate only a few secondary branches of MA or MV, while widely–projecting neurons innervate the entire arcade of MA and MV (**Fig. 5.1B**). The physiological implications of the multiple populations of vascular–projecting neurons are covered in detail below.

*The bystander effect does not explain discrepancies between DβH-sap applied to MA or MV, or both*

Several factors could contribute to the discrepancy in results from DβH-sap applied to different vascular targets. The first, is non–specific neuronal cell death mediated by a bystander effect, where saporin gains access to non-targeted cells via connexin channels designed for cell–cell communication (Elshami et al., 1996; Mesnil, Piccoli, Tiraby, Willecke, & Yamasaki, 1996). While presynaptic sympathetic neurons contain connexin36, which mediates cell to cell electrical coupling, there is no evidence of prevertebral neurons expressing connexin36. Furthermore, connexin channels were not observed in perivascular nerve fibers in hamster feed arteries (Looft-Wilson, Haug, Neufer, & Segal, 2004; Marina, Becker, & Gilbey, 2008). Therefore, cell to cell transport of saporin is unlikely, but further investigation into the presence of connexin channels in prevertebral neurons could make this mechanism plausible. A second factor is saporin released into the synaptic milieu after its target neuron undergoes cell death and is taken up by bystander neurons via bulk fluid phase endocytosis. However, bulk fluid phase endocytosis requires large quantities of saporin (Wiley & Lappi, 1994) and identification of saporin after it has eliminated its targeted neuron has never been reported. Depending on target, DβH–sap application suggested vastly different innervation fields of vascular–projecting neurons and the exact mechanism behind this discrepancy requires further investigation.

**Physiological Impacts of the Innervation Patterns of Vascular-Projecting Neurons**

*Widely-projecting prevertebral neurons combine with other factors to control the splanchnic circulation*

Applying DβH-sap to MA and MV suggested a population of widely-projecting neurons innervating each organ in the splanchnic circulation; therefore, I hypothesized that widely-projecting efferent fibers confer distinct control of end organs via unique composition of neuroeffector junctions at each target. Evidence exists for the differential control of MA and MV at the neuroeffector junction, in that stimulating perivascular nerves constricts MV at lower frequencies compared to MA, while both are constricted at higher frequencies (Hottenstein & Kreulen, 1987). The distinct responses of MA and MV to different frequencies is likely caused by differential postjunctional effects of NE via activation of $\alpha_2$ ARs to inhibit neurotransmitter release to a greater extent in arteries compared to veins, while also enhancing $\alpha_2$ AR mediated constriction of veins (Park et al., 2009; Sporkova et al., 2010). Furthermore, different neurotransmitters constricting MA and MV could account for the discrepancies in responses to stimulating perivascular nerves at different frequencies. This is possible because constriction of arteries are primarily mediated by ATP while constriction of veins are primarily mediated by NE (Gitterman & Evans, 2001a; Luo et al., 2003). Veins responding differently than arteries to low frequency sympathetic outflow could account for the preferential constriction of MV without similar constriction of MA during hemorrhage (Price et al., 1966). Similarly, higher frequency outflow could recruit MA and MV in physiological challenges like exercise where constriction of both MA and MV are observed (Qamar & Read, 1987). Therefore,

widely projecting splanchnic sympathetic neurons can have differential effects based on target due to unique compositions of neuroeffector junctions.

Combining widely-projecting neurons with local vasodilatory factors or sensory neurons, can shunt blood to regions requiring increased blood flow. For example, during hemorrhage splanchnic sympathetic activity is increased, but local factors vasodilate arterioles supplying the mucosa, but not the muscularis (Shepherd & Riedel, 1988), thus shunting blood to an area where oxygen consumption is high (Granger et al., 2011; Krejci et al., 2000). Similarly, during digestion hyperemia is localized to the segment of intestine where chyme (digested food) is present (Chou, 1983; Gallavan et al., 1980; Gallavan & Chou, 1985; Granger et al., 2011). The regional increases in mesenteric blood flow involve many hypothesized mechanisms, but I will focus on neurally–based mechanisms (Gallavan & Chou, 1985; Matheson et al., 2000). Postprandial sympathetic activation is seen in kidney, muscle, cardiac and adipose tissue to combat decreases in arterial pressure when blood is redistributed to the splanchnic circulation (van Baak, 2008), although splanchnic sympathetic nerve activity has not been measured during postprandial hyperemia. If splanchnic sympathetic nerve activity is increased during postprandial hyperemia, widely–projecting neurons would constrict the entire splanchnic circulation, therefore, an additional mechanism would be necessary to counteract vasoconstriction in intestinal compartments containing chyme. Such a role could be filled by primary sensory neurons, which have cell bodies located in dorsal root ganglia and send collaterals to the mesenteric vasculature and the gastrointestinal tract. Primary sensory neurons elicit inhibitory junction potentials in smooth muscle cells of mesenteric arteries through direct release of calcitonin gene related peptide (CGRP) or nitric oxide

onto mesenteric arteries in response to mechanical stimulation via colonic dissention (Holzer, 1992; Zheng et al., 1998). Primary sensory neurons could vasodilate mesenteric arteries providing blood supply to jejunal and ileal intestinal segments containing chyme via a similar mechanical mechanism seen in the colon. The opposing actions of widely–projecting sympathetic neurons and primary sensory neurons combine to constrict feed arteries to intestinal segments not immediately involved in the digestion process, thereby shunting blood to intestinal segments actively involved in the digestion process by vasodilating feed arteries supplying intestinal segments containing chyme. This allows blood to be distributed to the gastrointestinal tract during digestion while limiting the volume of blood to prevent decreases in arterial pressure.

*Different populations of vascular-projecting neurons serve different physiological functions*

DβH-MA or -MV suggested several distinct populations of vascular-projecting neurons, I hypothesized these different populations serve different physiological functions. The first population of neurons are those projecting widely to arteries and veins and are recruited during physiological states requiring decreases in blood flow to and mobilization of blood from the splanchnic circulation. Blood flow to the splanchnic organs is reduced and blood is redistributed from splanchnic veins to skeletal muscle during exercise (Qamar & Read, 1987), this response could be mediated by activating widely-projecting neurons, thereby constricting both splanchnic arteries and veins (**Fig. 5.2**).

The second population of neurons are those regionally-projecting to veins which are recruited in physiological states requiring splanchnic venoconstriction. Regional-, vein-projecting neurons are likely recruited during hemorrhage, where venoconstriction is

required to counter blood loss while preventing corresponding tissue ischemia (Price et al., 1966), **Fig. 5.3**). Regional-, vein-projecting would help control the amount of blood mobilized from the splanchnic circulation depending on the severity of hemorrhage. For instance, during 4% hemorrhage of total blood volume the spleen contributes a negligible volume to the blood lost while the gastrointestinal tract and the liver contribute 16% and 23% respectively. During 15% hemorrhage of total blood volume, the spleen contributes 19%, the gastrointestinal tract 21% and the liver 22% to the volume of blood lost (Greenway & Lister, 1974). It is likely the sympathetic innervation to splenic vasculature arises from a separate population of vascular-projecting neurons and is recruited in a distinct fashion from the rest of the splanchnic circulation. In support of this, DβH-MV reduced duodenal NE content but not splenic NE content, indicating separate populations of regional-, vein-projecting neurons project to MV and splenic vasculature, thereby providing separate control of the spleen during hemorrhage. Regional-, vein-projecting neurons are also likely recruited during the onset of hypertension. Neurogenically driven increases in MCFP are seen one day after inducing Ang II-salt hypertension, while neurogenically driven increases in mesenteric resistance are not consistently seen until ten days after inducing Ang II-salt hypertension (King et al., 2007; Kuroki et al., 2011), indicating preferential recruitment of veins over arteries during the initial onset of hypertension. Taken together, regional-, vein-projecting neurons can provide distinct control over veins and can account for the preferential recruitment of splanchnic venous reservoirs in hemorrhage and hypertension.

The third population of neurons are those regionally projecting to arteries that provide control over blood flow to different intestinal segments throughout the mesenteric

circulation. As discussed above, hyperemia is localized to the segment of the intestine where chyme is present and I hypothesized that regionally–projecting mesenteric sympathetic neurons can shunt blood to intestinal segments that contain chyme by vasoconstricting feed arteries supplying blood to regions that do not contain chyme (**Fig. 5.4**). Additionally, primary sensory neurons could vasodilate feed arteries of intestinal segments containing chyme via a mechanosensory-based mechanism described above. The combined vasoactive functions of regional–projecting sympathetic neurons and primary sensory neurons shunts blood flow to intestinal segments actively aiding in digestion, while limiting the volume of blood redistributed to the splanchnic circulation. This is particularly important to prevent even more substantial drops in arterial pressure as initiated by reduced splanchnic resistance during digestion (Kircher et al., 2003).

I hypothesized that the distinct populations of prevertebral neurons described above are organized into functional units much like motor units. Preganglionic input to postganglionic neurons is divergent with a ratio of 1:10 pre- to post-ganglionic neurons, and postganglionic neurons receives input from several preganglionic neurons as well as weak afferent inputs (Janig & McLachlan, 1992). A majority of action potentials in prevertebral neurons are driven by the summation of secondary inputs (Bratton et al., 2010). Functional units would be organized by preganglionic input, but controlled via summation of inputs from preganglionic neurons (Langley, 1893), vagal inputs (Rosas-Ballina et al., 2008), intestinofugal neurons in the gut (Kreulen & Szurszewski, 1979), and sensory neurons in the dorsal root ganglion (Crowcroft & Szurszewski, 1971). A summation of these inputs could occur to recruit functional units appropriate for certain physiological or pathophysiological conditions. For example, hypovolemia activates the

baroreceptor reflex to restore systemic arterial pressure by constricting splanchnic veins (Pelletier et al., 1971; Shen et al., 1990). I propose regional-, vein-projecting neurons are barosensitive and receive the majority of vagal input to prevertebral ganglia, allowing hypovolemia to preferentially constrict veins by activating baroreceptor mediated reflexes during hemorrhage. Therefore, prevertebral vascular- projecting neurons are organized into functional units that are activated based on the summation of many inputs to provide distinct control over the splanchnic circulation during different physiological states.

**Therapeutic Applications**

The current study set out to examine ablations of splanchnic vascular-projecting neurons to identify and generate additional therapeutic avenues for hypertension. Applying DβH-sap to vasculature generated a complete sympathectomy of the splanchnic region, similar to CGx (Li et al., 2010), aside from leaving sensory innervation to the splanchnic region intact. Afferent sensory fibers could play a large role in arterial pressure regulation, since sensory fibers are involved in feedback mechanisms that dilate mesenteric arteries. Similarly, renal injury can drive rises in systemic arterial pressure via the excitation of renal nerve afferents (Converse et al., 1993; Hausberg et al., 2002). I am currently performing an experiment to identify the long-term effects of sole sensory innervation (i.e. without sympathetic innervation) on the elevations of systemic arterial pressure during hypertension via complete sympathectomy mediated by injecting DβH-sap IP. The results of this experiment may uncover a substantial role of sensory innervation to the abdominal region in the regulation of arterial pressure, and provide an additional therapeutic target for the treatment of hypertension.

Complete ablation of the sympathetic innervation to the abdominal region lowers arterial pressure (Grimson & Orgain, 1949), but also removes of the ability of the splanchnic circulation to mobilize vast volumes of venous blood. For example, exercise requires vasoconstriction of the mesenteric circulation to shunt blood away from the splanchnic circulation to the skeletal muscle (Qamar & Read, 1987). In humans with splanchnic sympathectomy, the splanchnic circulation is not constricted and blood is not redistributed to the skeletal muscle, which results in dramatic decreases in arterial pressure during exercise, causing considerable morbidity (Puvi-Rajasingham, Smith, Akinola, & Mathias, 1998). Similarly, some patients experience orthostatic hypotension after splanchnic sympathectomy (Van Lieshout, Wieling, Wesseling, Endert, & Karemaker, 1990), presumably from insufficient vasoconstriction of the splanchnic circulation when standing. The current study suggested that incomplete ablation of either artery- or vein- projecting neurons achieved by DβH-MA or MV could ameliorate the negative effects of this therapy. DβH-MA or MV significantly attenuated but did not abolish acute rises in systemic arterial pressure, so partial ablation of arterial–projecting and venous–projecting neurons may leave enough vascular sympathetic innervation to maintain acute control of the splanchnic circulation during physiological states, like exercise, to prevent dramatic decreases in arterial pressure. However, it is unknown if partial sympathectomy would alleviate long–term increases in arterial pressure to the extent of complete splanchnic sympathectomy. Long-term studies in an animal model of hypertension are required to elucidate the therapeutic potential of DβH-MA or MV.

## Conclusions

This research set out to modulate specific subsets of prevertebral neurons to differently affect MA and MV. Using rAAV as a means to anterogradely trace the innervation fields of prevertebral neurons was unsuccessful. However, injecting rAAV directly into the CG transduced prevertebral neurons providing future avenues to elucidate the innervation patterns of vascular-projecting neurons. Interestingly, targeting vascular-projecting neurons with an immunotoxin ablated 94% of prevertebral neurons. Based on this result, I hypothesized that prevertebral neurons project widely throughout the mesenteric circulation. Widely-projecting prevertebral neurons would confer control of the splanchnic circulation to the number of prevertebral neurons recruited by various inputs, generating a graded control of the splanchnic circulation. Combined with unique neuroeffector junctions, individual control of end organs can be achieved. Alternatively, DβH-sap applied to either MA or MV produced smaller reductions in vascular TH-IR fibers than DβH-sap applied to both MA and MV indicating separate subpopulations of artery-projecting and vein-projecting neurons exist. As a result, I hypothesized the response of the splanchnic circulation during different physiological and pathophysiological conditions would be c differentially controlled by activating distinct populations of prevertebral neurons. Taken together, some insight to the innervation patterns of prevertebral neurons and how the sympathetic nervous system controls the splanchnic circulation has been revealed. However, further elucidating neural pathways of prevertebral neurons is essential to understanding the influences of the splanchnic circulation on systemic arterial pressure.

## Figures

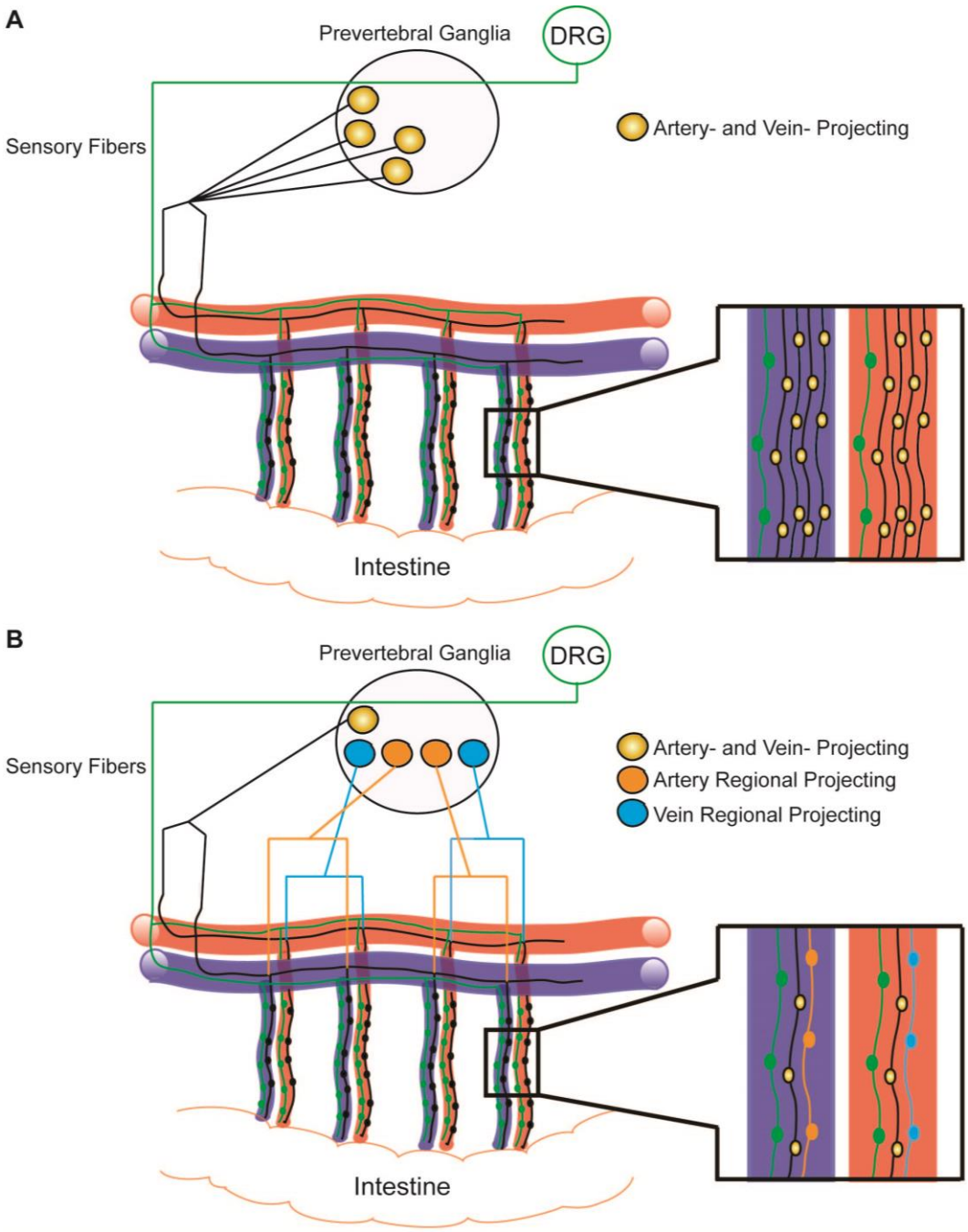


**Figure 5.1: Diagrammatic representations of innervation patterns of vascular–projecting neurons.** Widespread ablation of prevertebral neurons via DβH–sap application to mesenteric arteries and veins suggested vascular–projecting neurons have wide fields of innervation (**A**). Partial ablation of prevertebral neurons via DβH–sap application to mesenteric arteries or veins indicated that several different populations of vascular–projecting neurons with wide– or regional–innervation fields (**B**).

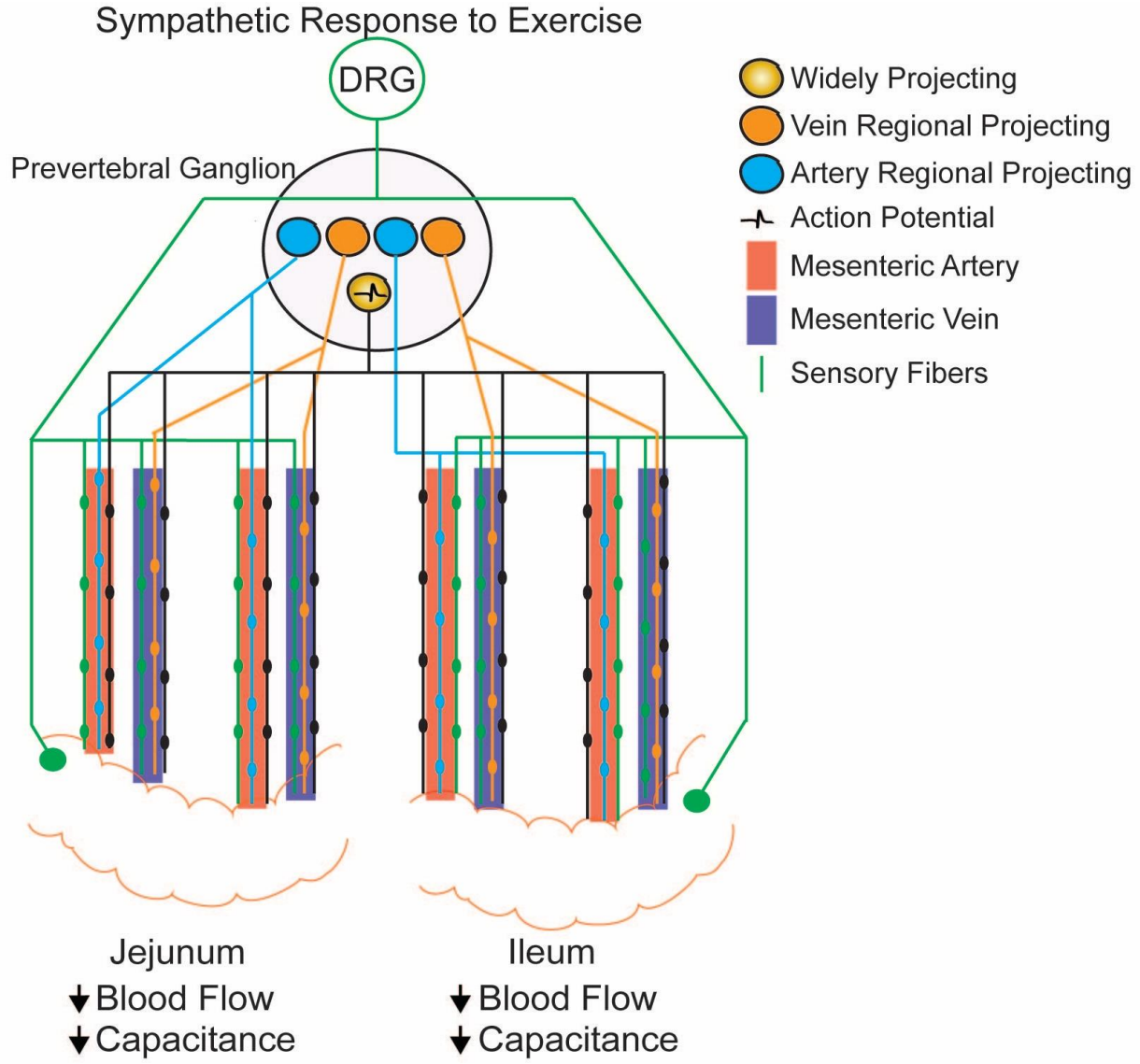


**Figure 5.2: Widely projecting neurons modulate the splanchnic sympathetic response to exercise.** During exercise, mesenteric arteries and veins are constricted to reduce splanchnic blood flow and redistribute large volumes of blood contained in splanchnic veins to the skeletal muscle. Widely–projecting neurons, depicted in gold, mediate the sympathetic response to exercise, via widespread splanchnic constriction and arteries and veins.

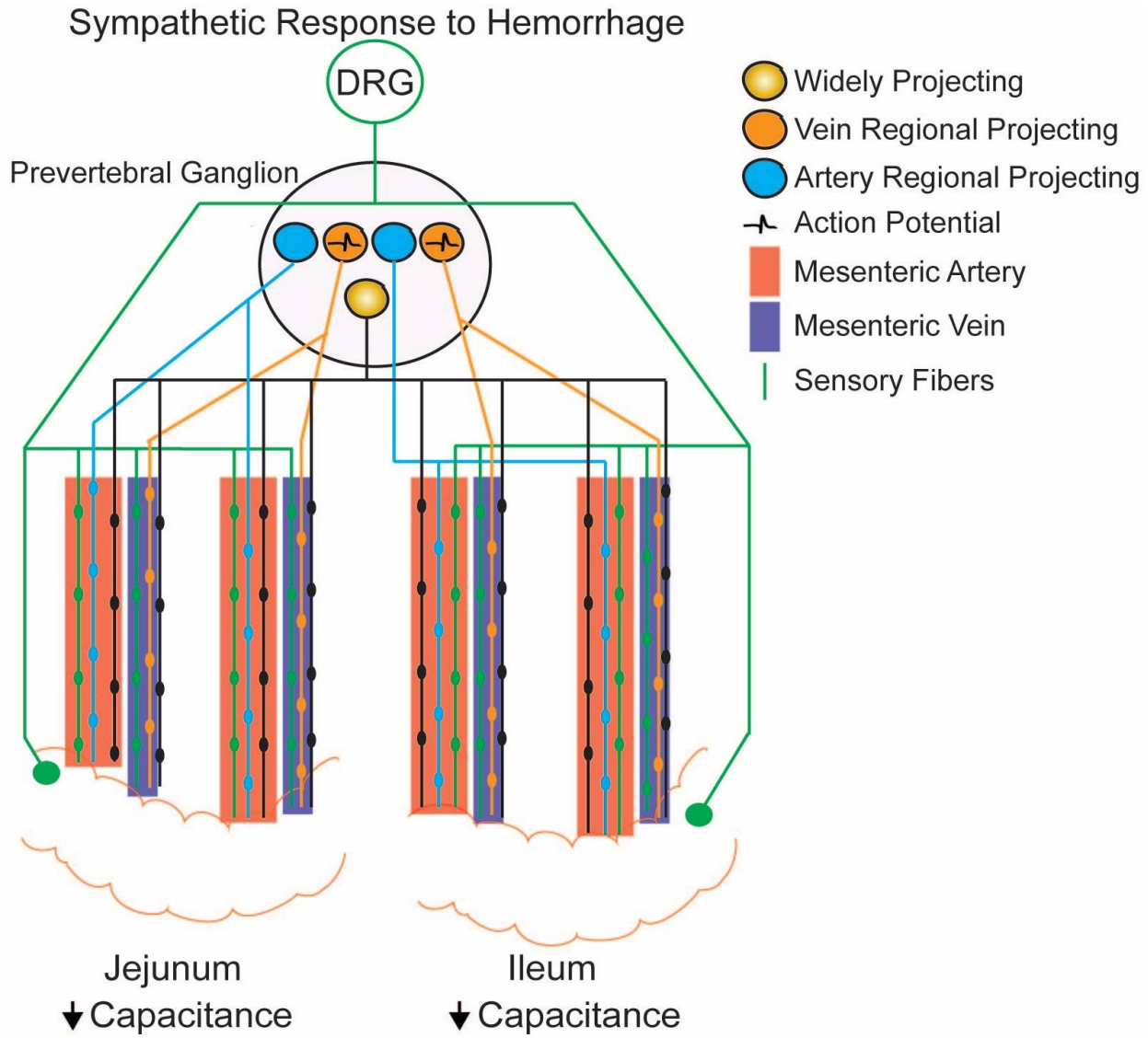


**Figure 5.3: Vein regional projecting neurons modulate the splanchnic sympathetic response to hemorrhage.** During hemorrhage, mesenteric veins are constricted to reduce account for blood loss without depleting central blood volume. Regional-, vein-projecting neurons, depicted in orange, mediate the sympathetic response to hemorrhage, via widespread venoconstriction.

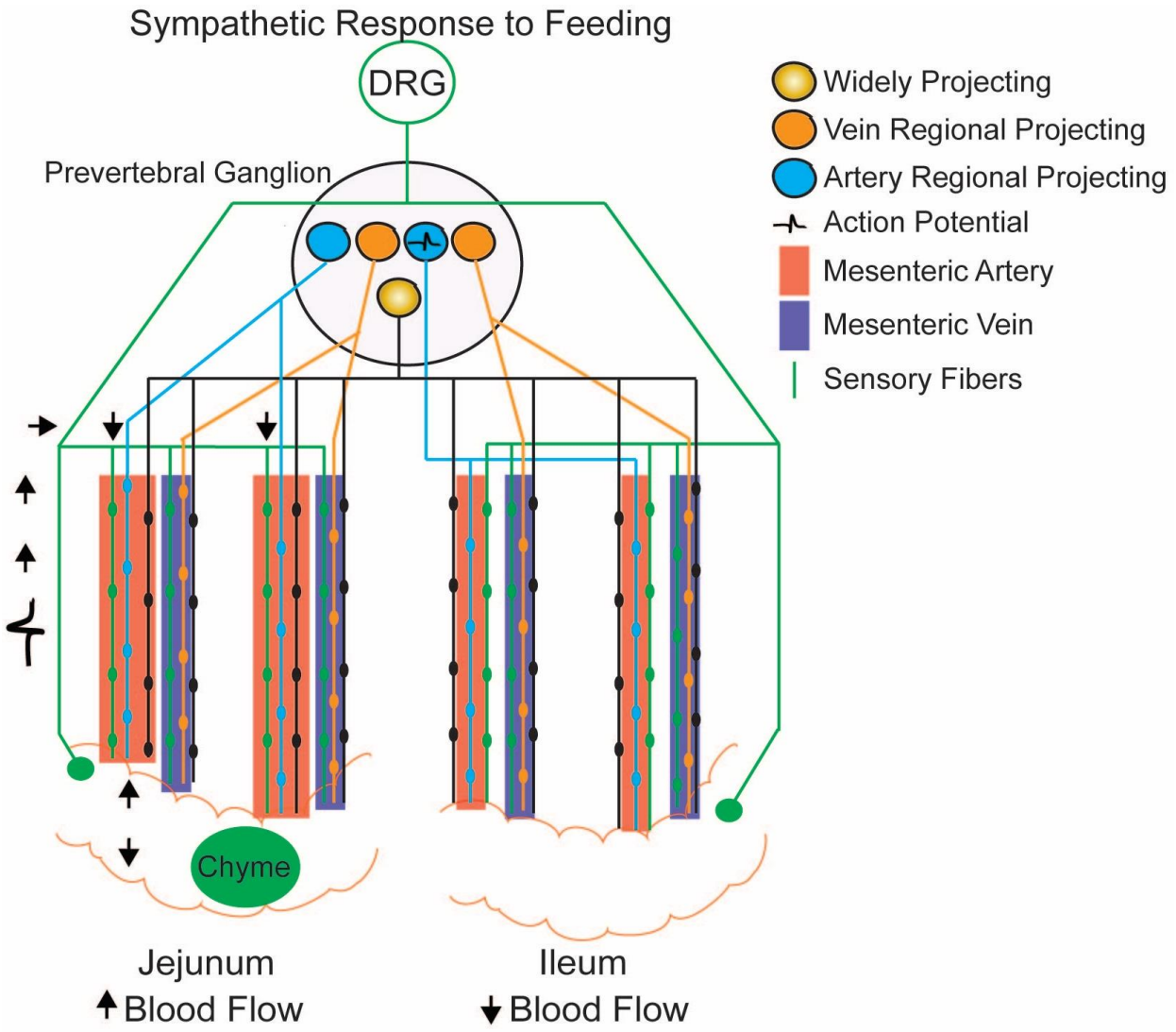


**Figure 5.4: Artery regional projecting neurons modulate the splanchnic sympathetic response to feeding.** During feeding, MA projecting to intestinal segments containing chyme are dilated, despite increased sympathetic activity. Regional-, artery-regional projecting neurons, depicted in light blue, mediate the sympathetic response to feeding, via regional constriction of arteries to intestinal segments not containing chyme. Sensory neurons mediate vasodilation of arteries feeding intestinal segments containing chyme via a mechanical feedback mechanism

# BIBLIOGRAPHY

## BIBLIOGRAPHY


Aceto, M. D., Martin, B. R., Uwaydah, I. M., May, E. L., Harris, L. S., Izazola-Conde, C., et al. (1979). Optically pure (+)-nicotine from (+/-)-nicotine and biological comparisons with (-)-nicotine. *Journal of Medicinal Chemistry*, *22*(2), 174–7.

Adams, D. J., Bevan, S., & Terrar, D. A. (1991). Modes of hexamethonium action on acetylcholine receptor channels in frog skeletal muscle. *British Journal of Pharmacology*, *102*(1), 135–45.

Aggarwal, A., Cutts, T. F., Abell, T. L., Cardoso, S., Familoni, B., Bremer, J., & Karas, J. (1994). Predominant symptoms in irritable bowel syndrome correlate with specific autonomic nervous system abnormalities. *Gastroenterology*, *106*(4), 945–50.

Ahluwalia, A., & Vallance, P. (1997). Evidence for functional responses to sensory nerve stimulation of rat small mesenteric veins. *The Journal of Pharmacology and Experimental Therapeutics*, *281*(1), 9–14.

Armitage, A. K. (1965). Effects of nicotine and tobacco smoke on blood pressure and release of catechol amines from the adrenal glands. *British Journal of Pharmacology and Chemotherapy*, *25*(2), 515–26.

Baloh, R. H., Tansey, M. G., Lampe, P. A., Fahrner, T. J., Enomoto, H., Simburger, K. S., et al. (1999). Artemin, a novel member of the GDNF ligand family, supports peripheral and central neurons and signals through the GFRalpha3-RET receptor complex. *Neuron*, *21*(6), 1291–302.

Barman, S. M., Orer, H. S., & Gebber, G. L. (2001). The role of the medullary lateral tegmental field in the generation and baroreceptor reflex control of sympathetic nerve discharge in the cat. *Annals of the New York Academy of Sciences*, *940*, 270–85.

Bartlett, J. S., Samulski, R. J., & McCown, T. J. (1998). Selective and rapid uptake of adeno-associated virus type 2 in brain. *Human Gene Therapy*, *9*(8), 1181–6.

Blacklow, N. R., Hoggan, M. D., Sereno, M. S., Brandt, C. D., Kim, H. W., Parrott, R. H., & Chanock, R. M. (1971). A seroepidemiologic study of adenovirus-associated virus infection in infants and children. *American Journal of Epidemiology*, *94*(4), 359–66.

Bloom, S. R., & Edwards, A. V. (1978). Certain pharmacological characteristics of the release of pancreatic glucagon in response to stimulation of the splanchnic nerves. *The Journal of Physiology*, *280*, 25–35.

Bloom, S. R., & Edwards, A. V. (1984). Characteristics of the neuroendocrine responses to stimulation of the splanchnic nerves in bursts in the conscious calf. *The Journal of Physiology*, *346*, 533–45.

Bloom, S. R., Edwards, A. V., & Vaughan, N. J. (1973). The role of the sympathetic innervation in the control of plasma glucagon concentration in the calf. *The Journal of Physiology*, *233*(2), 457–66.

Bratton, B., Davies, P., Jänig, W., & McAllen, R. (2010). Ganglionic transmission in a vasomotor pathway studied in vivo. *The Journal of Physiology*, *588*(Pt 9), 1647–59.

Brooks, A. R., Harkins, R. N., Wang, P., Qian, H. S., Liu, P., & Rubanyi, G. M. (2004). Transcriptional silencing is associated with extensive methylation of the CMV promoter following adenoviral gene delivery to muscle. *The Journal of Gene Medicine*, *6*(4), 395–404.

Brooksby, G. A., & Donald, D. E. (1972). Release of blood from the splanchnic circulation in dogs. *Circulation Research*, *31*(1), 105–18.

Browning, K. N., Zheng, Z., Kreulen, D. L., & Travagli, R. A. (1999). Two populations of sympathetic neurons project selectively to mesenteric artery or vein. *The American Journal of Physiology*, *276*(4 Pt 2), H1263–72.

Brunet, I., Gordon, E., Han, J., Cristofaro, B., Broqueres-You, D., Liu, C., et al. (2014). Netrin-1 controls sympathetic arterial innervation. *The Journal of Clinical Investigation*, *124*(7), 3230–40.

Brunsden, A. M., Brookes, S. J. H., Bardhan, K. D., & Grundy, D. (2007). Mechanisms underlying mechanosensitivity of mesenteric afferent fibers to vascular flow. *American Journal of Physiology - Gastrointestinal and Liver Physiology*, *293*(2), G422–8.

Burnstock, G. (2009). Purinergic cotransmission. *F1000 Biology Reports*, *1*, 46.

Cearley, C. N., & Wolfe, J. H. (2007). A single injection of an adeno-associated virus vector into nuclei with divergent connections results in widespread vector distribution in the brain and global correction of a neurogenetic disease. *The Journal of Neuroscience : the Official Journal of the Society for Neuroscience*, *27*(37), 9928–40.

Chamberlin, N. L., Du, B., de Lacalle, S., & Saper, C. B. (1998). Recombinant adeno-associated virus vector: use for transgene expression and anterograde tract tracing in the CNS. *Brain Research*, *793*(1-2), 169–75.

Chen, S., Yang, M., Miselis, R. R., & Aston-Jones, G. (1999). Characterization of transsynaptic tracing with central application of pseudorabies virus. *Brain Research*, *838*(1-2), 171–83.

Chou, C. C. (1983). Splanchnic and overall cardiovascular hemodynamics during eating and digestion. *Federation Proceedings*, *42*(6), 1658–61.

Converse, R. L., Jacobsen, T. N., Toto, R. D., Jost, C. M., Cosentino, F., Fouad-Tarazi, F., & Victor, R. G. (1993). Sympathetic overactivity in patients with chronic renal failure. *The New England Journal of Medicine*, *327*(27), 1912–8.

Crowcroft, P. J., & Szurszewski, J. H. (1971). A study of the inferior mesenteric and pelvic ganglia of guinea-pigs with intracellular electrodes. *The Journal of Physiology*, *219*(2), 421–41.

Damon, D. H., Teriele, J. A., & Marko, S. B. (2007). Vascular-derived artemin: a determinant of vascular sympathetic innervation? *American Journal of Physiology - Heart and Circulatory Physiology*, *293*(1), H266–73.

Davies, A. M. (1996). The neurotrophic hypothesis: where does it stand? *Philosophical Transactions of the Royal Society of London. Series B, Biological Sciences*, *351*(1338), 389–94.

De Fontgalland, D., Wattchow, D. A., Costa, M., & Brookes, S. J. H. (2008). Immunohistochemical characterization of the innervation of human colonic mesenteric and submucosal blood vessels. *Neurogastroenterology and Motility: the Official Journal of the European Gastrointestinal Motility Society*, *20*(11), 1212–26.

Dean, C., & Coote, J. H. (1986). A ventromedullary relay involved in the hypothalamic and chemoreceptor activation of sympathetic postganglionic neurones to skeletal muscle, kidney and splanchnic area. *Brain Research*, *377*(2), 279–85.

Dean, C., Seagard, J. L., Hopp, F. A., & Kampine, J. P. (1992). Differential control of sympathetic activity to kidney and skeletal muscle by ventral medullary neurons. *Journal of the Autonomic Nervous System*, *37*(1), 1–10.

Elshami, A. A., Saavedra, A., Zhang, H., Kucharczuk, J. C., Spray, D. C., Fishman, G. I., et al. (1996). Gap junctions play a role in the “bystander effect” of the herpes simplex virus thymidine kinase/ganciclovir system in vitro. *Gene Therapy*, *3*(1), 85–92.

Emmanuel, A. V., & Kamm, M. A. (2000). Laser Doppler flowmetry as a measure of extrinsic colonic innervation in functional bowel disease. *Gut*, *46*(2), 212–7.

Esler, M., Jennings, G., Korner, P., Blombery, P., Burke, F., Willett, I., & Leonard, P. (1984). Total, and organ-specific, noradrenaline plasma kinetics in essential hypertension. *Clinical and Experimental Hypertension. Part A: Theory and Practice*, *6*(1-2), 507–21.

Evans, R. J., & Surprenant, A. (1992). Vasoconstriction of guinea-pig submucosal arterioles following sympathetic nerve stimulation is mediated by the release of ATP. *British Journal of Pharmacology*, *106*(2), 242–9.

Felten, S. Y., & Olschowka, J. (1987). Noradrenergic sympathetic innervation of the spleen: II. Tyrosine hydroxylase (TH)-positive nerve terminals form synapticlike contacts on lymphocytes in the splenic white pulp. *Journal of Neuroscience Research*, *18*(1), 37–48.

Ferguson, M., Ryan, G. B., & Bell, C. (1986). Localization of sympathetic and sensory neurons innervating the rat kidney. *Journal of the Autonomic Nervous System*, *16*(4), 279–88.

Fink, G. D. (2008). Arthur C. Corcoran Memorial Lecture. Sympathetic activity, vascular capacitance, and long-term regulation of arterial pressure. *Hypertension*, *53*(2), 307–12.

Fink, G. D., Johnson, R. J., & Galligan, J. J. (2000). Mechanisms of increased venous smooth muscle tone in desoxycorticosterone acetate-salt hypertension. *Hypertension*, *35*(1 Pt 2), 464–9.

Foss, J. D., Fink, G. D., & Osborn, J. W. (2013). Reversal of genetic salt-sensitive hypertension by targeted sympathetic ablation. *Hypertension*, *61*(4), 806–11.

Foust, K. D., Poirier, A., Pacak, C. A., Mandel, R. J., & Flotte, T. R. (2007). Neonatal intraperitoneal or intravenous injections of recombinant adeno-associated virus type 8 transduce dorsal root ganglia and lower motor neurons. *Human Gene Therapy*, *19*(1), 61–70.

Freedman, M. A., Hallenbeck, G. A., & Code, C. F. (1952). The effect of vagotomy and of methantheline bromide on the diarrhea produced by celiac and superior mesenteric ganglionectomy. *Surgical Forum*, (38th Congress), 481–486.

Fujimori, A., Saito, A., Kimura, S., Watanabe, T., Uchiyama, Y., Kawasaki, H., & Goto, K. (1989). Neurogenic vasodilation and release of calcitonin gene-related peptide (CGRP) from perivascular nerves in the rat mesenteric artery. *Biochemical and Biophysical Research Communications*, *165*(3), 1391–8.

Furness, J. B. (1971). The adrenergic innervation of the vessels supplying and draining the gastrointestinal tract. *Zeitschrift Für Zellforschung Und Mikroskopische Anatomie*, *113*(1), 67–82.

Furness, J. B., & Costa, M. (1974). The adrenergic innervation of the gastrointestinal tract. *Ergebnisse der Physiologie Reviews of Physiology*, *69*(0), 2–51.

Furness, J. B., Koopmans, H. S., Robbins, H. L., Clerc, N., Tobin, J. M., & Morris, M. J. (2001). Effects of vagal and splanchnic section on food intake, weight, serum leptin and hypothalamic neuropeptide Y in rat. *Autonomic Neuroscience: Basic and Clinical*, *92*(1-2), 28–36.

Gallavan, R. H., & Chou, C. C. (1985). Possible mechanisms for the initiation and maintenance of postprandial intestinal hyperemia. *The American Journal of Physiology*, *249*(3 Pt 1), G301–8.

Gallavan, R. H., Chou, C. C., Kvietys, P. R., & Sit, S. P. (1980). Regional blood flow during digestion in the conscious dog. *The American Journal of Physiology*, *238*(2), H220–5.

Galligan, J. J., Hess, M. C., Miller, S. B., & Fink, G. D. (2001). Differential localization of P2 receptor subtypes in mesenteric arteries and veins of normotensive and hypertensive rats. *The Journal of Pharmacology and Experimental Therapeutics*, *296*(2), 478–85.

Gibbins, I. L. (1992). Vasoconstrictor, vasodilator and pilomotor pathways in sympathetic ganglia of guinea-pigs. *Neuroscience*, *47*(3), 657–72.

Gibbins, I. L., Hoffmann, B., & Morris, J. L. (1998). Peripheral fields of sympathetic vasoconstrictor neurons in guinea pigs. *Neuroscience Letters*, *248*(2), 89–92.

Gitterman, D. P., & Evans, R. J. (2001a). Nerve evoked P2X receptor contractions of rat mesenteric arteries; dependence on vessel size and lack of role of L-type calcium channels and calcium induced calcium release. *British Journal of Pharmacology*, *132*(6), 1201–8.

Gitterman, D. P., & Evans, R. J. (2001b). Properties of P2X and P2Y receptors are dependent on artery diameter in the rat mesenteric bed. *British Journal of Pharmacology*, *131*(8), 1561–8.

Glatzel, M., Flechsig, E., Navarro, B., Klein, M. A., Paterna, J. C., Büeler, H., & Aguzzi, A. (2000). Adenoviral and adeno-associated viral transfer of genes to the peripheral nervous system. *Proceedings of the National Academy of Sciences of the United States of America*, *97*(1), 442–7.

Glebova, N. O., & Ginty, D. D. (2004). Heterogeneous requirement of NGF for sympathetic target innervation in vivo. *The Journal of Neuroscience: the Official Journal of the Society for Neuroscience*, *24*(3), 743–51.

Gootman, P. M., & Cohen, M. I. (1970). Efferent splanchnic activity and systemic arterial pressure. *The American Journal of Physiology*, *219*(4), 897–903.

Gourine, A. V., Wood, J. D., & Burnstock, G. (2009). Purinergic signalling in autonomic control. *Trends in Neurosciences*, *32*(5), 241–8.

Granger, D. N., Kvietys, P. R., & Korthuis, R. J. (2011). *Microcirculation of the intestinal mucosa*. Hoboken, NJ: John Wiley & Sons.

Greene, L. A., & Tischler, A. S. (1976). Establishment of a noradrenergic clonal line of rat adrenal pheochromocytoma cells which respond to nerve growth factor. *Proceedings of the National Academy of Sciences of the United States of America*, *73*(7), 2424–8.

Greenway, C. V., & Lister, G. E. (1974). Capacitance effects and blood reservoir function in the splanchnic vascular bed during non-hypotensive haemorrhage and blood volume expansion in anaesthetized cats. *The Journal of Physiology*, *237*(2), 279–94.

Grimson, K. S., & Orgain, E. S. (1949). Results of treatment of patients with hypertension by total thoracic and partial to total lumbar sympathectomy, splanchnicectomy and celiac ganglionectomy. *Annals of Surgery*, *129*(6), 850–71.

Gurney, A. M., & Rang, H. P. (1997). The channel-blocking action of methonium compounds on rat submandibular ganglion cells. 1983. *British Journal of Pharmacology*, *120*(4 Suppl), 471-90.

Han, S. P., Naes, L., & Westfall, T. C. (1990). Inhibition of periarterial nerve stimulation-induced vasodilation of the mesenteric arterial bed by CGRP (8-37) and CGRP receptor desensitization. *Biochemical and Biophysical Research Communications*, *168*(2), 786–91.

Hausberg, M., Kosch, M., Harmelink, P., Barenbrock, M., Hohage, H., Kisters, K., et al. (2002). Sympathetic nerve activity in end-stage renal disease. *Circulation*, *106*(15), 1974–9.

Hill, C. E., Hirst, G. D., & Van Helden, D. F. (1983). Development of sympathetic innervation to proximal and distal arteries of the rat mesentery. *The Journal of Physiology*, *338*, 129-147.

Holzer, P. (1992). Peptidergic sensory neurons in the control of vascular functions: mechanisms and significance in the cutaneous and splanchnic vascular beds. *Reviews of Physiology, Biochemistry and Pharmacology*, *121*, 49–146.

Honma, Y., Araki, T., Gianino, S., Bruce, A., Heuckeroth, R., Johnson, E., & Milbrandt, J. (2002). Artemin is a vascular-derived neurotropic factor for developing sympathetic neurons. *Neuron*, *35*(2), 267–82.

Hottenstein, O. D., & Kreulen, D. L. (1987). Comparison of the frequency dependence of venous and arterial responses to sympathetic nerve stimulation in guinea-pigs. *The Journal of Physiology*, *384*, 153–67.

Hsieh, N. K., Liu, J. C., & Chen, H. I. (2000). Localization of sympathetic postganglionic neurons innervating mesenteric artery and vein in rats. *Journal of the Autonomic Nervous System*, *80*(1-2), 1–7.

Hukkanen, M., Konttinen, Y. T., Rees, R. G., Gibson, S. J., Santavirta, S., & Polak, J. M. (1992). Innervation of bone from healthy and arthritic rats by substance P and calcitonin gene related peptide containing sensory fibers. *The Journal of Rheumatology*, *19*(8), 1252–9.

Ikushima, S., Muramatsu, I., Sakakibara, Y., Yokotani, K., & Fujiwara, M. (1982). The effects of d-nicotine and l-isomer on nicotinic receptors. *The Journal of Pharmacology and Experimental Therapeutics*, *222*(2), 463–70.

Jacobowitz, D. M., Ziegler, M. G., & Thomas, J. A. (1975). In vivo uptake of antibody to dopamine-beta-hydroxylase into sympathetic elements. *Brain Research*, *91*(1), 165–70.

Janig, W., & McLachlan, E. M. (1992). Characteristics of function-specific pathways in the sympathetic nervous system. *Trends in Neurosciences*, *15*(12), 475–81.

Julius, S. (1988). Transition from high cardiac output to elevated vascular resistance in hypertension. *American Heart Journal*, *116*(2 Pt 2), 600–6.

Kandlikar, S. S., & Fink, G. D. (2011). Splanchnic sympathetic nerves in the development of mild DOCA-salt hypertension. *American Journal of Physiology - Heart and Circulatory Physiology*, *301*(5), H1965–73.

Kaplitt, M. G., Leone, P., Samulski, R. J., Xiao, X., Pfaff, D. W., O'Malley, K. L., & During, M. J. (1994). Long-term gene expression and phenotypic correction using adeno-associated virus vectors in the mammalian brain. *Nature Genetics*, *8*(2), 148–54.

Karim, F., & Hainsworth, R. (1976). Responses of abdominal vascular capacitance to stimulation of splachnic nerves. *The American Journal of Physiology*, *231*(2), 434–40.

Kaspar, B. K., Lladó, J., Sherkat, N., Rothstein, J. D., & Gage, F. H. (2003). Retrograde viral delivery of IGF-1 prolongs survival in a mouse ALS model. *Science*, *301*(5634), 839–42.

Katafuchi, T., Ichijo, T., Take, S., & Hori, T. (1993a). Hypothalamic modulation of splenic natural killer cell activity in rats. *The Journal of Physiology*, *471*, 209–21.

Katafuchi, T., Take, S., & Hori, T. (1993b). Roles of sympathetic nervous system in the suppression of cytotoxicity of splenic natural killer cells in the rat. *The Journal of Physiology*, *465*, 343–57.

Katsuki, M., Hirooka, Y., Kishi, T., & Sunagawa, K. (2015). Decreased proportion of Foxp3+ CD4+ regulatory T cells contributes to the development of hypertension in genetically hypertensive rats. *Journal of Hypertension*, *33*(4), 773-83.

Kidokoro, Y., Miyazaki, S., & Ozawa, S. (1982). Acetylcholine-induced membrane depolarization and potential fluctuations in the rat adrenal chromaffin cell. *The Journal of Physiology*, *324*, 203–20.

Kihara, K., & de Groat, W. C. (1997). Sympathetic efferent pathways projecting to the bladder neck and proximal urethra in the rat. *Journal of the Autonomic Nervous System*, *62*(3), 134–42.

Kim, D. W., Harada, T., Saito, I., & Miyamura, T. (1993). An efficient expression vector for stable expression in human liver cells. *Gene*, *134*(2), 307–308.

King, A. J., Osborn, J. W., & Fink, G. D. (2007). Splanchnic circulation is a critical neural target in angiotensin II salt hypertension in rats. *Hypertension*, *50*(3), 547–56.

Kircher, P., Lang, J., Blum, J., Gaschen, F., Doherr, M., Sieber, C., & Gaschen, L. (2003). Influence of food composition on splanchnic blood flow during digestion in unsedated normal dogs: a Doppler study. *Veterinary Journal*, *166*(3), 265–272.

Kirik, D., Rosenblad, C., Burger, C., Lundberg, C., Johansen, T. E., Muzyczka, N., et al. (2002). Parkinson-like neurodegeneration induced by targeted overexpression of alpha-synuclein in the nigrostriatal system. *The Journal of Neuroscience : the Official Journal of the Society for Neuroscience*, *22*(7), 2780–91.

Klein, R. L., Meyer, E. M., Peel, A. L., Zolotukhin, S., Meyers, C., Muzyczka, N., & King, M. A. (1998). Neuron-specific transduction in the rat septohippocampal or nigrostriatal pathway by recombinant adeno-associated virus vectors. *Experimental Neurology*, *150*(2), 183–94.

Korecka, J., Ulusoy, A., Verhaagen, J., & Bossers, K. (2011). *Comparison of AAV serotypes for gene delivery to dopaminergic neurons in the Substantia Nigra*. *Journal of Neurochemistry, 109*(3), 838-845.

Kosuga, M., Enosawa, S., Li, X. K., Suzuki, S., Matsuo, N., Yamada, M., et al. (2001). Strong, long-term transgene expression in rat liver using chicken beta-actin promoter associated with cytomegalovirus immediate-early enhancer (CAG promoter). *Cell Transplantation*, *9*(5), 675–80.

Krejci, V., Hiltebrand, L., Banic, A., Erni, D., Wheatley, A. M., & Sigurdsson, G. H. (2000). Continuous measurements of microcirculatory blood flow in gastrointestinal organs during acute haemorrhage. *British Journal of Anaesthesia*, *84*(4), 468–75.

Kreulen, D. L. (1984). Integration in autonomic ganglia. *The Physiologist*, *27*(1), 49–55.

Kreulen, D. L. (1986). Activation of mesenteric arteries and veins by preganglionic and postganglionic nerves. *The American Journal of Physiology*, *251*(6 Pt 2), H1267–75.

Kreulen, D. L., & Peters, S. (1986). Non-cholinergic transmission in a sympathetic ganglion of the guinea-pig elicited by colon distension. *The Journal of Physiology*, *374*, 315–34.

Kreulen, D. L., & Szurszewski, J. H. (1979). Reflex pathways in the abdominal prevertebral ganglia: evidence for a colo-colonic inhibitory reflex. *The Journal of Physiology*, *295*, 21–32.

Kuntz, A., & Saccomanno, G. (1944). Reflex inhibition of intestinal motility mediated through decentralized prevertebral ganglia. *Journal of Neurophysiology*, *7*(3), 163–170.

Kuroki, M. T., Guzman, P. A., Fink, G. D., & Osborn, J. W. (2011). Time-dependent changes in autonomic control of splanchnic vascular resistance and heart rate in ANG II-salt hypertension. *American Journal of Physiology - Heart and Circulatory Physiology*, *302*(3), H763–9.

Langley, J. N. (1893). The Arrangement of the Sympathetic Nervous System, based chiefly on Observations upon Pilo-motor Nerves. *The Journal of Physiology*, *15*(3), 176–248.21.

Li, M., Galligan, J., Wang, D., & Fink, G. (2010). The effects of celiac ganglionectomy on sympathetic innervation to the splanchnic organs in the rat. *Autonomic Neuroscience: Basic and Clinical*, *154*(1-2), 66–73.

Lillehei, C. W., & Wangensteen, O. H. (1948). Effect of celiac ganglionectomy upon experimental peptic ulcer formation. *Proceedings of the Society for Experimental Biology and Medicine. Society for Experimental Biology and Medicine*, *68*(2), 369–72.

Lindh, B., Hökfelt, T., & Elfvin, L. G. (1988). Distribution and origin of peptide-containing nerve fibers in the celiac superior mesenteric ganglion of the guinea-pig. *Neuroscience*, *26*(3), 1037–71.

Long, J. B., Jay, S. M., Segal, S. S., & Madri, J. A. (2009). VEGF-A and Semaphorin3A: modulators of vascular sympathetic innervation. *Developmental Biology*, *334*(1), 119–32.

Looft-Wilson, R. C., Haug, S. J., Neufer, P. D., & Segal, S. S. (2004). Independence of connexin expression and vasomotor conduction from sympathetic innervation in hamster feed arteries. *Microcirculation*, *11*(5), 397–408.

Lovick, T. A. (1987). Differential control of cardiac and vasomotor activity by neurones in nucleus paragigantocellularis lateralis in the cat. *The Journal of Physiology*, *389*, 23–35.

Lovick, T. A., & Hilton, S. M. (1985). Vasodilator and vasoconstrictor neurones of the ventrolateral medulla in the cat. *Brain Research*, *331(2), 353-7*

Luft, F. C., Wilcox, C. S., Unger, T., Kühn, R., Demmert, G., Rohmeiss, P., et al. (1989). Angiotensin-induced hypertension in the rat. Sympathetic nerve activity and prostaglandins. *Hypertension*, *14*(4), 396–403.

Lundgren, O., & Svanvik, J. (1973). Mucosal hemodynamics in the small intestine of the cat during reduced perfusion pressure. *Acta Physiologica Scandinavica*, *88*(4), 551–63.

Lundin, S., Ricksten, S. E., & Thorén, P. (1984). Renal sympathetic activity in spontaneously hypertensive rats and normotensive controls, as studied by three different methods. *Acta Physiologica Scandinavica*, *120*(2), 265–72.

Luo, M., Hess, M. C., Fink, G. D., Olson, L. K., Rogers, J., Kreulen, D. L., et al. (2003). Differential alterations in sympathetic neurotransmission in mesenteric arteries and veins in DOCA-salt hypertensive rats. *Autonomic Neuroscience: Basic and Clinical*, *104*(1), 47–57.

Löser, P., Jennings, G. S., Strauss, M., & Sandig, V. (1998). Reactivation of the previously silenced cytomegalovirus major immediate-early promoter in the mouse liver: involvement of NFkappaB. *Journal of Virology*, *72*(1), 180–90.

Macleod, G. T., Lavidis, N. A., & Bennett, M. R. (1994). Calcium dependence of quantal secretion from visualized sympathetic nerve varicosities on the mouse vas deferens. *The Journal of Physiology*, *480 (Pt 1)*, 61–70.

Macrae, I. M., Furness, J. B., & Costa, M. (1986). Distribution of subgroups of noradrenaline neurons in the coeliac ganglion of the guinea-pig. *Cell and Tissue Research*, *244*(1), 173–80.

Manitt, C., Nikolakopoulou, A. M., Almario, D. R., Nguyen, S. A., & Cohen-Cory, S. (2009). Netrin participates in the development of retinotectal synaptic connectivity by modulating axon arborization and synapse formation in the developing brain. *The Journal of Neuroscience: the Official Journal of the Society for Neuroscience*, *29*(36), 11065–77.

Marina, N., Becker, D. L., & Gilbey, M. P. (2008). Immunohistochemical detection of connexin36 in sympathetic preganglionic and somatic motoneurons in the adult rat. *Autonomic Neuroscience: Basic and Clinical*, *139*(1-2), 15–23.

Marlett, J. A., & Code, C. F. (1979). Effects of celiac and superior mesenteric ganglionectomy on interdigestive myoelectric complex in dogs. *The American Journal of Physiology*, *237*(5), E432–43.

Marley, E., & Paton, W. D. (1961). The output of sympathetic amines from the cat's adrenal gland in response to splanchnic nerve activity. *The Journal of Physiology*, *155*, 1–27.

Mason, M. R. J., Ehlert, E. M. E., Eggers, R., Pool, C. W., Hermening, S., Huseinovic, A., et al. (2010). Comparison of AAV serotypes for gene delivery to dorsal root ganglion neurons. *Molecular Therapy: the Journal of the American Society of Gene Therapy*, *18*(4), 715–24.

Matheson, P. J., Wilson, M. A., & Garrison, R. N. (2000). Regulation of intestinal blood flow. *The Journal of Surgical Research*, *93*(1), 182–96.

May, C. N. (1996). Prolonged systemic and regional haemodynamic effects of intracerebroventricular angiotensin II in conscious sheep. *Clinical and Experimental Pharmacology and Physiology*, *23*(10-11), 878–84.

May, C. N. (2006). Differential regional haemodynamic changes during mineralocorticoid hypertension. *Journal of Hypertension*, *24*(6), 1137–46.

McAllen, R. M., May, C. N., & Shafton, A. D. (1995). Functional anatomy of sympathetic premotor cell groups in the medulla. *Clinical and Experimental Hypertension*, *17*(1-2), 209–21.

McLachlan, E. M. (2003). Transmission of signals through sympathetic ganglia--modulation, integration or simply distribution? *Acta Physiologica Scandinavica*, *177*(3), 227–35.

Meehan, A. G., Hottenstein, O. D., & Kreulen, D. L. (1991). Capsaicin-sensitive nerves mediate inhibitory junction potentials and dilatation in guinea-pig mesenteric artery. *The Journal of Physiology*, *443*, 161–74.

Mesnil, M., Piccoli, C., Tiraby, G., Willecke, K., & Yamasaki, H. (1996). Bystander killing of cancer cells by herpes simplex virus thymidine kinase gene is mediated by connexins. *Proceedings of the National Academy of Sciences of the United States of America*, *93*(5), 1831–5.

Murphy, S. M., Matthew, S. E., Rodgers, H. F., Lituri, D. T., & Gibbins, I. L. (1998). Synaptic organisation of neuropeptide-containing preganglionic boutons in lumbar sympathetic ganglia of guinea pigs. *The Journal of Comparative Neurology*, *398*(4), 551–67.

Nakazato, Y., Sekine, H., Isogaya, M., & Ito, S. (1987). Atropine-and hexamethonium-resistant motor response to greater splanchnic nerve stimulation in the dog stomach. *Journal of the Autonomic Nervous System*, *20*(1), 35.

Neuhuber, W. L., Sandoz, P. A., & Fryscak, T. (1986). The central projections of primary afferent neurons of greater splanchnic and intercostal nerves in the rat. *Anatomy and Embryology*, *174*(1), 123–144.

Nilsson, H., Ljung, B., Sjöblom, N., & Wallin, B. G. (1985). The influence of the sympathetic impulse pattern on contractile responses of rat mesenteric arteries and veins. *Acta Physiologica Scandinavica*, *123*(3), 303–9.

Osborn, J. W., Fink, G. D., & Kuroki, M. T. (2011). Neural mechanisms of angiotensin II-salt hypertension: implications for therapies targeting neural control of the splanchnic circulation. *Current Hypertension Reports*, *13*(3), 221–8.

Osborn, J. W., Fink, G. D., Sved, A. F., Toney, G. M., & Raizada, M. K. (2007). Circulating angiotensin II and dietary salt: converging signals for neurogenic hypertension. *Current Hypertension Reports*, *9*(3), 228–35.

Pang, C. C. (2001). Autonomic control of the venous system in health and disease: effects of drugs. *Pharmacology &Amp; Therapeutics*, *90*(2-3), 179–230.

Park, J., Galligan, J. J., Fink, G. D., & Swain, G. M. (2009). Alterations in sympathetic neuroeffector transmission to mesenteric arteries but not veins in DOCA-salt hypertension. *Autonomic Neuroscience: Basic and Clinical*, *152*(1-2), 11–20.

Pediani, J. D., McGrath, J. C., & Wilson, S. M. (1999). P2Y receptor-mediated Ca2+ signalling in cultured rat aortic smooth muscle cells. *British Journal of Pharmacology*, *126*(7), 1660–6.

Peel, A. L., Zolotukhin, S., Schrimsher, G. W., Muzyczka, N., & Reier, P. J. (1997). Efficient transduction of green fluorescent protein in spinal cord neurons using adeno-associated virus vectors containing cell type-specific promoters. *Gene Therapy*, *4*(1), 16–24.

Pelletier, C. L., Edis, A. J., & Shepherd, J. T. (1971). Circulatory reflex from vagal afferents in response to hemorrhage in the dog. *Circulation Research*, *29*(6), 626–34.

Perko, M. J., Nielsen, H. B., Skak, C., Clemmesen, J. O., Schroeder, T. V., & Secher, N. H. (1998). Mesenteric, coeliac and splanchnic blood flow in humans during exercise. *The Journal of Physiology*, *513 (Pt 3)*, 907–13.

Picklo, M. J., Wiley, R. G., Lonce, S., Lappi, D. A., & Robertson, D. (1995). Anti-dopamine beta-hydroxylase immunotoxin-induced sympathectomy in adult rats. *The Journal of Pharmacology and Experimental Therapeutics*, *275*(2), 1003–10.

Polito, L., Bortolotti, M., Farini, V., Battelli, M. G., Barbieri, L., & Bolognesi, A. (2008). Saporin induces multiple death pathways in lymphoma cells with different intensity and timing as compared to ricin. *The International Journal of Biochemistry &Amp; Cell Biology*, *41*(5), 1055–61.

Price, H. L., Deutsch, S., Marshall, B. E., Stephen, G. W., Behar, M. G., & Neufeld, G. R. (1966). Hemodynamic and metabolic effects of hemorrhage in man, with particular reference to the splanchnic circulation. *Circulation Research*, *18*(5), 469–74.

Pucovský, V., Gordienko, D. V., & Bolton, T. B. (2002). Effect of nitric oxide donors and noradrenaline on Ca 2+ release sites and global intracellular Ca 2+ in myocytes from guinea-pig small mesenteric arteries. *The Journal of Physiology*, *539*(1), 25.

Purves, D., & Wigston, D. J. (1983). Neural units in the superior cervical ganglion of the guinea-pig. *The Journal of Physiology*, *334*, 169–178.

Puvi-Rajasingham, S., Smith, G. D., Akinola, A., & Mathias, C. J. (1998). Abnormal regional blood flow responses during and after exercise in human sympathetic denervation. *The Journal of Physiology*, *505 (Pt 3)*, 841–9.

Qamar, M. I., & Read, A. E. (1987). Effects of exercise on mesenteric blood flow in man. *Gut*, *28*(5), 583–7.

Quinson, N., Robbins, H. L., Clark, M. J., & Furness, J. B. (2001). Locations and innervation of cell bodies of sympathetic neurons projecting to the gastrointestinal tract in the rat. *Archives of Histology and Cytology*, *64*(3), 281–94.

Ramey, E. R., & Goldstein, M. S. (1957). The adrenal cortex and the sympathetic nervous system. *Physiological Reviews*, *37*(2), 155–95.

Raper, R. F., Sibbald, W. J., Hobson, J., & Rutledge, F. S. (1991). Effect of PGE1 on altered distribution of regional blood flows in hyperdynamic sepsis. *Chest*, *100*(6), 1703–11.

Reilly, P. M., Wilkins, K. B., Fuh, K. C., Haglund, U., & Bulkley, G. B. (2001). The mesenteric hemodynamic response to circulatory shock: an overview. *Shock*, *15*(5), 329–43.

Robert, J. H., Toledano, A. E., Toth, L. S., Premus, G., & Dreiling, D. A. (1988). Hypovolemic shock, pancreatic blood flow, and pancreatitis. *International Journal of Pancreatology: Official Journal of the International Association of Pancreatology*, *3*(4), 283–92.

Rosas-Ballina, M., Ochani, M., Parrish, W. R., Ochani, K., Harris, Y. T., Huston, J. M., et al. (2008). Splenic nerve is required for cholinergic antiinflammatory pathway control of

TNF in endotoxemia. *Proceedings of the National Academy of Sciences of the United States of America*, *105*(31), 11008–13.

Rowell, L. B., Blackmon, J. R., Kenny, M. A., & Escourrou, P. (1984). Splanchnic vasomotor and metabolic adjustments to hypoxia and exercise in humans. *The American Journal of Physiology*, *247*(2 Pt 2), H251–8.

Ruitenberg, M. J., Eggers, R., Boer, G. J., & Verhaagen, J. (2002). Adeno-associated viral vectors as agents for gene delivery: application in disorders and trauma of the central nervous system. *Methods*, *28*(2), 182–94.

Samsel, R. W., & Schumacker, P. T. (1994). Systemic hemorrhage augments local O2 extraction in canine intestine. *Journal of Applied Physiology*, *77*(5), 2291–8.

Sapru, H. N., Gonzalez, E. R., & Krieger, A. J. (1982). Greater splanchnic nerve activity in the rat. *Brain Research Bulletin*, *8*(3), 267–72.

Sawchenko, P. E., & Swanson, L. W. (1981). A method for tracing biochemically defined pathways in the central nervous system using combined fluorescence retrograde transport and immunohistochemical techniques. *Brain Research*, *210*(1-2), 31–51.

Shen, Y. T., Knight, D. R., Thomas, J. X., & Vatner, S. F. (1990). Relative roles of cardiac receptors and arterial baroreceptors during hemorrhage in conscious dogs. *Circulation Research*, *66*(2), 397–405.

Shepherd, A. P., & Riedel, G. L. (1988). Intramural distribution of intestinal blood flow during sympathetic stimulation. *The American Journal of Physiology*, *255*(5 Pt 2), H1091–5.

Shimazu, T. (1981). Central nervous system regulation of liver and adipose tissue metabolism. *Diabetologia*, *20 Suppl*, 343–56.

Singh, K. K., Park, K. J., Hong, E. J., Kramer, B. M., Greenberg, M. E., Kaplan, D. R., & Miller, F. D. (2008). Developmental axon pruning mediated by BDNF-p75NTR-dependent axon degeneration. *Nature Neuroscience*, *11*(6), 649–58.

Smit, A. A., Halliwill, J. R., Low, P. A., & Wieling, W. (1999). Pathophysiological basis of orthostatic hypotension in autonomic failure. *The Journal of Physiology*, *519* (Pt 1), 1–10.

Sporkova, A., Perez-Rivera, A., & Galligan, J. J. (2010). Interaction between alpha(1)- and alpha(2)-adrenoreceptors contributes to enhanced constrictor effects of norepinephrine in mesenteric veins compared to arteries. *European Journal of Pharmacology*, *643*(2-3), 239–46.

Stjärne, L., & Stjärne, E. (1995). Geometry, kinetics and plasticity of release and clearance of ATP and noradrenaline as sympathetic cotransmitters: roles for the neurogenic contraction. *Progress in Neurobiology*, *47*(1), 45–94.

Tang, Y. W., Mitchell, P. S., Espy, M. J., Smith, T. F., & Persing, D. H. (1999). Molecular diagnosis of herpes simplex virus infections in the central nervous system. *Journal of Clinical Microbiology*, *37*(7), 2127–36.

Thomas, C. E., Storm, T. A., Huang, Z., & Kay, M. A. (2004). Rapid uncoating of vector genomes is the key to efficient liver transduction with pseudotyped adeno-associated virus vectors. *Journal of Virology*, *78*(6), 3110–22.

Todorov, L. D., Bjur, R. A., & Westfall, D. P. (1994). Temporal dissociation of the release of the sympathetic co-transmitters ATP and noradrenaline. *Clinical and Experimental Pharmacology and Physiology*, *21*(11), 931–2.

Toung, T., Reilly, P. M., Fuh, K. C., Ferris, R., & Bulkley, G. B. (2000). Mesenteric vasoconstriction in response to hemorrhagic shock. *Shock*, *13*(4), 267–73.

Trudrung, P., Furness, J. B., Pompolo, S., & Messenger, J. P. (1994). Locations and chemistries of sympathetic nerve cells that project to the gastrointestinal tract and spleen. *Archives of Histology and Cytology*, *57*(2), 139–50.

Uechi, M., Asai, K., Osaka, M., Smith, A., Sato, N., Wagner, T. E., et al. (1998). Depressed heart rate variability and arterial baroreflex in conscious transgenic mice with overexpression of cardiac Gsalpha. *Circulation Research*, *82*(4), 416–23.

Van Lieshout, J. J., Wieling, W., Wesseling, K. H., Endert, E., & Karemaker, J. M. (1990). Orthostatic hypotension caused by sympathectomies performed for hyperhidrosis. *The Netherlands Journal of Medicine*, *36*(1-2), 53–7.

Vander, A. J. (1965). Effect of catecholamines and the renal nerves on renin secretion in anesthetized dogs. *The American Journal of Physiology*, *209*(3), 659–62.

Wehrwein, E. A., Yoshimoto, M., Guzman, P., Shah, A., Kreulen, D. L., & Osborn, J. W. (2014). Role of cardiac sympathetic nerves in blood pressure regulation. *Autonomic Neuroscience: Basic and Clinical*, *183*, 30–5.

Wiley, R. G., & Lappi, D. A. (1994). *Suicide transport and immunolesioning*. Austin, TX: RG Landes Co. Molecular Biology Intelligence Unit.

Worlicek, M., Knebel, K., Linde, H. J., Moleda, L., Schölmerich, J., Straub, R. H., & Wiest, R. (2010). Splanchnic sympathectomy prevents translocation and spreading of E coli but not S aureus in liver cirrhosis. *Gut*, *59*(8), 1127–1134.

Wu, Z., Asokan, A., & Samulski, R. J. (2006). Adeno-associated virus serotypes: vector toolkit for human gene therapy. *Molecular Therapy: the Journal of the American Society of Gene Therapy*, *14*(3), 316–27.

Yamamoto, J., Goto, Y., Nakai, M., Ogino, K., & Ikeda, M. (1983). Circulatory pressure-volume relationship and cardiac output in DOCA-salt rats. *Hypertension*, *5*(4), 507–13.

Zhang, G.-R., Zhao, H., Abdul-Muneer, P. M., Cao, H., Li, X., & Geller, A. I. (2014). Neurons can be labeled with unique hues by helper virus-free HSV-1 vectors expressing Brainbow. *Journal of Neuroscience Methods*, *240*, 77–88.

Zheng, H., Qiao, C., Wang, C.-H., Li, J., Li, J., Yuan, Z., et al. (2009). Efficient retrograde transport of adeno-associated virus type 8 to spinal cord and dorsal root ganglion after vector delivery in muscle. *Human Gene Therapy*, *21*(1), 87–97.

Zheng, Z., Shimamura, K., Anthony, T. L., Travagli, R. A., & Kreulen, D. L. (1998). Nitric oxide is a sensory nerve neurotransmitter in the mesenteric artery of guinea pig. *Journal of the Autonomic Nervous System*, *67*(3), 137–44.

Ziegler, M. G., Thomas, J. A., & Jacobowitz, D. M. (1976). Retrograde axonal transport of antibody to dopamine-beta-hydroxylase. *Brain Research*, *104*(2), 390–5.

van Baak, M. A. (2008). Meal-induced activation of the sympathetic nervous system and its cardiovascular and thermogenic effects in man. *Physiology &Amp; Behavior*, *94*(2), 178–86.

van Eijndhoven, H. W. F., van der Heijden, O. W. H., Fazzi, G. E., Aardenburg, R., Spaanderman, M. E. A., Peeters, L. L. H., & De Mey, J. G. R. (2003). Vasodilator reactivity to calcitonin gene-related peptide is increased in mesenteric arteries of rats during early pregnancy. *Journal of Vascular Research*, *40*(4), 344–50.